Synthesis and characterization of amine functionalized cellulose-silica composites for heavy metal adsorption from contaminated water.

by

Mayenzeke Trueman Mazibuko

Submitted in fulfillment of the requirements for the degree of

Master of Applied Science in Chemistry (MAppSc)

Department of Chemistry, Faculty of Applied Sciences

at the

Durban University of Technology

February 2025

Supervisor: Dr. TH Mokhothu
Co-supervisor: Prof. PS Mdluli
Co-supervisor: Dr. V Paul

Declaration

I, Mayenzeke Trueman Mazibuko, hereby declare that this research project is my original work and has not been submitted for any degree or examination at any other institution. All sources used have been duly acknowledged, and every effort has been made to ensure the accuracy and integrity of the data and findings presented in this study. My work its only publication was in the form of conference papers and journal publications, as listed below:

Conference paper and abstracts arising from this study.

Mayenzeke Trueman Mazibuko, Mokhothu Thabang Hendrica, Phumlane Selby Mdluli, and Vimla Paul, 2021. Synthesis and characterization of amine-functionalized cellulose Silica composites for heavy metal adsorption in contaminated water. 14th Green Chemistry postgraduate summer school. 4th-10th July 2021, Venezia, Italy, Zoom.

Mayenzeke Trueman Mazibuko, Mokhothu Thabang Hendrica, Phumlane Selby Mdluli, and Vimla Paul, 2021. Synthesis and characterization of amine-functionalized cellulose-silica composites for heavy metal adsorption in contaminated water. The South African Chemical Institute-KwaZulu-Natal Section (SACI KZN): 2021 SACI KZN Postgraduate Research Colloquium. 7th July 2021, Zoom.

Mayenzeke Trueman Mazibuko, Mokhothu Thabang Hendrica, Phumlane Selby Mdluli, and Vimla Paul, 2022. Synthesis and characterization of amine-functionalized cellulose-silica composites for heavy metal adsorption in contaminated water. 15th Green Chemistry postgraduate summer school. 3rd-8th July 2022, Venezia, Italy, Zoom.

Mayenzeke Trueman Mazibuko, Mokhothu Thabang Hendrica, Phumlane Selby Mdluli, and Vimla Paul, 2022. Amine functionalized cellulose-silica composites for heavy metal adsorption in contaminated water. Durban University of Technology faculty research day, Musgrave, Durban, South Africa.

Journal papers published and submitted arising from this study.

Mayenzeke Trueman Mazibuko, Stanley Chibuzor Onwubu, Mokhothu Thabang Hendric, Vimla Paul, and Phumlane Selby Mdluli, 2024. Unlocking Heavy Metal Remediation Potential: A Review of Cellulose–Silica Composites. Sustainability, 16(8), p.3265.
https://doi.org/10.3390/su16083265

Mayenzeke Trueman Mazibuko, Stanley Chibuzor Onwubu, Phumlane Selby Mdluli, Vimla Paul, Mokhena Clement Teboho, Mokhothu Thabang, 2024. Amine-functionalized cellulose-silica composites for the remediation of hexavalent chromium (Cr IV) in contaminated water. Results in Chemistry, 11, p.101796.
https://doi.org/10.1016/j.rechem.2024.101796

Mayenzeke Trueman Mazibuko

……..
Dr T.H. Mokhothu

……
Prof PS Mdluli

……
Dr V Paul

.

Dedication

This work is dedicated to my family, whose unwavering support and encouragement have been my foundation through every challenge and triumph. To my mentors and colleagues, thank you for your guidance and inspiration, which have enriched this journey.

Above all, I dedicate this research to the communities affected by water contamination, hoping that these efforts contribute toward cleaner, safer water and a healthier, sustainable future. May this work inspire further advancements in environmental protection and the well-being of future generations**.**

Acknowledgments

I am deeply grateful to everyone who contributed to the completion of this research. I would like to acknowledge the following individuals.

I would like to express my profound gratitude to my supervisor, Dr. Thabang Hendrica Mokhothu, for his unwavering support, consistent supervision, and invaluable guidance throughout every stage of this project. His enthusiasm for research, critical insights, and commitment to excellence set the tone for producing high-quality work. Dr. Mokhothu's belief in my potential greatly encouraged me, fostering my growth in research methodology, academic report writing, and personal development.

I am especially thankful for his patience and dedication, which ensured that all my academic and project-related requirements were met efficiently, facilitating the timely completion of this work. Furthermore, I deeply appreciate the financial assistance he provided, which played a crucial role in covering travel costs for outsourcing laboratory experiments and attending conferences. His support was instrumental in the success of this research, and for that, I am sincerely grateful.

Dr. Stanley Chibuzor Onwubu: I would like to extend my heartfelt gratitude to him for his invaluable support and mentorship in report writing throughout this research journey. His expertise, constructive feedback, and meticulous attention to detail were instrumental in enhancing the quality of my work. Dr. Onwubu's guidance not only improved the presentation and clarity of my findings but also instilled in me a deeper understanding of effective scientific communication.

I am also sincerely grateful to my co-supervisors, Prof. Phumlane Selby Mdluli and Dr. Vimla Paul, for their invaluable contributions. Their expertise and guidance provided me with a broader perspective on the research and helped refine my approach to the study. Their input was crucial to the success of this work, and I am thankful for the opportunity to learn from them.

I would like to express my sincere gratitude to Dr. Teboho Mokhena for his invaluable guidance and assistance in enhancing my understanding of heavy metal adsorption, particularly in the areas of equilibrium and kinetics studies. His expertise and thoughtful input were crucial in shaping the analytical aspects of this research, ensuring a comprehensive approach to these critical components. Thank you for your unwavering support and contributions to this study.

I am deeply grateful to my family and friends for their constant support and encouragement throughout this journey. To my siblings, your prayers and unwavering belief in me were a source of strength that carried me through challenging moments. Your regular calls, encouragement, and faith in my abilities served as the balm that sustained me and kept me motivated as I worked on this dissertation.

Finally, I also wish to acknowledge the generous support from the National Research Foundation and ESKOM-TESP, whose funding made this research possible. My sincere thanks extend to the Durban University of Technology and MinTek for providing access to their facilities and resources, which were essential for conducting the experiments and analyses required for this study. Thank you all for your vital contributions, which have made this work possible. Your support has been truly indispensable, and I am forever grateful for it.

Abstract

The pressing challenge of heavy metal pollution in water sources demands innovative and sustainable solutions. This project explored recent advancements in heavy metal remediation techniques, focusing on the utilization of cellulose–silica composites and tailored surface modification techniques. The synthesis strategies and properties of cellulose–silica adsorbents highlight their enhanced adsorption capacities and structural robustness for removing heavy metal pollutants from aqueous environments. The study investigated various surface modification approaches, including thiol functionalization, amino acid grafting, and silane coupling agents, for optimizing the surface chemistry and morphology of cellulose–silica composites. Mechanistic insights into the adsorption processes and kinetics of modified adsorbents were studied, along with considerations for optimizing adsorption performance under different environmental conditions.

The adsorption method for hexavalent chromium (Cr (VI) removal from domestic and industrial wastewater is widely desirable due to public health concerns about the heavy metal. The study aimed to investigate the adsorption of Cr (VI) using a novel adsorbent: an amine-functionalized cellulose-silica composite derived from banana pseudo-stem. The in-situ sol-gel method was used to create cellulose-silica silane functionalized composites and analyzed them through different characterization techniques such as attenuated total reflectance-Fourier transform infrared spectroscopy (ATR-FTIR), X-ray diffraction (XRD), thermogravimetric analysis (TGA), Brunauer–Emmett–Teller (BET), Scanning Electron Microscopy (SEM), and transmission electron microscopy (TEM) techniques. ATR-FTIR depicted key organic constituents in raw banana pseudo-stem fibers (BF) and the formation of Si–O bonds in Bleached Cellulose-Silica (BC–SiO_2) composite and further enhanced by the grafting of N-[3-(trimethoxysilyl)propyl]ethylenediamine (DAPTMS) onto the BC-SiO_2 surface in BC-SiO_2-DAPTMS. Functionalization with varying DAPTMS concentrations (2, 4, and 10%) was employed to enhance the composites' adsorption capacity, binding affinity, and thermal stability. Comprehensive characterization using ATR-FTIR, XRD, TGA, BET, SEM, and TEM revealed structural and thermal modifications, with higher DAPTMS concentrations improving adsorption performance.

The modifications of BC with SiO_2 followed by DAPTMS result in the BC-SiO_2-DAPTMS composite, which has reduced crystallinity as shown by XRD and enhanced thermal stability as demonstrated by TGA, while BET analysis showed altered surface area and pore characteristics in BC-SiO_2-DAPTMS (2%). The SEM and TEM imaging provided visual evidence of structural modifications and improved dispersion in BC-SiO_2-DAPTMS composites. The effects of initial Cr (VI) concentration, adsorbent weight dosage, contact time, and pH on the removal efficiency of Cr (VI) using amine-functionalized cellulose–silica composites were also investigated. The results highlighted significant differences in adsorption performance based on the composite formulation and operating conditions. The initial Cr (VI) concentration effect revealed that BC-SiO_2-DAPTMS (4%) consistently achieved the highest removal efficiencies, peaking at 97.14% at 0.3 mg/L. BC-SiO_2-DAPTMS (10%) followed closely, with efficiency stabilizing around 95.53% at higher concentrations. BC-SiO_2-DAPTMS (2%) exhibited lower but improving performance with increasing concentrations. Adsorbent weight dosage experiments demonstrated that increasing weight enhanced removal efficiency, with BC-SiO_2-DAPTMS (10%) achieving optimal performance (95.46%) at 1 g, though benefits plateaued beyond this weight.

The impact of contact time showed BC-SiO_2-DAPTMS (10%) achieving equilibrium after 50 minutes, with a maximum removal efficiency of 91.29%. BC-SiO_2-DAPTMS (4%) exhibited a similar trend, but with a slightly lower maximum efficiency of 84.30%. The pH study indicated that acidic conditions (pH 1–4) were most favourable for Cr (VI) removal, with BC-SiO_2-DAPTMS (10%) reaching the highest removal efficiency (89.27% at pH 3) and maintaining superior performance across all pH levels. Overall, BC-SiO_2-DAPTMS (10%) demonstrated the best performance across all conditions, followed by BC-SiO_2-DAPTMS (4%), underscoring the importance of higher DAPTMS functionalization for enhanced Cr (VI) adsorption. These findings offer valuable insights into optimizing composite design and operational parameters for effective Cr(VI) remediation in contaminated water systems. The kinetic modelling followed the pseudo-second order (PSO) model, while the Freundlich and Langmuir isotherms provided insights into the adsorption mechanisms. The overall results demonstrated that the BC-SiO_2-DAPTMS composites, particularly at 4% and 10% DAPTMS concentrations, are effective, scalable, and sustainable adsorbents for Cr (VI) remediation, offering significant potential for practical water treatment applications. The study offered valuable insights into the development of effective adsorbent materials for sustainable heavy metal remediation applications.

Table of Contents

List of Figures

List of tables

List of Symbols and Abbreviations

$Ag@TiO_2/SiO_2$: silver-imprinted Titania/silica nanospheres

APTES: 3-Aminopropyl)triethoxysilane

APTMS: 3-aminopropyl)trimethoxysilane

AR: Analytical Reagent

ATR-FTIR: Attenuated Total Reflectance - Fourier Transform Infrared Spectroscopy

ATSDR: Agency for Toxic Substances and Disease Registry

α-Fe_2O_3: Hematite (Iron (III) Oxide)

BC: Bleached Cellulose

BC-SiO_2: Bleached Cellulose-Silica Composite

BC-SiO_2-DAPTMS: Bleached Cellulose-Silica- N-[3-(Trimethoxysilyl)propyl]ethylenediamine

BET: Brunauer-Emmett-Teller

BF: Banana stem fibers

C_2H_6O: Ethanol

CA: Cellulose Acetate

CC: Commercial Cellulose

C_{eq}: Equilibrium Concentration in Solution

C_i: Initial Concentration

$Cr(OH)_3$: Chromium Hydroxide

Cr (VI): Hexavalent Chromium

Cr^{3+}: Trivalent Chromium

C_t: Concentration at Time t

Cu (II): Copper ions in the +2-oxidation state

CuKα: Copper K-alpha radiation

DAPTMS: N-[3-(trimethoxysilyl)propyl]ethylenediamine

DPC: Diphenyl carbazide

DTA: Differential Thermal Analysis

DTG: Differential Thermogravimetric Analysis

EDS: Energy Dispersive X-ray Spectrometer

EDX: Energy Dispersive X-ray

HCl: Hydrochloric Acid

HMS: Hydroxy Magnesium Silicate

IARC: International Agency for Research on Cancer

k_1: Rate Constant for Pseudo-First Order Adsorption

k_2: Rate Constant for Pseudo-Second Order Adsorption

$K_2Cr_2O_7$: Potassium Dichromate

K_f: Freundlich Adsorption Capacity Constant

KOH: Potassium Hydroxide

M: Mass

n: Freundlich Adsorption Intensity Constant

NaOCl: Sodium Hypochlorite

NaOH: Sodium Hydroxide

NTP: National Toxicology Program

PCB: Printed Circuit Boards

PCBs: Polychlorinated Biphenyls

Pd (II): Palladium (II) ions

PEO: Polyethylene Oxide

PFO: Pseudo-First Order (kinetic model)

PSO: Pseudo-Second Order (kinetic model)

q_{eq}: Amount of Cr (VI) Adsorbed at Equilibrium

Q_t: Quantity of Cr (VI) Adsorbed per Unit of Adsorbent at Time t

R%: Removal Percentage

rpm: Revolutions Per Minute

SAPS: South African Police Service

SEM: Scanning Electron Microscope

SiO_2: Silica (Silicon Dioxide)

SiO_2@Cel-TEPA: Silica/Cellulose Carrier Particles Functionalized with Tetraethylenepentamine

SPL: Substances Priority List

TEM: Transmission Electron Microscopy

TEOS: Tetraethoxysilane

TGA: Thermogravimetric Analysis

TMOA-Br: Trimethyloctadecylammonium Bromide

TMSPDETA: N-(3-Trimethoxysilylpropyl)diethylenetriamine

V: Volume

WHO: World Health Organization

XRD: X-Ray Diffraction

Chapter One

Introduction

1.1 Background and context of the study

Heavy metals, a varied category of elements with various chemical properties, have become a significant environmental worry because of their toxicity, persistence, and pervasiveness in ecosystems. Characterized by a density greater than water (Ismanto *et al.* 2023) these metals often accumulate as insoluble pollutants, leading to severe ecological and health consequences (Hojjati-Najafabadi *et al.* 2022; Vasileva-Tcankova 2022). Industrial processes, mining, and agriculture are major contributors to their release into the environment, posing serious risks to human health, animal life, and food security. Once heavy metals infiltrate soil and water systems, they are absorbed by plants, reducing agricultural productivity and compromising food safety (Sharma and Agrawal 2005; Wang and Chen 2009). In aquatic environments, the issue is made worse by pollution from automobile emissions, industrial runoff, and atmospheric deposition (Sörme and Lagerkvist 2002).

To combat heavy metal pollution, various techniques have been developed for heavy metal removal from wastewater, ranging from traditional techniques like ion exchange, membrane filtration, chemical precipitation, flotation, and adsorption to more advanced hybrid approaches (Malik, Jain and Yadav 2017). Chemical precipitation is widely favoured for its simplicity and cost-effectiveness, especially at high metal concentrations, but produces large volumes of sludge, complicating disposal and reducing efficiency for trace metals (Leal-Gutiérrez *et al.* 2021). Reverse osmosis, ultrafiltration, and nanofiltration are membrane filtration methods that efficiently remove dissolved metals and solids, though they are energy-intensive and prone to membrane fouling, leading to higher costs (Xiang *et al.* 2022). Ion exchange, often used for metals like chromium and nickel, is efficient but limited in large-scale applications due to high operational costs and resin regeneration requirements (Jasim and Ajjam 2024). Non-conventional methods, like electrochemical treatments (e.g., electrocoagulation and electrooxidation), have shown

potential in removing metals like arsenic and lead, offering high efficiency but requiring complex equipment and significant energy, limiting their use in less developed regions (Yadav *et al.* 2024).

Adsorption with low-cost materials, such as cellulose-silica composites and activated carbon, is gaining traction due to its cost-effectiveness and high removal rates for metals like Cr (VI) and Pb (II). Adsorption efficiency is determined by the adsorbent's surface area and chemical modifications (Alguacil *et al.* 2018). Emerging materials, like electrospun nanofibers and functionalized nanoparticles, offer enhanced capacities for selective heavy metal removal, though challenges like scalability and cost remain (Najafabadi *et al.* 2015). Ion exchange, adsorption, and membrane filtration are the most researched methods, according to a review by Fu and Wang. Adsorption by inexpensive adsorbents is known to be very successful for low-concentration heavy metal wastewater, offering an alternative to activated carbon (Fu and Wang 2011). Lead (Pb), zinc (Zn), mercury (Hg), nickel (Ni), cadmium (Cd), copper (Cu), chromium (Cr), arsenic (As), and Zn are the most common heavy metals. Heavy metals like Cr, Pb, and Cd are notorious pollutants due to their toxicity, persistence in the environment, and potential to bioaccumulate in living organisms (Pohl 2020). The highly hazardous heavy metal hexavalent chromium (Cr (VI)) finds widespread use in sectors like textile dyeing, leather tanning, and metal plating. The International Agency for Research on Cancer (IARC) has categorized it as a Group 1 carcinogen, highlighting its severe health risks, like those posed by cadmium. Additionally, Cr (VI) is designated as a hazardous material by the Agency for Toxic Substances and Disease Registry (ATSDR) (A.T.S.D.R 2022). The World Health Organization (WHO) has set a maximum permissible concentration of 0.05 mg/L for chromium in drinking water, underscoring its toxicity (W.H.O 2017). Furthermore, according to the National Toxicology Program (NTP), Cr (VI) is a known human carcinogen (N.T.P 2016). The acceptable limits for total chromium and Cr (VI) in drinking water in South Africa are 100 and 50 µg/ℓ, respectively (Loock et al., 2014).

Cr (VI) is mostly difficult to remediate because of its high solubility with mobility in water. Traditionally, Cr (VI) ions are eliminated using chemical reagent treatments that convert Cr (VI) to Cr (III) and precipitate it as $Cr(OH)_3$. Modern approaches include membrane separation, ion exchange, and Cr (VI) procedures (Terry 2004; Alvarez-Ayuso and Nugteren 2005; Li, Li and Yang

2016; Sun *et al.* 2017), highlighting developments in technologies for environmental remediation. However, recent developments in removal techniques have resulted in increased effectiveness, with adsorption emerging as a very efficient and cost-effective option. Low-cost adsorbents generated from industrial and agricultural waste have gained popularity due to their environmental and economic benefits. Nevertheless, these materials often show low adsorption efficiency, limiting their overall effectiveness in heavy metal removal (Cretescu, Soreanu and Harja 2015; Komkiene and Baltrenaite 2016; Romero-Cano, Gonzalez-Gutierrez and Baldenegro-Perez 2016). Although promising, the use of cellulose extracted from natural fibers for heavy metal remediation remains relatively underexplored.

Gonzalez-Lopez *et al.* reported an overview of Cr (VI) removal, which was examined by the application of chemically modified polysaccharides, such as cellulose, chitosan, starch, and alginate. Focus on approaches such as functional group grafting, cross-linking, and surface changes to improve adsorption effectiveness. The review emphasized the financial and environmental benefits of mechanisms like chelation, ion exchange, and electrostatic attraction (González-López et al. 2021). Wang and Lee examined the processes involved in the reduction and adsorption of Cr (VI) onto cellulose. Their research highlights cellulose's dual function in both reducing Cr (VI) to trivalent chromium [Cr (III)] and adsorbing the reduced Cr (III). Through a series of batch experiments, they evaluated how factors like pH, temperature, and Cr (VI) concentration affect the reaction. The findings show that cellulose effectively serves as a reducing agent and adsorbent, with optimal reduction occurring in acidic conditions. Initial Cr (VI) concentration and the surface characteristics of cellulose also play important roles in the reaction rate. FTIR and XPS analyses confirm the reduction of Cr (VI) and the attachment of Cr (III) to oxygen-containing functional groups on the cellulose (Wang and Lee 2011).

However, Cellulose contains neutral -OH groups, which are not highly reactive toward anionic species like Cr (VI). It has a limited surface area and lacks specific binding sites, which ultimately decreases its adsorption efficacy. To overcome these limitations, incorporating cellulose with silica nanoparticles has become a promising strategy. Silica provides a high surface area, enhanced porosity, and a suitable platform for further functionalization, such as grafting amine groups,

thereby improving the overall adsorption capacity and selectivity of the composite for efficient heavy metal removal. Utilizing the high surface area of silica and the mechanical strength and biodegradability of cellulose nanofibrils (CNFs) as adsorbents for Cr (III), Agaba *et al.* created silica-cellulose composites by reinforcing precipitated silica agglomerates with CNFs (Agaba et al. 2018). Although unmodified silica nanoparticles have a large surface area and a porous structure, their native surface chemistry, which consists mostly of silanol (Si-OH) groups, lacks the active binding sites required for successful Cr (VI) ion adsorption. To overcome this limitation, surface modification using functional amine groups is required. Among available options, APTMS ((3-aminopropyl)trimethoxysilane) is preferred due to its rapid hydrolysis, strong covalent bonding to silica, and the introduction of primary amine groups that facilitate both electrostatic attraction and redox conversion of Cr (VI) to Cr (III), which exhibits excellent adsorption performance in acidic conditions. Compared to other agents, APTMS offers an optimal combination of surface reactivity, simplicity, and proven effectiveness in environmental remediation applications. This combination of cellulose-silica composites and amine-functionalized silica offers a promising and sustainable solution for heavy metal remediation (Lee *et al.* 2018).

Because of their wide availability, environmental friendliness, and adjustable surface qualities, composite materials, especially those based on cellulose and silica matrices, have demonstrated significant promise in heavy metal adsorption (Gupta *et al.* 2023). To improve cellulose-silica composites' capacity to adsorb heavy metals, amine functionalization has been investigated (Hong *et al.* 2015). Adsorption effectiveness is improved when amine groups are added to the composite surface, because they increase the affinity for metal ions through complexation and ion exchange mechanisms (Bisla, Kawamura and Yoshitake 2022). The production, characterisation, and use of amine-functionalized cellulose-silica composites in heavy metal removal have all been examined in earlier research. Yousif et al., 2019 successfully detected and removed copper (II) ions from contaminated waters using cellulose/silica carrier particles functionalized with tetraethylenepentamine (SiO_2@Cel-TEPA). Even at negligible quantities, the produced SiO_2@Cel-TEPA material demonstrated excellent sensitivity to Cu (II) ions and retained its functionality for recycling and reuse without experiencing appreciable performance loss.

The adsorption capabilities of amino-silanized cellulose membranes for the selective removal of hexavalent chromium ions were also investigated by Jamroz et al. A combination of silica and an amino-functional silane modifier was applied to the surface of cellulose fibers to create novel adsorbents. Three versions were synthesized: cellulose-1N, cellulose-2N, and cellulose-3N, each with a different number of nitrogen atoms in the modifying agent. Cellulose-1N was functionalized with (3-aminopropyl)triethoxysilane (APTES), which contains one nitrogen atom; cellulose-2N with DAPTMS, which contains two nitrogen atoms; and cellulose-3N with N-(3-trimethoxysilylpropyl)diethylenetriamine (TMSPDETA), which contains three nitrogen atoms. They highlighted how surface amine functional groups can improve adsorption efficiency and how the quantity of protonated amino groups on the membrane surface is correlated with the adsorption capacity (Jamroz *et al.* 2019).

Agricultural by-products have drawn interest lately as inexpensive, environmentally friendly adsorbent materials. Banana stem fibers, an abundant agricultural waste, combine eco-friendliness, low density, and cost-effectiveness, making them suitable for large-scale applications. This study addresses a gap in existing research by developing a new cellulose-silica composite with amine functionalization made from Banana stem fibers for Cr (VI) adsorption. The composite was synthesized via the in-situ sol-gel method, using Tetraethoxysilane (TEOS) as the silica precursor, and N-[3-(trimethoxysilyl)propyl]ethylenediamine (DAPTMS) is an amine silane coupling agent. The incorporation of amine groups into the cellulose-silica matrix enhances adsorption efficiency through mechanisms like complexation and ion exchange. The sol-gel process also enables the integration of silica nanoparticles, increasing surface area and functional groups for Cr (VI) binding. The composite's adsorption performance was assessed under various circumstances, such as pH, initial metal concentration, contact time, and adsorbent dosage. Kinetic and equilibrium analyses were performed to optimize the procedure. This research aims to develop a sustainable, efficient, and economical adsorbent for the cleanup of Cr (VI), with broader applications in wastewater treatment and environmental sustainability.

1.2 Research problem

The contamination of ecosystems by heavy metals, particularly Cr (VI), has become a serious environmental and public health issue due to their persistence and bioaccumulation potential (Pohl 2020). Industrial operations such as metal plating, mining, and manufacturing are key contributors to this pollution, which infiltrates water and soil, compromising food safety and biodiversity (Sharma and Agrawal 2005; Wang and Chen 2009). While existing methods like chemical precipitation, ion exchange, and membrane filtration are effective, they come with drawbacks, including high operational costs, energy demands, and challenges related to waste management (Leal-Gutiérrez *et al.* 2021; Xiang *et al.* 2022; Jasim and Ajjam 2024). Adsorption using sustainable, low-cost materials has gained attention as a viable alternative for heavy metal removal (Malik, Jain and Yadav 2017). However, many conventional adsorbents, such as activated carbon, struggle to effectively remove trace levels of metals (Alguacil *et al.* 2018).

Only one fruit is produced by the banana tree. Banana pseudo stems are cut down and left as biomass after banana fruit is harvested, allowing a new tree to grow and yield additional fruit. Although their potential for heavy metal cleanup is still largely unexplored, Banana stem fibers, a plentiful agricultural by-product, offer an economical and environmentally favorable alternative for large-scale applications. Unmodified Banana stem fibers are too dense and compact to allow for high water permeance, with few active sites and low efficiency for Cr (VI) ions. As a result, chemical modification increases reactive sites, surface area, and porosity. Thus, extracted cellulose from banana stem fiber and functionalizing it with silica and amine groups has been shown to significantly increase adsorption capacity, notably for Cr (VI) ions (Lee *et al.* 2018). Research on creating amine-functionalized cellulose-silica composites from Banana stem fibers for heavy metal removal is lacking, despite the serious environmental and health risks posed by heavy metal pollution. By creating a new amine-functionalized cellulose-silica composite from Banana stem fibers and assessing its efficacy in adsorbing Cr (VI), this study aims to fill this gap. The research will explore its performance under different conditions, optimizing its adsorption capacity through equilibrium and kinetic analyses, to provide a sustainable and cost-effective solution for heavy metal remediation.

1.3 Aim

The aim of the study was to synthesize and characterize amine-functionalized cellulose-silica composites for Cr (VI) ion adsorption.

1.4 Objectives

1.4.1 Cellulose extraction from the banana stem:

1. To extract cellulose from agricultural residue by chemical processes.
2. To characterize the extracted cellulose using attenuated total reflectance-Fourier transform infrared spectroscopy (ATR-FTIR), thermogravimetric analysis (TGA), transmission electron microscopy (TEM), scanning electron microscopy (SEM), X-ray diffraction (XRD) to characterize the structure, morphology, thermal stability, and surface properties of the extracted cellulose.

1.4.2 Synthesis of Amine-Functionalized Composites:

1. To prepare cellulose/silica composites functionalized with an amine-based coupling agent by in-situ sol-gel process.
2. To functionalize the synthesized composites with amine groups to enhance their Cr (VI) adsorption capacity. The functionalization process involves introducing varying amounts of the amine-based silane coupling agent to achieve different levels of amine functional groups on the cellulose-silica composite surface. This variation in amine-based silane coupling agent concentrations (2%, 4%, and 10%) is critical for investigating the impact of different functionalization levels on the adsorption capacity and effectiveness of the composite for Cr (VI) ion removal.

1.4.3 Characterization of Composites:

1. To characterize the amine silane-functionalized cellulose-silica composite using TGA, TEM, SEM, XRD, ATR-FTIR, and Brunauer–Emmett–Teller (BET) analysis to characterize the structure, morphology, thermal stability, and surface properties of the synthesized composites.

1.4.4 Optimization of Adsorption Conditions:

1. To investigate the effect of different parameters such as pH, contact time, initial Cr (VI) concentration, and adsorbent dosage on the adsorption performance.
2. To optimize the adsorption conditions to achieve maximum Cr (VI) removal efficiency.

1.4.5 Adsorption Studies:

3. To determine the Cr (VI) ion concentration using UV/Visible spectroscopy for trace levels adsorbed by amine silane-functionalized cellulose-silica composites.
4. To conduct batch adsorption experiments to evaluate the adsorption capacity and kinetics of Cr (VI) removal by the functionalized composites.
5. To apply isotherm models (e.g., Langmuir and Freundlich) to understand the adsorption mechanism and calculate adsorption parameters.

1.5 Rationale, significance, and impact of the study

This research offers significant benefits for environmental sustainability, public health, and the economy, particularly in South Africa. Although South Africa is a water-scarce country with limited rainfall below the global average, the country faces growing challenges in maintaining clean water due to expanding urbanization, industrialization, and agricultural operations (Edokpayi

et al. 2020). The water condition is further exacerbated by the activities of the sectors, which have resulted in increased contamination of water supplies with hazardous heavy metals such as Cr (VI), lead, and cadmium (Pohl 2020). Given the negative impact of heavy metals on the environment and public health (N.T.P 2016; A.T.S.D.R 2022), there is a need for an environmentally sustainable technique that could help remediate these metals from the environment. The development of a Banana stem fiber adsorbent functionalized with silica nanoparticles provides an economical and scalable technique to remove heavy metals from contaminated water. Environmentally, using biodegradable Banana stem fibers saves waste and promotes healthier ecosystems as a resource-efficient alternative to remedial approaches. This is high towards a greener and cleaner environment. In terms of public health, the study improves water treatment efficiency, hence supporting South Africa's objective of universal access to safe water by 2030, which is critical for decreasing health risks in impacted populations.

Economically, it provides a low-cost alternative to pricey treatments, aiding rural and resource-constrained communities while generating value for local banana farmers by reusing agricultural waste. This aligns with the government's objective of universal clean water access by 2030, as defined in the National Development Plan (NDP) 2030, which creates an urgent need for sustainable and inexpensive alternatives (Ojo 2018). Globally, this work serves as an example of sustainable water treatment in developing and water-scarce countries, thereby contributing to larger efforts in water security and sustainable development. Thus, this study directly supports several specific targets under the United Nations Sustainable Development Goal (SDG 6) (Clean Water and Sanitation). It addresses Target 6.3 by improving water quality through pollution reduction and minimizing hazardous chemicals. By creating affordable methods to remove toxic metals like Cr (VI) from contaminated water, this study promotes safer, more sustainable water sources for rural and underserved communities. It also aligns with Target 6.4, enhancing water-use efficiency and helping alleviate water scarcity by providing a sustainable treatment solution that repurposes natural resources, such as agricultural by-products. Furthermore, the research contributes to Target 6.6 by protecting and restoring water-related ecosystems, reducing heavy metal contamination, supporting biodiversity, and conserving essential ecosystems that rely on clean water (UN-Water 2021).

Additionally, this research aligns with SDG 12: Responsible Consumption and Production, by supporting circular economy principles, specifically repurposing agricultural waste (Banana stem fibers) into effective adsorbents for water treatment. Finally, it also supports SDG 3: Good Health and Well-being, by improving public health through the removal of toxic metals from drinking water, reducing exposure to harmful contaminants. This aligns with South Africa's National Development Plan 2030, addressing water quality issues, particularly in rural and resource-limited areas (Jaishankar *et al.* 2014).

Overall, this research has the potential to significantly improve environmental sustainability, public health, and the economy, aligning with worldwide efforts to secure water security and promote sustainable development, particularly in South Africa.

1.6 Delimitation and scope of the study

This study focuses on investigating the potential of cellulose-silica composites for heavy metal remediation, with a particular emphasis on hexavalent chromium [Cr (VI)] removal from aqueous solutions. The scope includes the synthesis, functionalization, and characterization of cellulose-silica composites, specifically amine-functionalized composites, which have shown promise in enhancing adsorption capacity and selectivity. Techniques such as ATR-FTIR, XRD, TGA, BET, SEM, and TEM are utilized for in-depth structural and surface analysis, enabling insights into composite performance in various environmental conditions. The study is confined to laboratory-scale experiments to evaluate the adsorption kinetics, and equilibrium isotherms, aiming to optimize the conditions for effective Cr (VI) remediation. The study's delimitations include excluding adsorption thermodynamics, field applications, or large-scale implementations of the composites and focusing only on Cr (VI) as the primary contaminant of interest. Additionally, while other heavy metals may be relevant in broader environmental contexts, this study limits its scope to Cr (VI) to ensure a detailed examination of adsorption mechanisms and efficacy specific to this contaminant.

1.7 Structure of the thesis

The dissertation is divided into five chapters.

Chapter One: provides an extensive introduction to the study. This directed the chapter toward the aim and objectives, problem statement, research rationale, significance impact, and delimitation and scope of the study.

Chapter Two: presents an overview of the literature on the unlocking heavy metal remediation potential: a review of cellulose–silica composites. This comprehensive review explores recent advancements in heavy metal remediation techniques, focusing on the utilization of cellulose–silica composites and tailored surface modification techniques. To improve the surface chemistry and morphology of cellulose–silica composites, the paper explores several surface modification techniques, such as silane coupling agents, amino acid grafting, and thiol functionalization.

Chapter Three: Is presented in an article format and focuses on the amine-functionalized cellulose-silica composites for the remediation of hexavalent chromium [Cr (VI)] in contaminated water. This section investigates the assessment of Cr (VI) adsorption with a new adsorbent: a Banana stem fiber-based cellulose-silica composite functionalized with an amine.

Chapter Four: This chapter presents the manuscript submitted for peer review that explores the efficacy of varying concentrations of N-[3-(trimethoxysilyl)propyl]ethylenediamine (DAPTMS) modified bleached cellulose-silica (BC-SiO_2) composites for the removal of Cr (VI) from wastewater. The study evaluates the influence of DAPTMS concentrations (4% and 10%) on the structural, physicochemical properties, and adsorption performance of the composites.

Chapter Five: serves as the final chapter, summarizes the key conclusions derived from the study, highlighting the main findings and their implications. It also discusses the limitations encountered during the research and provides recommendations for future studies.

1.8 References

A.T.S.D.R. 2022. The ATSDR 2022 Substance Priority List. Available: https://www.atsdr.cdc.gov/spl/#2019spl (Accessed on 3 May 2020)

Abdelkhalek, A., Ali, S. S., Sheng, Z., Zheng, L. and Hasanin, M. 2022. Lead Removal from Aqueous Solution by Green Solid Film Based on Cellulosic Fiber Extracted from Banana Tree Doped in Polyacrylamide. Fibers and Polymers, 23 (5): 1171-1181.

Abdel-Khalek, A. A., Hamed, A. and Hasheesh, W. S. 2021. Does the adsorbent capacity of orange and banana peels toward silver nanoparticles improve the biochemical status of Oreochromis niloticus? Environmental Science and Pollution Research, 28: 33445-33460.

Agaba, A., Cheng, H., Zhao, J., Zhang, C., Tebyetekerwa, M., Rong, L., Sui, X. and Wang, B. 2018. Precipitated silica agglomerates reinforced with cellulose nanofibrils as adsorbents for heavy metals. RSC advances, 8 (58): 33129-33137.

Alguacil, F. J., Alcaraz, L., García-Díaz, I. and López, F. A. 2018. Removal of Pb2+ in wastewater via adsorption onto an activated carbon produced from winemaking waste. Metals, 8 (9): 697.

Alvarez-Ayuso, E. and Nugteren, H. 2005. Purification of chromium (VI) finishing wastewaters using calcined and uncalcined Mg-Al-CO3-hydrotalcite. Water Research, 39 (12): 2535-2542.

Bisla, V., Kawamura, I. and Yoshitake, H. 2022. Cross-linked cellulose acetate aminosilane (CAAS) for aqueous arsenic (V) adsorption. Carbohydrate Polymer Technologies and Applications, 4: 100259.

Edokpayi, J. N., Enitan-Folami, A. M., Adeeyo, A. O., Durowoju, O. S., Jegede, A. O. and Odiyo, J. O. 2020. Recent trends and national policies for water provision and wastewater treatment in South Africa. In: Water conservation and wastewater treatment in BRICS nations. Elsevier, 187-211.

Fu, F. and Wang, Q. 2011. Removal of heavy metal ions from wastewaters: a review. Journal of Environmental Management, 92 (3): 407-418.

González-López, M. E., Laureano-Anzaldo, C. M., Pérez-Fonseca, A. A., Arellano, M. and Robledo-Ortíz, J. R. 2021. Chemically modified polysaccharides for hexavalent chromium adsorption. Separation & Purification Reviews, 50 (4): 333-362.

Gupta, A. D., Kirti, N., Katiyar, P. and Singh, H. 2023. A critical review on three-dimensional cellulose-based aerogels: synthesis, physico-chemical characterizations and applications as adsorbents for heavy metals removal from water. Cellulose, 30 (6): 3397-3427.

Hojjati-Najafabadi, A., Mansoorianfar, M., Liang, T., Shahin, K. and Karimi-Maleh, H. 2022. A review on magnetic sensors for monitoring of hazardous pollutants in water resources. Science of the Total Environment, 824: 153844.

Hong, G.-W., Ramesh, S., Kim, J.-H., Kim, H.-J. and Lee, H.-S. 2015. Synthesis and properties of cellulose-functionalized POSS-SiO_2/TiO_2 hybrid composites. Journal of Nanoscience and Nanotechnology, 15 (10): 8048-8054.

Ismanto, A., Hadibarata, T., Widada, S., Indrayanti, E., Ismunarti, D. H., Safinatunnajah, N., Kusumastuti, W., Dwiningsih, Y. and Alkahtani, J. 2023. Groundwater contamination status in Malaysia: level of heavy metal, source, health impact, and remediation technologies. Bioprocess and Biosystems Engineering, 46 (3): 467-482.

Jaishankar, M., Tseten, T., Anbalagan, N., Mathew, B. B. and Beeregowda, K. N. 2014. Toxicity, mechanism and health effects of some heavy metals. Interdisciplinary toxicology, 7 (2): 60-72.

Jamroz, E., Kocot, K., Zawisza, B., Talik, E., Gagor, A. and Sitko, R. 2019. A green analytical method for ultratrace determination of hexavalent chromium ions based on micro-solid phase extraction using amino-silanized cellulose membranes. Microchemical Journal, 149: 104060.

Jasim, A. Q. and Ajjam, S. K. 2024. Removal of heavy metal ions from wastewater using ion exchange resin in a batch process with kinetic isotherm. South African Journal of Chemical Engineering, 49: 43-54.

Komkiene, J. and Baltrenaite, E. 2016. Biochar as adsorbent for removal of heavy metal ions [Cadmium (II), Copper (II), Lead (II), Zinc (II)] from aqueous phase. International Journal of Environmental Science and Technology, 13: 471-482.

Leal-Gutiérrez, M. J., Cuéllar-Briseño, R., Castillo-Garduño, A. M., Bernal-González, M., Chávez-Castellanos, Á. E., Solís-Fuentes, J. A., Durán-Domínguez-de-Bazúa, M.-d.-C. and Bazúa-Rueda, E. R. 2021. Precipitation of heavy metal ions (Cu, Fe, Zn, and Pb) from mining flotation effluents using a laboratory-scale upflow anaerobic sludge blanket reactor. Water, Air, & Soil Pollution, 232 (5): 197.

Lee, J., Kim, J.-H., Choi, K., Kim, H.-G., Park, J.-A., Cho, S.-H., Hong, S. W., Lee, J.-H., Lee, J. H. and Lee, S. 2018. Investigation of the mechanism of chromium removal in (3-aminopropyl) trimethoxysilane functionalized mesoporous silica. Scientific reports, 8 (1): 12078.

Li, L., Li, Y. and Yang, C. 2016. Chemical filtration of Cr (VI) with electrospun chitosan nanofiber membranes. Carbohydrate polymers, 140: 299-307.

Loock, M., Beukes, J. and Van Zyl, P. 2014. A survey of Cr (VI) contamination of surface water in the proximity of ferrochromium smelters in South Africa. Water SA, 40 (4): 709-716.

Malik, D., Jain, C. and Yadav, A. K. 2017. Removal of heavy metals from emerging cellulosic low-cost adsorbents: a review. Applied Water Science, 7: 2113-2136.

Mokhothu, T., Luyt, A., Morselli, D., Bondioli, F. and Messori, M. 2015. Influence of in situ-generated silica nanoparticles on EPDM morphology, thermal, thermomechanical, and mechanical properties. Polymer Composites, 36 (5): 825-833.

N.T.P. 2016. Report on Carcinogens, fourteenth edition, Department of Health and Human Services Available: https://ntp.niehs.nih.gov/go/roc14 (Accessed 10 February 2024)

Najafabadi, H. H., Irani, M., Rad, L. R., Sojoudi, A. and Haririan, I. 2015. Removal of Cu^{2+}, Pb^{2+}, and Cr^{6+} from aqueous solutions using a chitosan/graphene oxide composite nanofibrous adsorbent. RSC advances, 5 (21): 16532-16539.

Ojo, T. A. 2018. Water access challenges and coping strategies in informal settlements: The case of Iscor settlement in Pretoria West. Unpublished doctoral dissertation, University of South Africa, Pretoria.

Pohl, A. 2020. Removal of heavy metal ions from water and wastewater by sulfur-containing precipitation agents. Water, Air, & Soil Pollution, 231 (10): 503.

Prasad, S., Yadav, K. K., Kumar, S., Gupta, N., Cabral-Pinto, M. M., Rezania, S., Radwan, N. and Alam, J. 2021. Chromium contamination and effect on environmental health and its remediation: A sustainable approach. Journal of Environmental Management, 285: 112174.

Romero-Cano, L. A., Gonzalez-Gutierrez, L. V. and Baldenegro-Perez, L. A. 2016. Biosorbents prepared from orange peels using Instant Controlled Pressure Drop for Cu (II) and phenol removal. Industrial Crops and Products, 84: 344-349.

Romero-Cano, L. A., Gonzalez-Gutierrez, L. V. and Baldenegro-Perez, L. A. 2016. Biosorbents prepared from orange peels using Instant Controlled Pressure Drop for Cu (II) and phenol removal. Industrial Crops and Products, 84: 344-349.

Sarin, V., Singh, T. S. and Pant, K. 2006. Thermodynamic and breakthrough column studies for the selective sorption of chromium from industrial effluent on activated eucalyptus bark. Bioresource Technology, 97 (16): 1986-1993.

Sharma, R. K. and Agrawal, M. 2005. Biological effects of heavy metals: an overview. Journal of Environmental Biology, 26 (2): 301-313.

Sörme, L. and Lagerkvist, R. 2002. Sources of heavy metals in urban wastewater in Stockholm. Science of the Total Environment, 298 (1-3): 131-145.

Sun, J., Zhang, Z., Ji, J., Dou, M. and Wang, F. 2017. Removal of Cr6+ from wastewater via adsorption with high-specific-surface-area nitrogen-doped hierarchical porous carbon derived from silkworm cocoon. Applied Surface Science, 405: 372-379.

Terry, P. A. 2004. Characterization of Cr ion exchange with hydrotalcite. Chemosphere, 57 (7): 541-546.

UN-Water. 2021. Sustainable Development Goal 6: Synthesis Report on Water and Sanitation. Available: https://www.unwater.org (Accessed 29 October 2024)

Vasileva-Tcankova, R. S. 2022. Global Ecological Problems of Modern Society. Acta Scientifica Naturalis, 9 (2): 63-86.

W.H.O. 2017. Guidelines for drinking-water quality. Available: https://www.who.int/publications/i/item/9789241549950 (Accessed 12 November 2022)

Wang, J. and Chen, C. 2009. Biosorbents for heavy metals removal and their future. Biotechnology advances, 27 (2): 195-226.

Wang, S.-L. and Lee, J.F. 2011. Reaction mechanism of hexavalent chromium with cellulose. Chemical Engineering Journal, 174 (1): 289-295.

Xiang, H., Min, X., Tang, C.-J., Sillanpää, M. and Zhao, F. 2022. Recent advances in membrane filtration for heavy metal removal from wastewater: A mini review. Journal of Water Process Engineering, 49: 103023.

Yadav, P., Singh, R. P., Singh, G., Verma, H., Singh, S. K., Dahiya, P. and Kumar, A. 2024. Contamination removal from wastewater using electrochemical approaches. In: Advances in Chemical Pollution, Environmental Management and Protection. Elsevier, 261-273.

Yousif, A. M., Zaid, O. F., El-Said, W. A., Elshehy, E. A. and Ibrahim, I. A. 2019. Silica Nanospheres-Coated Nanofibrillated Cellulose for Removal and Detection of Copper (II) Ions in Aqueous Solutions. Industrial & Engineering Chemistry Research, 58 (12): 4828-4837.

Chapter Two

Unlocking Heavy Metal Remediation Potential: A Review of Cellulose–Silica Composites

This chapter has been published as:

Mayenzeke Trueman Mazibuko, Stanley Chibuzor Onwubu, Mokhothu Thabang Hendrica, Vimla Paul and Phumlane Selby Mdluli, 2024. Unlocking Heavy Metal Remediation Potential: A Review of Cellulose–Silica Composites. Sustainability, 16(8), p.3265. https://doi.org/10.3390/su16083265

2.1 Abstract

This comprehensive review explores recent advancements in heavy metal remediation techniques, focusing on the utilization of cellulose–silica composites and tailored surface modification techniques. We examine the synthesis strategies and properties of cellulose–silica adsorbents, highlighting their enhanced adsorption capacities and structural robustness for removing heavy metal pollutants from aqueous environments. The review investigates various surface modification approaches, including thiol functionalization, amino acid grafting, and silane coupling agents, for optimizing the surface chemistry and morphology of cellulose–silica composites. Mechanistic insights into the adsorption processes and kinetics of modified adsorbents are discussed, along with considerations for optimizing adsorption performance under different environmental conditions. This review provides valuable perspectives on the development of effective adsorbent materials for sustainable heavy metal remediation applications.

Keywords: heavy metal remediation; cellulose–silica composites; surface modification; adsorption kinetics; environmental sustainability; surface chemistry

2.2 Introduction

The term “heavy metals” encompasses a diverse group of elements with varied chemical compositions and significant biological roles. According to (Ismanto *et al.* 2023), heavy metals are defined as metallic compounds with a relative density higher than water. Heavy metal ions often

manifest as insoluble, poisonous, biohazardous, and persistent pollutants. These contaminants pose serious threats to human health, animal welfare, and ecosystem integrity, necessitating urgent remediation efforts. Moreover, the unchecked discharge of heavy metal ions into water bodies, stemming from industrial activities, mining operations, and agricultural practices, has led to widespread environmental degradation (Hojjati-Najafabadi *et al.* 2022; Vasileva-Tcankova 2022). Soil and plants, in particular, accumulate heavy metals, compromising agricultural productivity and food safety (Sharma and Agrawal 2005; Wang and Chen 2009). Furthermore, heavy metal contamination in water sources, including sewage and stormwater, originates from diverse sources such as industrial runoff, vehicular emissions, and atmospheric deposition (Sörme and Lagerkvist 2002). To mitigate the adverse impacts of heavy metal pollution, effective remediation strategies are urgently needed. There are many techniques used today to treat wastewater. A few common techniques for cleaning wastewater include precipitation, neutralization, membrane filtration, ion exchange, flotation, and adsorption. Additionally, technologies for treatment have been developed that integrate physical and chemical processes, such as the electrochemical process (Malik, Jain and Yadav 2017). These are further elaborated below:

2.2.1 Chemical Precipitation

Chemical precipitation is a popular and cost-effective technique for removing heavy metals from wastewater due to its simplicity. This method involves adding chemicals to the wastewater to produce an insoluble precipitate. Variations such as heavy metal chelating precipitation, hydroxide precipitation, and sulphide precipitation are commonly used. Lime and limestone are frequently employed as precipitant agents due to their convenience and efficiency in treating inorganic effluents. However, challenges such as excessive chemical usage, sludge disposal, and overproduction of sludge need to be addressed (Wang *et al.* 2005).

2.2.2 Ion Exchange

Ion exchange relies on the ability of wastewater to exchange cations for metals. Various materials, both natural (such as alumina, carbon, and silicates) and man-made (like zeolites and resins), are

used in this process. Zeolites are particularly common in ion exchange due to their effectiveness in aqueous media. However, ion exchange lacks selectivity and is highly sensitive to pH variations (Nasef and Ujang 2012).

2.2.3 Membrane Process

Membrane filtration techniques, including ultrafiltration (Gao *et al.* 2011), nanofiltration (Mohammad *et al.* 2015), reverse osmosis (Joo and Tansel 2015), and electrodialysis (Mei and Tang 2018), are used to filter out heavy metals from aqueous solutions. Each variation targets specific contaminants, such as oils, suspended particles, and heavy metals. These processes are effective but may require high-energy inputs and maintenance costs (Van der Bruggen *et al.* 2003).

2.2.4 Flotation

Large-scale flotation is a method for removing toxic metal ions from wastewater. Additional flotation techniques include precipitate flotation, dissolved air flotation (DAF), and ion flotation. DAF is used more frequently for removing heavy metals from aqueous solutions as compared to other flotation techniques (Gharai and Venugopal 2016).

2.2.5 Coagulation Process

The coagulation process is used to produce colloids. Coagulating substances like aluminium, ferrous sulphate, and ferric chloride are used to neutralize contaminants in wastewater or water. Many researchers have shown that it is an important technique. Polyaluminum chloride (PAC) and ferric chloride solution are used as coagulants to remove heavy metals (Jiang 2015).

2.2.6 Electrochemical Process

In electrochemical processes, metal is removed from an electrolyte solution while being influenced by an external direct current. The coagulation process weakens colloidal particles and triggers the

sedimentation process by adding a coagulant. An increase in the rate of coagulation requires the flocculation process, which quickens the conversion of weak particles into bulky floccules (Radjenovic and Sedlak 2015).

2.2.7 Adsorption Process

Adsorption is a reasonably affordable, useful, and simple technology. It has excellent metal removal efficiency and is utilized as a quick method for treating different types of wastewaters. According to reports, adsorption is the most popular technique for removing various contaminants, particularly metal ions (Mubarak *et al.* 2021; Solyman and Ahmed 2022). This is likely due to adsorption's high efficacy, ease of use, lack of waste production, and low cost. This technique is gaining acceptance due to the possibility of recovering the metal and reusing the adsorbent (Worch 2012). Adsorption is a cost-effective method for efficiently removing heavy metals from wastewater by binding metal ions to solid surfaces. While activated carbon (AC) remains a popular adsorbent due to its high surface area and microporous structure (Bhatnagar *et al.* 2013). There is increasing interest in low-cost bio-absorbents (Sharma, Sofi and Wani 2018). Low-cost bio-absorbents, including agricultural waste materials and bio-adsorbents like microbial biomass, have gained attention due to their affordability and effectiveness in metal removal (Dong and Ge 2019; Zhao and Liu 2019). These bio-absorbents, derived from agricultural waste materials, industrial by-products, and natural waste materials, offer affordability and effectiveness in metal removal but typically exhibit low efficiency (Rana, Bandyopadhyay and Maiti 2022). This is because their density may limit water permeability and the efficiency of heavy metal removal. Therefore, chemical modification of cellulose with silica enhances adsorption and desorption performance due to silica's porous structure, high surface area, and surface chemistry.

2.2.8 Cellulose–Silica Composites

Among the various adsorption techniques, cellulose and silica-based materials have emerged as promising adsorbents for heavy metal removal (Gupta *et al.* 2023). Cellulose, a polysaccharide found in plant cell walls, offers excellent sorption capacity and biocompatibility. It comprises

glucose units that are joined-(1,4) together to make up a long linear polysaccharide with a molecular formula of $(C_5H_8O_4)_m$ (Figure 2.1). Materials with a high cellulose content include plant fibers, woods, stalks, stems, shells, straw, grasses, etc. (Carpenter, de Lannoy and Wiesner 2015). Cellulose is a substance of interest for a variety of applications because of its amazing physicochemical characteristics, which include colourlessness, a lack of odour or taste, great mechanical strength, superior sorption capacity, hydrophilicity, and biocompatibility. Because of its low density and reactive surface with OH side groups, cellulose can graft chemical species onto its surface. Silica, on the other hand, offers chemical stability, surface reactivity, and the ability to modify surface properties.

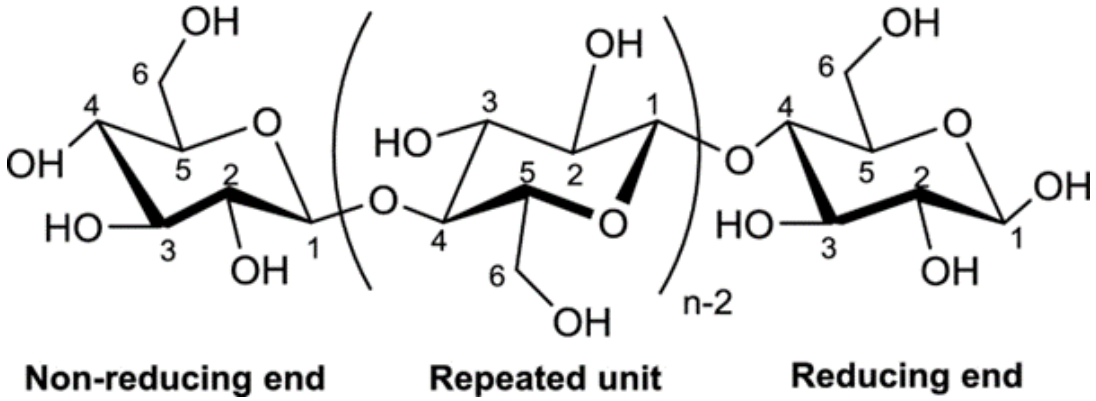

Figure 2.1 The structure of cellulose (Carpenter, de Lannoy and Wiesner 2015).

When coupled with silica and different functional groups, these composites exhibit enhanced adsorption capacity and selectivity for heavy metals. While the understanding of heavy metal contaminants and their environmental implications has been extensively studied and reviewed in the scientific literature, previous reviews have often overlooked the potential synergistic effects of coupling cellulose and silica with different functional groups to enhance adsorption capacity and selectivity. While previous reviews have touched upon individual aspects of heavy metal remediation potential, there are notable gaps in the overall understanding of the field. For instance, while some reviews have examined the sources and environmental impacts of heavy metals (Hojjati-Najafabadi *et al.* 2022; Vasileva-Tcankova 2022), others have delved into the mechanisms of heavy metal adsorption by various materials (Sachan, Ramesh and Das 2021). Additionally, many reviews have failed to systematically compare the adsorption capacities and efficiency of

different adsorbents, hindering the identification of optimal materials for real-world applications. Despite these efforts, there remains a need for a comprehensive review that synthesizes the latest advancements in heavy metal adsorption using cellulose and silica coupling agents, addressing the limitations of previous reviews and offering new insights into the field.

2.2.9 Purpose of the Review

This paper comprehensively reviews recent advancements in the field of heavy metal adsorption using cellulose and silica coupling agents. By synthesizing findings from a wide range of studies, we offer new insights into the potential applications of these materials for environmental remediation. Moreover, we systematically compare the adsorption capacities and efficiency of different cellulose and silica-based adsorbents, enabling researchers to identify the most promising materials for further investigation. Overall, our review aims to bridge the gap between theory and practice, offering practical guidance for researchers and policymakers working in the field of heavy metal remediation. The objectives of this review, therefore, include:

To review recent advancements in heavy metal adsorption using cellulose and silica coupling agents.

To compare the adsorption capacities and efficiency of different cellulose and silica-based adsorbents reported in recent literature.

To identify key research gaps and propose directions for future research in the field of heavy metal remediation.

2.3 Literature Review

This section provides a concise and precise description of the relevant literature on recent advancements in heavy metal remediation techniques, focusing on the utilization of cellulose–silica composites and tailored surface modification techniques.

The information in this study was sourced from published books and literature downloaded from websites and online journal hubs, including Google Scholar, PubMed, Science Direct, SciFinder, and Scopus. Appropriate keywords such as “heavy metal adsorption”, “cellulose”, “silica”, “coupling agents”, “removal efficiency”, and “adsorbent capacity” were used to narrow down the search results. These included studies published in the English language within the last five years to ensure relevance and currency of information. In addition, the included articles focus on the adsorption of heavy metals (e.g., Pb, Cd, Cu, Zn) using cellulose and silica-based adsorbents. Also, extracted relevant data from selected articles, including the type of adsorbent (cellulose, silica, or their coupling agents), heavy metal ions studied, adsorption capacity (in mg/g or percentage removal), experimental conditions (pH, temperature, contact time), and key findings into EndNote software (version 21). Thereafter, the extracted data were analyzed to identify trends, patterns, and discrepancies in the adsorption capacities of cellulose, silica, and their coupling agents for different heavy metal ions.

2.3.1 Natural Fiber

The effects of toxic heavy metals on the environment and human health are a big problem. The continued decrease in water quality and the degree of contamination have been noted by scientists, who are concerned about them. Many methods for removing heavy metals from water and waste have recently undergone extensive research. Because non-renewable resources are used, and costs are high, heavy metal removal and remediation are provided at a high price by current technology. A variety of materials have frequently been employed as adsorbents, and many researchers are now utilizing adsorption techniques for this purpose. Due to its many advantages, such as stability, usability, low cost, simplicity of use, and performance, adsorption has proven to be a viable method

for purification (Ince and Ince 2017). Adsorption technology employs a range of inexpensive adsorbent materials, including metal oxides, biosorbents, clays, activated carbons, and zeolites, to drastically lower the concentrations of heavy metal ions. Because it depends on so many variables, the process of metal adsorption onto adsorbent material, especially on agricultural wastes, is extremely intricate. The phases of complexation, chemisorption, and adsorption–complexation on pores and surfaces, microprecipitation, and ion exchange are all included in this process. Metal ions from water are attached to certain functional groups, including amido, hydroxy, carboxyl, and sulphydryl, when biological materials are employed in the adsorption process (Kalia, Kaith and Kaur 2009; Ince and Ince 2017).

Due to their low density, high strength/weight ratio, and reduction, natural fibers are vital lightweight composite and reinforcement materials. The microstructure and chemical composition of fibers, with the fiber cross-sectional area having the largest degree of change, affect the mechanical properties of fibers. Natural fibers have hydrophilic properties because they include hemicellulose, which makes them easily absorb water. As a result, they are less suited to a matrix with hydrophobic characteristics (Kalia, Kaith and Kaur 2009). Higher cellulose concentration and crystallinity frequently result in better fiber strength, whereas lignin has the reverse effect. Additionally, variations in fiber anatomical qualities between and within species have an impact on the density and mechanical characteristics of fibers.

Natural-fiber-reinforced composites have gained popularity recently because of their low weight, non-abrasive, flammable, non-toxic, affordable, and biodegradable qualities. Of the various natural fibers, the fibers from flax, bamboo, sisal, hemp, ramie, jute, and wood are especially important (Kalia, Kaith and Kaur 2009). The advancement and increase in industrial alternatives can be attributed to the study of replacing synthetic fiber in fiber-reinforced composites with natural fibers. Natural fibers have the benefits of being inexpensive, biodegradable, and low in density. However, due to their relatively high moisture sorption and low matrix compatibility, natural fibers in composites are primarily disadvantageous. As a result, chemical treatments are taken into consideration to change the fiber surface's properties (Li, Tabil and Panigrahi 2007).

Lignocellulosic natural fibers, such as kenaf, sisal, coir, jute, ramie, and pineapple leaf (PALF), have the potential to replace glass or other conventional reinforcing components in composites. Many qualities of these fibers make them a desirable substitute for conventional materials. They have high properties like modulus and are rigid, impact-resistant, and flexible. They are also widely accessible, renewable, and biodegradable. Additional desirable characteristics include affordability, low density, decreased equipment abrasion, reduced skin and respiratory irritation, vibration damping, and enhanced energy recovery (Sgriccia, Hawley and Misra 2008).

2.3.1.1 Natural Fiber and Heavy Metal Adsorption Capacity

The adsorption of heavy metals from wastewater has been performed using a variety of natural plant fibers. Natural plant fibers are composed primarily of cellulose, a few extractives, and amorphous polymers (hemicelluloses and lignin). Agricultural waste (cellulosic and non-wood) from crops generates a lot of waste after processing. Waste frequently contains a lot of cellulose. As a result, heavy metal adsorbents made from agricultural waste are increasingly being used in research and development. Agricultural by-products are frequently utilized for adsorption, either modified or unmodified. The adsorption of heavy metal ions from contaminated water has been successfully applied using banana, orange, and lemon peels, rice husk, rice straw, peanut shell, bran, and sugar cane bagasse (García Raurich, Martínez Roldán and Monagas Asensio 2020; Huzaisham *et al.* 2020; Šabanović *et al.* 2020).

Because of hazardous heavy metals, environmental pollution is a major issue in many densely inhabited areas of the world. The health of people is negatively impacted by the household and industrial pollutants that lead to various environmental issues. Before disposing of aqueous waste in the environment, some metals from industrial discharges must be removed. To evaluate the effectiveness of uptakes, a monitor was used to compare the adsorption of zinc (Zn (II)) and lead (Pb (II)) ions on Banana stem fibers. The fiber in the banana stem was extracted mechanically and then treated with an alkali (NaOH) to make it softer. Parallel-laid webs were used to create needle-punched fabrics. When heavy-phase adsorption was initially studied in its foundational forms, the findings demonstrated that the concentration of heavy metals, the amount of adsorbent utilized,

and pH levels all had a substantial impact on the adsorption capacity of Banana stem fibers. Banana stem fibers removed 98% of zinc and 95.5% of lead with remarkable efficiency in batch trials. The findings indicated that the ideal pH range was found to be between 6.5 and 7.0, and that the equilibrium time for adsorption was 60 min (Ariharasudhan *et al.* 2022a).

The optimization of several variables has been a major problem in wastewater treatment plants to reach the appropriate limits on effluent discharge. Banana peels were used in the optimization study Afolabi et al. conducted in 2021 to assess the removal of lead (II) from wastewater. Using batch adsorption tests, the central composite design was used to investigate the interactive effects of the operating parameters (initial concentration, solution pH, adsorbent dosage, and particle size). The response surface design yielded the greatest results, with a removal percentage of 98.146%, at an initial concentration of 100 mg/L, pH of 5, adsorbent dosage of 0.55 g, and particle size of 75 μm.

In a comparable investigation, (Cheah, Yue and Ting 2021) discovered that heat and chemical preparation of banana peels, aside from acid pre-treatment, improved metal removal efficacy. The study found that pre-treatment can improve the removal of metal by banana peels; chemical pre-treatment was shown to be more successful than heat treatment, and detergent was found to be a practical and useful pre-treatment agent. (Bhagat, Gedam and Pathak 2020) examined the effectiveness of banana peel strip (BP) in eliminating copper and zinc ions from water. A cheap source of biomass generated from agricultural waste, BP demonstrated good adsorption capabilities when absorbing Cu^{2+} and Zn (II) from wastewater effluent.

One study investigated the capacity of Banana stem fiber needle-felted fabric to absorb heavy metal ions (Pb (II) and Zn (II)) across various conditions, including pH, contact duration, and concentration. Results revealed that the uptake of Pb (II) and Zn (II) varied depending on the initial solution's pH, the amount of adsorbent used, contact duration, and concentration. Higher pH, concentration, and contact duration correlated with increased absorption of Pb (II) and Zn (II) ions (measured in mg/g). Notably, lead and zinc exhibited significant absorption at pH 7 irrespective of time or concentration, while deviations from this pH level resulted in lower absorption rates,

attributed to the use of chemicals (NaOH, HCl) to alter the solution's pH. Batch tests demonstrated that Banana stem fibers effectively removed 95.5% of lead and 98% of zinc.

Heavy metal ion contamination of freshwater sources represents a serious risk to the safety of drinking water. Therefore, it is essential to treat water to remove specific contaminants, such as copper ions. Adsorbents or continuous membrane/filter procedures are frequently used to do this. For example, alternative combinations of these processes that could be applied as a treatment in this case include adsorption or ion-exchange membranes/filters. As a result, environmentally friendly alternatives to traditional adsorption membrane/filter materials include those made from renewable resources. For instance, filters made of natural fibers and nanocellulose were coated with (2,2,6,6-Tetramethylpiperidin-1-yl)oxy (TEMPO) and made from flax and agave fibers, as well as other kinds of CNF. Although it has been demonstrated that anionic TEMPO-oxidized cellulose nanofibrils (TCNF) have a considerable affinity for heavy metal ions, their usage in nanopaper membranes is limited by their low permeability. Additionally, pure nanopapers have not yet been employed to effectively and efficiently adsorb metal ions (Mautner *et al.* 2019) (See Figure 2.2).

Pure nanopapers have yet to be used successfully to adsorb metal ions with great permeance and efficiency. The permeance and copper adsorption capacity of these filters were used to evaluate how well they performed. This novel kind of filter made from industrial crop residue was demonstrated to have extremely high permeances, which allowed it to adsorb large amounts of Cu^{2+} ions during a continuous filtration process. For the active adsorption agent TEMPO-CNF, this translates to an adsorption capacity of more than 60 mg/g.

Due to the presence of hydroxyl functional groups, cellulosic biomaterials have strong adsorption potential. Banana stem fibers and other lignocellulosic fibers are made of cellulose, hemicellulose, lignin, pectin, wax, and water-soluble components. This fiber is readily available and easy to produce, which is an appealing quality that makes it an appropriate substitute for synthetic fibers that might be dangerous (Barreto *et al.* 2010). Sheng *et al.* (2018) modified banana pseudo-stem fiber using cellulose xanthogenation and steam explosion techniques to improve the capacity of

the fiber to absorb heavy metal ions Pb (II) and Cd (II). Steam explosion Banana stem fibers cellulose xanthogenate's (SEBF-CX) adsorption kinetics fit in with the pseudo-second order model. Pb (II) and Cd (II) adsorption in the pseudo-second order model, however, were 99.0099 and 67.3401 mg/g, respectively. Compared to raw Banana stem fibers (RBF), the metal ion adsorption capacities of SEBF-CX and SEBF were higher. The three fibers tested, among them SEBF-CX, were the best and might be employed as an effective absorbent to remove heavy metal ions from contaminated water.

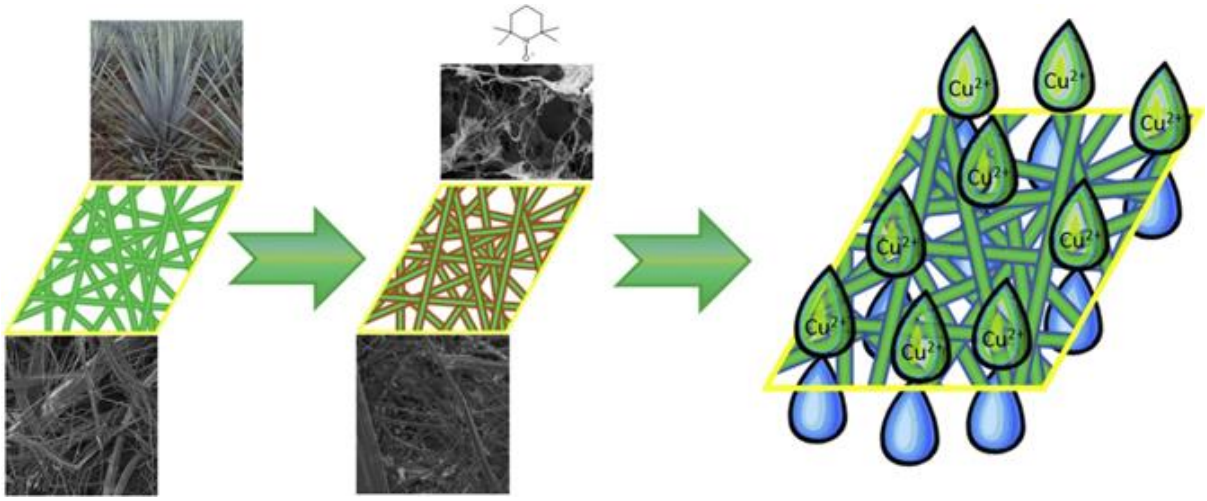

Figure 2.2 Natural fiber–nanocellulose composite filters for the removal of heavy metal ions from water (Mautner *et al.* 2019).

Furthermore, (Selambakkannu *et al.* 2018) created a bio-adsorbent derived from banana trunk fibers, modified synthetically for potential application in heavy metal adsorption from wastewater (See Figure 2.3). Initially, the fiber underwent grafting with a glycidyl methacrylate (GMA) polymer via electron beam irradiation. Subsequently, the GMA-grafted fiber was functionalized with an imidazole (IMI) group through an epoxide ring-opening process, yielding an amine density of 2.00 mmol/g.

The effective removal of metal ions from the aqueous solutions was carried out by the IMI functional group. This comprehensive kinetic and mechanistic study employs IMI-functionalized GMA-grafted Banana stem fibers to remove metal ions (Cu^{2+}, Pb (II), and Zn (II)) via adsorptive

removal. The saturation of the adsorbent, however, caused the removal % to decline as the initial metal ion concentration rose. The adsorption capacities for the metal ions Cu^{2+}, Pb (II), and Zn (II) were 71.6, 84.2, and 60.1 mg/g, respectively, using IMI-GMA-grafted fiber. On real sewage water that had been collected from a nearby household area, IMI-functionalized GMA-grafted fibers were tested as a metal ion adsorbent. Within one hour of contact time, a 100% removal of the target metal ions was accomplished. This test demonstrated that bio-sorbent made from fodder crops, in this case the banana trunk, may be adapted and used as a cost-efficient treatment for threatening environmental issues.

Polypropylene is also used because of its importance in producing strong composite materials for a variety of applications. The chitosan biopolymer is composed of several amino and hydroxyl groups and efficiently removes Cd ions from wastewater. For the adsorptive removal of cadmium (Cd) ions from wastewater, (Alaswad *et al.* 2020) prepared polypropylene (PP)/sisal fiber (SF)/Banana stem fibers (BF), and chitosan-based hybrid chitosan (CS/SF/BF) composite materials (See Figure 2.4).

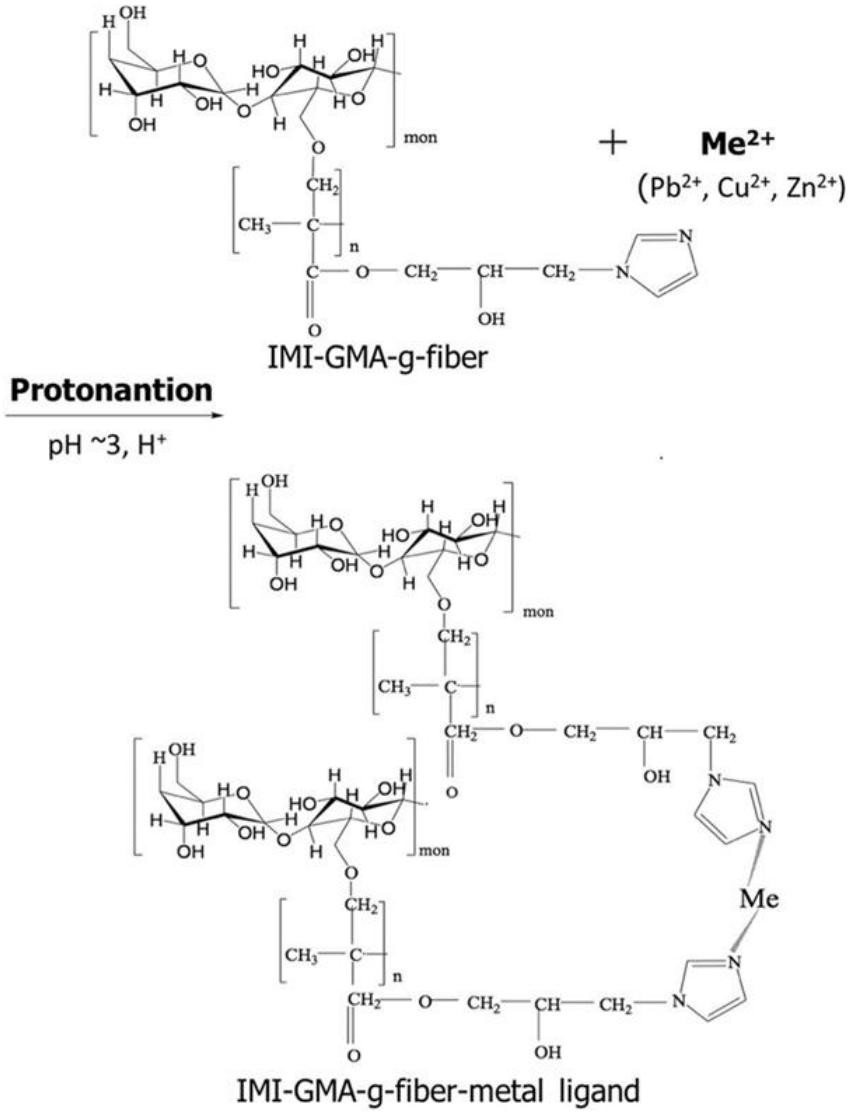

Figure 2.3 Metal ion adsorption mechanism by IMI-functionalized GMA-grafted Banana stem fibers (Selambakkannu *et al.* 2018).

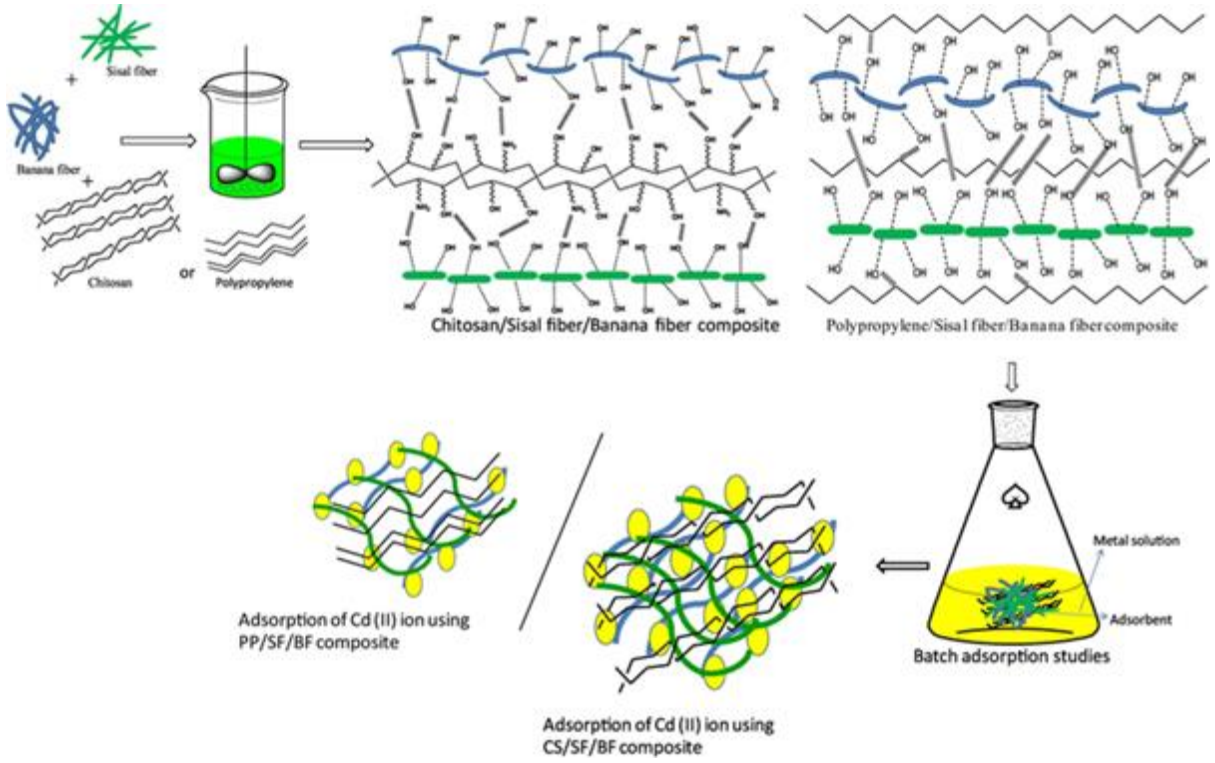

Figure 2.4 Schematic representation for the preparation of ternary chitosan/sisal fiber (SF)/Banana stem fibers (BF) composite, polypropylene (PP)/SF/BF fiber composite (Alaswad *et al.* 2020).

The developed ternary hybrid composites were characterized, and the sample with the best amorphous/less crystalline nature was chosen for the adsorption tests. For the PP/SF/BF composite and bio (CS/SF/BF) composite, the C_{max} value for the Cd (II) ion was determined to be 304 and 419 mg/g, respectively. Pseudo-first-order kinetics, pseudo-second order kinetics, and intraparticle diffusion studies were used to analyze the kinetic adsorption data. For pseudo-second order kinetics, PP/SF/BF and CS/SF/BF fiber composites both exhibited very high R^2 values. As a result, the biocomposite developed from chitosan, sisal, and Banana stem fibers showed the greatest ability to adsorb and remove Cd (II) ions.

In the current work, the removal of lead ions from solid forms (as strips) by adsorption on green cellulosic fiber/polyacrylamide (GCFP) was investigated. Solid strips were developed in place of hydrogel to carry out the adsorption process without losing any water. The investigations included several operating parameters, including contact time, initial Pb concentration, adsorbent dosage,

and pH value. The findings of the kinetic investigation demonstrated that for the adsorption of Pb ions, the pseudo-second order kinetic model offered improved correlation. The results showed that GCFP films are highly effective at removing lead ions from water. At pH = 7, an adsorbent dosage of 0.4 g, an initial Pb concentration of 50 ppm, and a contact time of 60 min, GCFP removed 98% (about 128 mg/g) of the Pb. These findings supported the GCFP film's strong attraction to Pb, which caused the metal to adsorb from the solution and fill the pores and active surface areas of the film (Abdelkhalek *et al.* 2022).

2.3.1.2 Cellulose and Heavy Metal Adsorption Capacity

Numerous sources, including plants, animals, aquatic life, and microorganisms, can yield cellulose. Wood pulp is one of the most widely used sources of cellulose (Aldaz, Figueroa and Bravo 2020). The ecosphere's most readily available and renewable source of organic polymers is cellulose (Wang *et al.* 2021). An organic polymer called cellulose holds the anhydroglucose units of a long, straight-chain molecule. The (1,4)-glycosidic connections bind these anhydroglucose units together (Aldaz, Figueroa and Bravo 2020; Maksoud *et al.* 2020). The abundance of OH groups in the cellulose structure allows for several processes to take place that can change the surface charge. This suggests that cellulose performance in various applications will be enhanced.

Cellulose has been derived from a variety of naturally occurring substances, including bacteria and plants, that are typically receptive and biodegradable. The fact that cellulose can be extracted from every portion of a fruit indicates that the fruit truly contains some cellulose and is therefore safe to eat. A new bacterial-cellulose composite has also been shown to be effective at adsorbing heavy metals like Pb (II), Cu^{2+}, Ni^{2+}, and Cr (VI). (Su *et al.* 2022) developed a poly(hexamethylenediamine-tannic acid)–bacterial cellulose (HTABC) composite using abundant, inexpensive, and nontoxic natural material in a simple one-step technique for the decontamination of highly poisonous Cr (VI) (See Figure 2.5). The as-synthesized HTA-BC exhibited great capacity (534.8 mg/g) and good selectivity for Cr (VI) scavenging. It was functionalized with rich amino and phenolic hydroxyl groups.

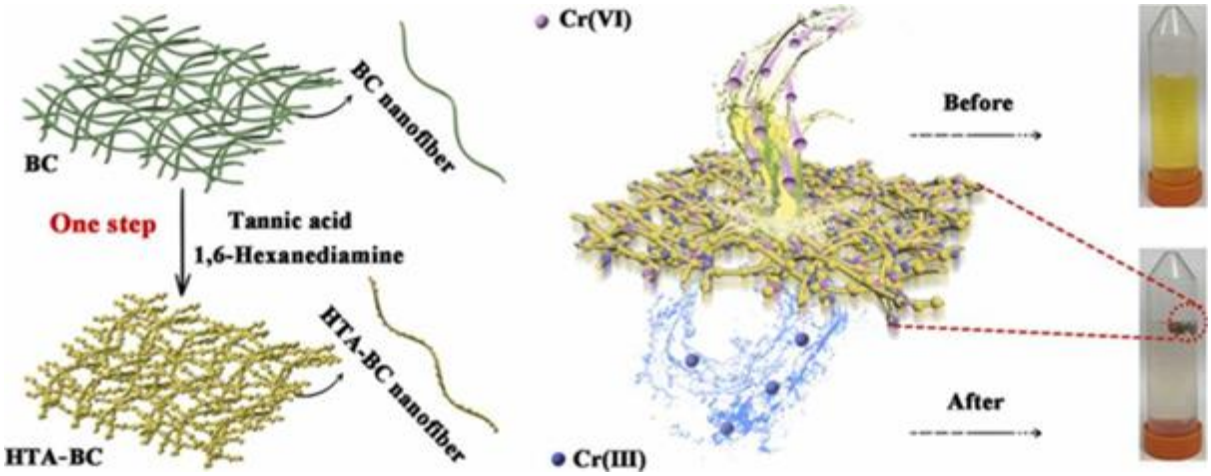

Figure 2.5 Schematic illustration of the possible polymerization mechanism of the HTA and the formation of HTA-BC (Su *et al.* 2022).

The HTA-BC composite, as it developed, had a strong capacity for adsorption and great selectivity for the removal of Cr (VI). The pseudo-second order kinetic model had higher regression coefficients ($R^2 > 0.987$) for the adsorption kinetic parameters of Cr (VI) by HTA-BC. The findings also showed that HTA-BC's adsorption behavior toward Cr (VI) fitted the Langmuir model. The HTA-BC composite could effectively lower the content of the spiked Cr (VI) below the allowable levels for drinking water by treating real water samples.

The literature indicates that cellulose is a novel class of adsorbent substance that has demonstrated the ability to successfully extract heavy metals from aqueous solutions, the most well-known method of which is via adsorption membranes (Karim *et al.* 2017; Mautner, Kobkeatthawin and Bismarck 2017). These nanopapers, however, are too dense to permit high water permeability, making the materials ineffective for removing heavy metals (Mautner *et al.* 2019). Therefore, modifying cellulose may greatly improve its adsorption capacity and encourage adsorption processes such as ion exchange, complexation, and electrostatic interaction. Very high adsorption capabilities have been obtained by functionalizing cellulose with amine groups, thiol groups, and other substances like nano-bentonite and chitosan (Syeda and Yap 2022).

The heavy metals in wastewater and natural water bodies have significantly harmed ecosystems and reduced the quality of the water environment. A uniquely efficient activated

carbon/carborundum microcrystalline cellulose core-shell nanocomposite (AC/CB/MCC) was developed by (Mubarak, Zayed and Ahmed 2022) to be used for the detoxification of As^{3+} and Cu^{2+} ions from aqueous solutions. The kinetic analyses showed that, among the models considered, the pseudo-second order model is the most advantageous for ion adsorption. The maximal adsorption capabilities for the adsorption of Cu^{2+} and As^{2+} ions were 423.55 and 422.9 mg/g, respectively, at pH 7.0, 298 K, and 500 mg of the AC/CB/MCC adsorbent dose. It was indicated that the AC/CB/MCC nanocomposite can be employed as a substitute and effective nano-adsorbent for the removal of hazardous heavy metal ions from polluted effluents, such as Cu^{2+} and As^{3+} ions. Numerous researchers have discussed the chemical modification of cellulose by esterification with EDTA for the recovery of metal ions, as well as the removal of metal ions from aqueous solutions by materials that link EDTA to cellulose derivatives (d'Halluin *et al.* 2017; Jilal *et al.* 2018). In situ synthesized chelating (amino acetic acid groups) adsorbent grafted on cellulose and its heavy metal ion adsorption capabilities from aqueous solutions were developed by (Hu *et al.* 2022) (See Figure 2.6).

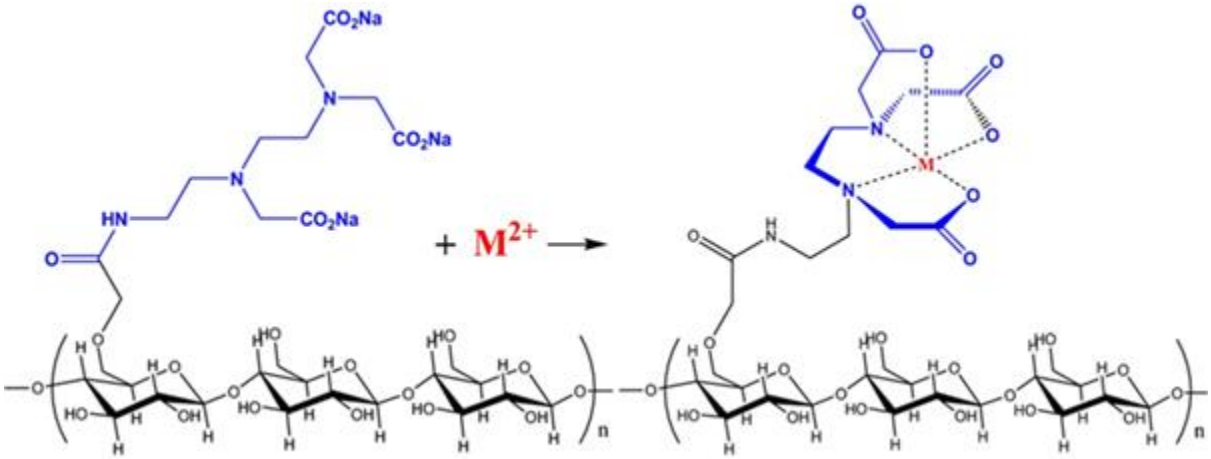

Figure 2.6 The proposed structure of the modified cellulose with an amino acetic acid group and its chelating center with metal ions being adsorbed (Hu *et al.* 2022).

The findings showed that this modified cellulose had good adsorption capability for a variety of metal ions and displayed adsorption characteristics comparable to those of EDTA. The maximum adsorption capacity for Cu^{2+} on modified cellulose with an amino acetic acid group was 80.3 mg/g, while the maximum adsorption capacity for Pb (II) was 266.7 mg/g. By using the Freundlich and

Langmuir models, the adsorption of Cu^{2+} and Pb (II) from single metal ion aqueous solutions onto this adsorbent was assessed and examined. The adsorption of both Cu^{2+} and Pb (II) ions was found to best fit the Langmuir isotherm model. The adsorbent saw a maximum quantity of Cu^{2+} and Pb (II) adsorption at pH 5.

2.3.2 Silica and Heavy Metal Adsorption Capacity

Due to their distinctive characteristics, such as a larger surface area, tunable pore diameters, excellent chemical and thermal stability, selectivity towards heavy metal ions, and ease of surface modification, silica nanoparticles from renewable sources have emerged as a leader in the various groups of nanoparticles. Studies (Rangaraj and Venkatachalam 2017; Rovani *et al.* 2018) reported that silica nanoparticles can be synthesized from a variety of agricultural by-products and plants, including rice husk, maize cob, sugarcane bagasse, and bamboo residues.

Traditional mesoporous silica adsorbents have limited capacities or slow kinetics (Di Natale, Gargiulo and Alfè 2020). Mesoporous silica is thought to be an effective substrate for capturing pollutants as well as an excellent catalyst carrier because of its large surface area, rapid mass transfer inside nanostructures, excellent hydrothermal stability, tunable pore sizes, and ease of organic modification. Particularly, organic modification and inorganic hybridization can be approached under relatively mild preparation conditions (Wang *et al.* 2015; Hao *et al.* 2016). However, due to its capacity to remove heavy metal ions, silica has been used in adsorption techniques as a heavy metal ion remover in aqueous solutions. Due to its high efficiency, simplicity, and ease of use, adsorption has been widely used as a successful approach for removing a lot of heavy metal ions (Abdelrahman *et al.* 2020; Abdelrahman *et al.* 2021; Youssef *et al.* 2021).

The testing of synthetic sorbents (SHNPs), developed by mixing colloidal hydrophilic nanoparticles (HNPs) with silica for useful water treatment applications, is described in (Di Natale, Gargiulo and Alfè 2020) (See Figure 2.7). Silica improves both the functionality and ease of removal of the used sorbent from the HNPs. The supported HNPs (SHNPs) show remarkable removal efficiency, particularly at neutral pH and low temperature (10 °C), which are typical

conditions for natural-water remediation and some types of industrial wastewater. At a reference value of 0.2 mM, the SHNPs' highest adsorption capacities for Cd (II), Pb (II), and Ni^{2+} ions are 0.042, 0.027, and 0.055 mmol/g, respectively.

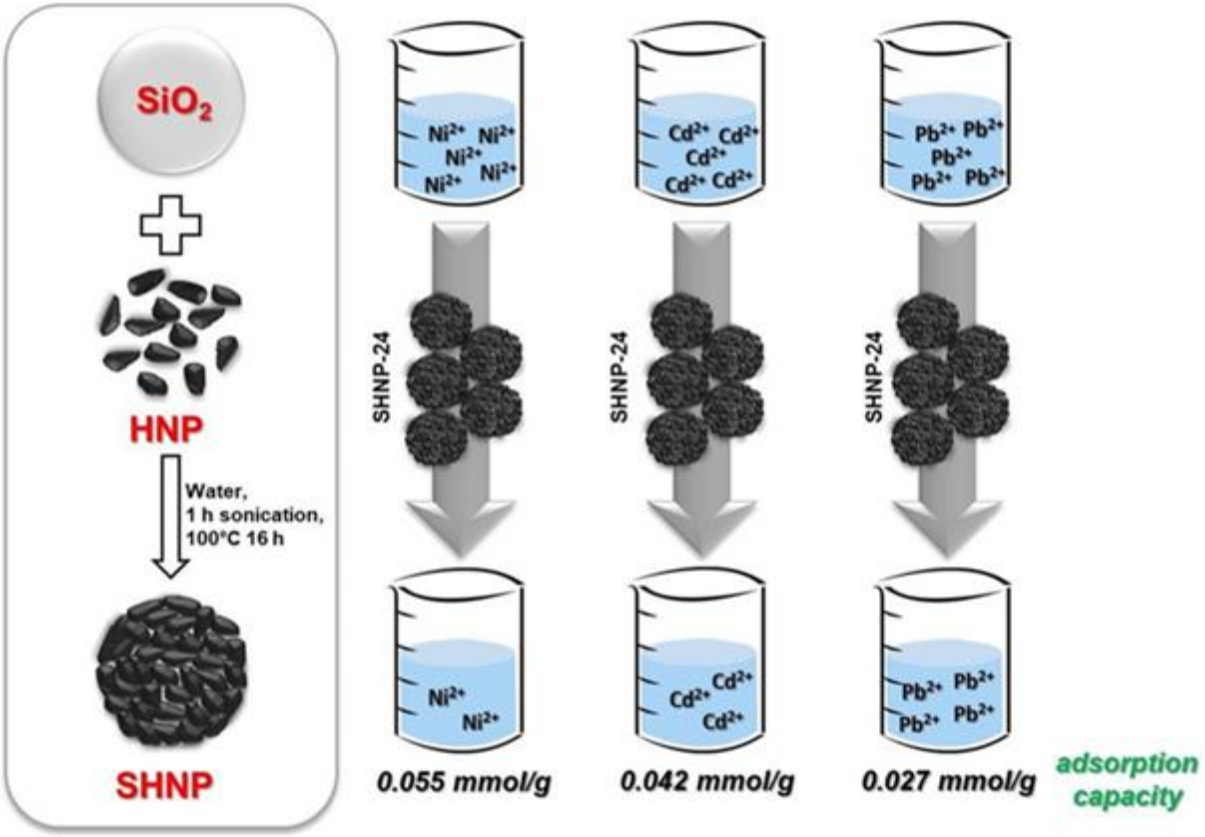

Figure 2.7 Adsorption of heavy metals on silica-supported hydrophilic carbonaceous nanoparticles (SHNPs) (Di Natale, Gargiulo and Alfè 2020).

The sorbents demonstrate significant adsorption capabilities per gram of active phase (0.54 mg/g for Cd (II) ions, 13.48 mg/g for Ni^{2+} ions, and 8.87 mg/g for Pb (II) ions) at the corresponding quality level accepted by Italian legislation on wastewater, indicating a potential application for them in water treatment operations.

As a possible absorbent for heavy metal ions, (Sachan, Ramesh and Das 2021) produced silicon nanoparticles (SNPs) from the dried leaf biomass of Saccharum ravannae (SRL), Saccharum officinarum (SOL), and Oryza sativa (OSL). SNPs were also used to remove copper ($Cu^{2+)}$ and

lead (Pb (II)) from wastewater as suitable adsorbent materials (See Figure 2.8). The adsorption outcomes demonstrated significant capacity in removing heavy metal ions (Pb (II) and Cu^{2+}) with varying values for different types of nanoparticles: 140.06 and 149.25 mg/g for SRL SNPs, 338.55 and 179.45 mg/g for SOL SNPs, and 334.7 and 274.02 mg/g for OSL SNPs. These synthesized nanoparticles exhibited notable adsorption capabilities along with high reusability for eliminating heavy metal ions from synthetic wastewater, achieving over 95% removal efficiency. The adsorption behaviour aligned well with the Freundlich isotherm model and followed pseudo-second order kinetics, elucidating the adsorption mechanism for Pb (II) and Cu^{2+} using SRL, SOL, and OSL SNPs.

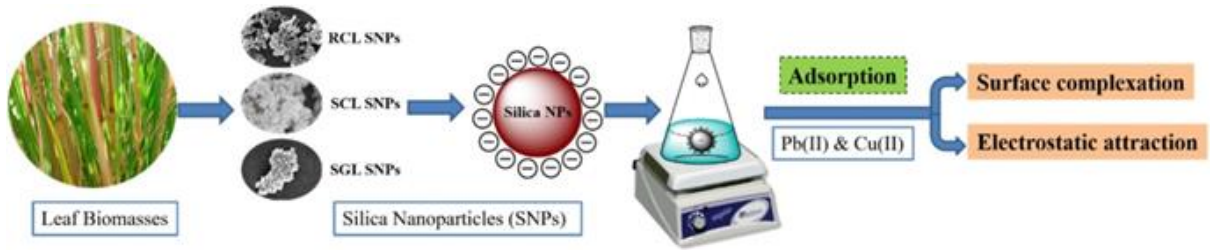

Figure 2.8 Green synthesis of silica nanoparticles from leaf biomass and its application to remove heavy metals from synthetic wastewater: a comparative analysis (Sachan, Ramesh and Das 2021).

(Al-Wasidi *et al.* 2022a) synthesized a unique composite based on Schiff base synthesis on silica nanoparticles (See Figure 2.9). First, 3-aminopropyltrimethoxysilane was used to modify silica nanoparticles, which contain silanol groups (Si-OH). A new Schiff base/silica composite was developed after the modified silica reacted with 1-hydroxy-2-acetonaphthone.

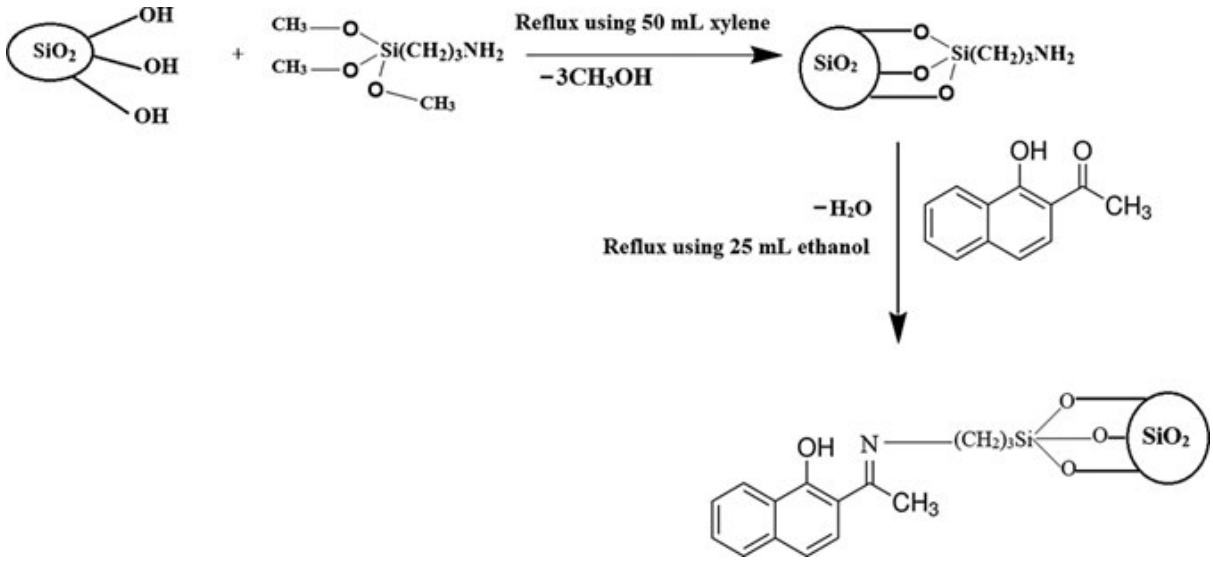

Figure 2.9 The synthetic steps of the composite (Al-Wasidi *et al.* 2022a).

For the effective removal of Ni^{2+}, Cu^{2+}, Zn (II), and Hg^{2+} ions from aqueous solutions, the synthesized composite was used. The composite has a maximal absorption capacity of 68.630, 50.942, 45.126, and 40.420 mg/g for Cu^{2+}, Hg^{2+}, Zn (II), and Ni^{2+} ions, respectively. The findings demonstrated that at pH = 6.5, contact time = 90 min, and adsorption temperature = 298 K, the greatest percentage removal of the examined metal ions was accomplished.

Bifunctional magnetic mesoporous silica (NZVI-SH-HMS) was successfully synthesized by (Li *et al.* 2021) for the efficient removal of Pb (II) and Cd (II) ions from aqueous solutions. First, a bi-functionalized magnetic mesoporous silica (NZVI-SH-HMS) material was manufactured at room temperature using the sol-gel and wet impregnation processes, with thiol and nanoscale zero-valent iron bound on the surface (See Figure 2.10).

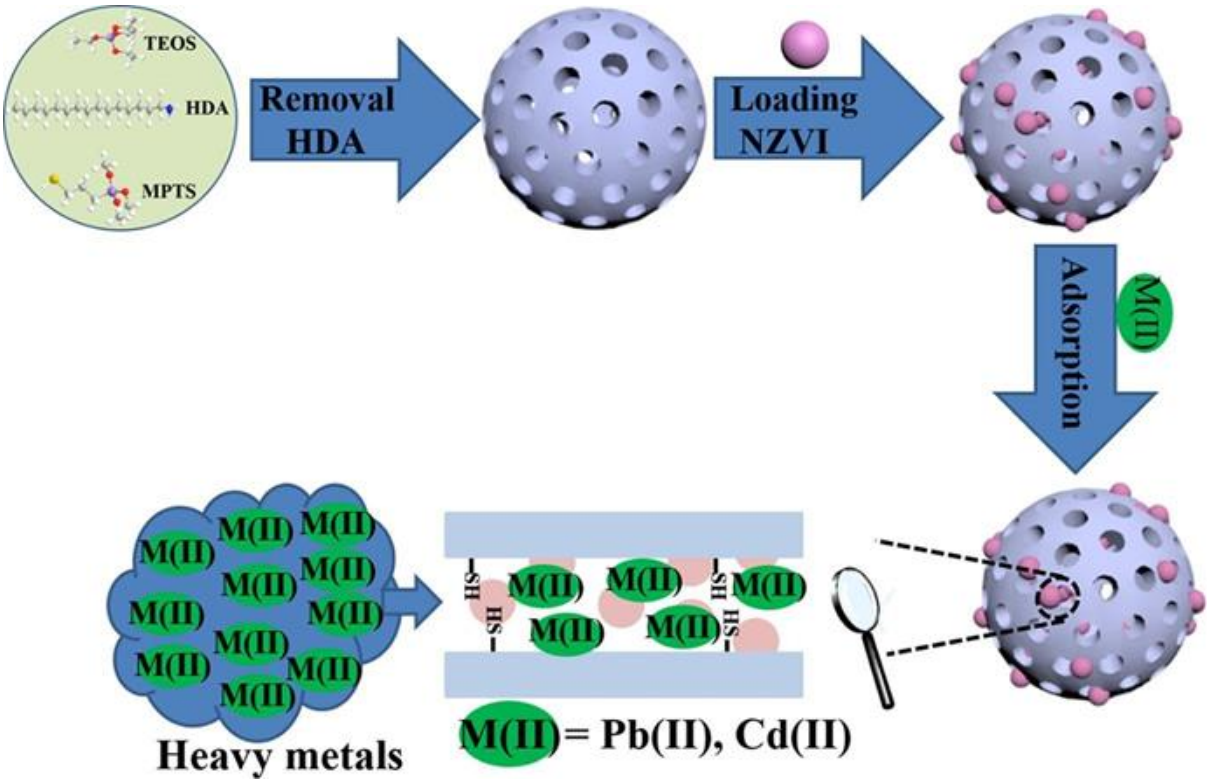

Figure 2.10 Highly effective removal of lead and cadmium ions from wastewater by bifunctional magnetic mesoporous silica (Li *et al.* 2021).

NZVI-SH-HMS had maximal adsorption capabilities of 487.8 mg/g for Pb (II) and 330.0 mg/g for Cd (II), respectively. Data on the pseudo-second order kinetics and isotherm of adsorption were well-fitted to the Langmuir isotherm model. The reusability and regeneration studies showed NZVI-SH-HMS had a large capability for removing heavy metals from the actual water environment and retained outstanding adsorption performance.

To increase the mechanical strength and heavy metal ion adsorption of silica aerogel, (Parale *et al.* 2023) developed a novel in situ sulphur-doping manufacturing process. Three-dimensional monolithic silica aerogels were initially developed by polymerizing (3-glycidoxypropyl) trimethoxysilane and (3-mercaptopropyl)trimethoxysilane using an adjustable one-pot epoxy-thiol reaction, then by using the sol-gel method and supercritical drying (See Figure 2.11). The heavy metals were eventually removed using the produced aerogels, with Pd^{2+} being adsorbed nearly 100% of the time. The Langmuir adsorption model was able to fit an adsorption capacity of up to

689.65 mg/g. The suggested technique is a novel approach for the in-situ synthesis of sulphur-doped silica aerogels with improved mechanical properties for heavy metal removal.

Groundwater contamination by heavy metals in the environment has grown to be a major threat to the health of living things. To reduce the hazards involved, heavy metals in contaminated water must be removed. (Amin *et al.* 2023) investigated mesoporous silica and chitosan nanoparticles that had been synthesized and coated with magnetite to absorb heavy metals from wastewater (See Figure 2.12). First, due to the mono-dispersity offered by this approach, magnetite nanoparticles (MNPs) were developed via the thermal degradation of the iron oleate precursor. The particles were given a mesoporous silica layer coating using the surfactant cetyltrimethylammonium bromide (CTAB). By stirring in a chitosan solution, the coated particles were subjected to chitosan coating.

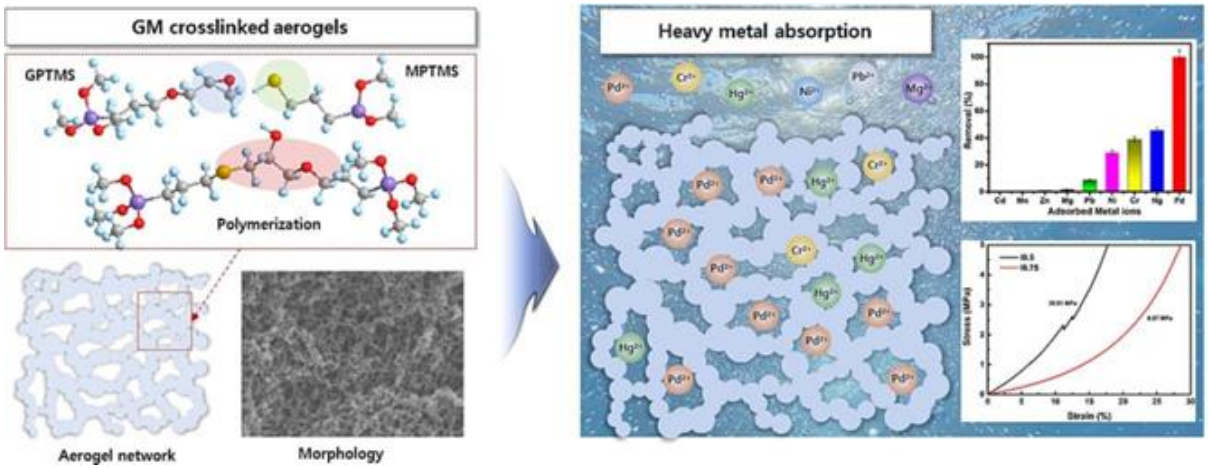

Figure 2.11 Cross-linked silica aerogels were synthesized using one-pot epoxy-thiol polymerization and the sol-gel process and heavy metal adsorption (Parale *et al.* 2023).

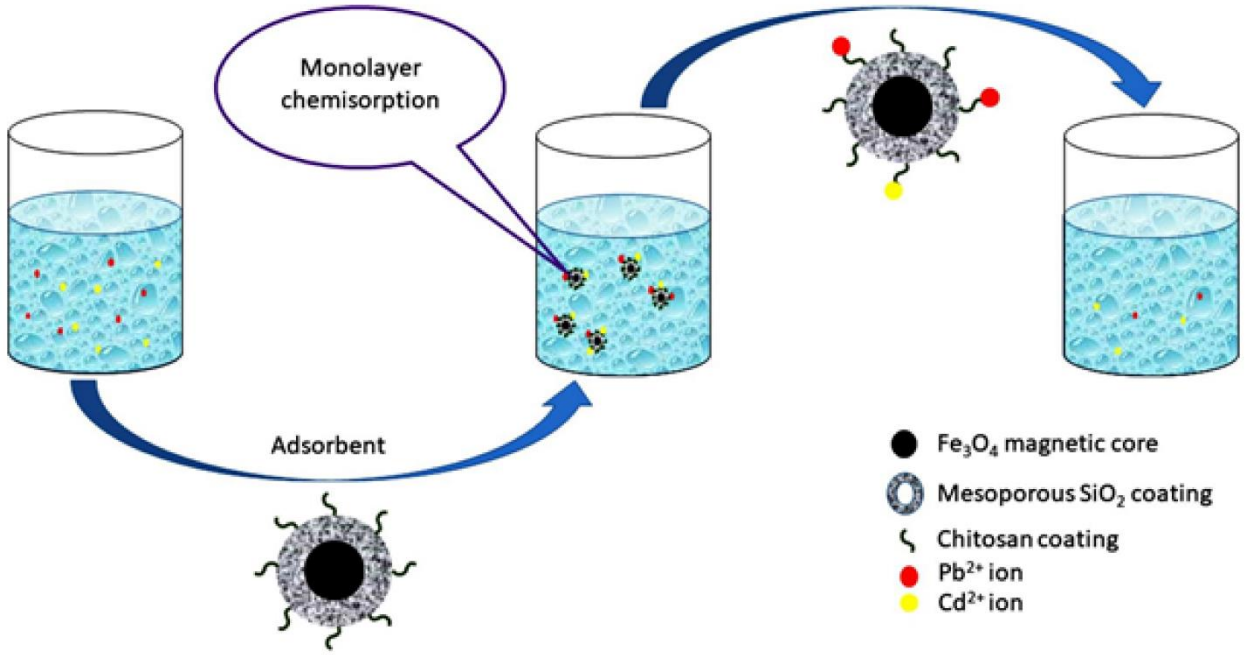

Figure 2.12 Heavy metal adsorption from wastewater by mesoporous silica and chitosan-coated magnetite nanoparticles (Amin *et al.* 2023).

In known concentrations of heavy metal salt solutions, the particles were utilized as an adsorbent. It is a favorable sign for future investigation and analysis because the produced adsorbent showed a reasonable adsorption capacity of 150.33 and 126.26 mg/g for Pb (II) and Cd (II), respectively. The pseudo-second order kinetic model and the Langmuir isotherm model are superior fits for the adsorption data of Pb (II) and Cd (II) based on the value of R^2 ($R^2 \geq 0.99$).

A new composite was developed in this study by (Al-Wasidi *et al.* 2022a), based on the production of a Schiff base on silica nanoparticles. A silanol group (Si-OH) was added to silica nanoparticles using (3-aminopropyl) trimethoxysilane.

A novel Schiff base/silica composite was made by mixing the modified silica with 4,6diacetylresorcinol (See Figure 2.9). Pb (II), Cu^{2+}, Co^{2+}, and Ni^{2+} ions were efficiently removed from aqueous solutions using the produced composite. The composite had a maximal absorption capacity of 107.066, 89.767, 80.580, or 70.972 mg/g for Pb (II), Cu^{2+}, Co^{2+}, and Ni^{2+} ions, respectively. The examined metal ions' adsorption processes were chemical, spontaneous, and well-matched with the pseudo-second order kinetic model and Langmuir equilibrium isotherm.

2.3.3 Cellulose with Silica Nanoparticles and Heavy Metal Adsorption (Cd, Pb, Cr)

Recent research has shown that nanotechnology has enormous potential for improving the efficiency of water prevention and purification while reducing costs. In this field, nanocellulose has attracted attention for two applications where it has effectively eliminated pollutants as a membrane and an adsorbent. This potential stems from its elevated aspect ratio, expansive specific surface area, outstanding water retention, and environmental inertness. Beyond these merits, the existence of active sites facilitates the integration of chemical groups, potentially enhancing the surface's efficacy in binding pollutants (Abouzeid *et al.* 2018).

Heavy metals such as Cd (II), Pb (II), Mn^{2+}, and others pose a serious threat to the environment since they are non-biodegradable. Using environmentally acceptable nanomaterials, heavy metal pollution can be minimized thanks to the development of nanobiotechnology. Specially designed bio-nanomaterials usually exhibit properties like longer shelf life, self-healing nature, adaptability in varied environments, and cost-effectiveness in comparison to nanoparticles generated using physicochemical procedures. Due to their excellent selectivity and adsorption capacity, bio-nanomaterials can effectively remove heavy metals from wastewater, even when they are present in incredibly low quantities. To reduce expenses and create a way for environmental sustainability, bio-nanotechnology is applied in their clean-up (Malik *et al.* 2022).

The characteristics of nanoparticles have been extensively investigated due to their restricted capacity to adsorb some heavy metal ions. According to (Rajendran *et al.* 2022) there has been research on the effects of experimental conditions on the uptake of metal ions, including the dose of the adsorbent, pH, substrate concentration, response time, temperature, and electrostatic force. Furthermore, the use of polymeric membranes for the adsorption of dangerous particles may lead to the development of next-generation reusable and portable water filtration systems. Because they conduct both membrane filtration and adsorption, membranes for membrane adsorption (MA) are very effective at eliminating trace quantities of contaminants such as cationic heavy metals, anionic phosphates, and nitrates (Khulbe and Matsuura 2018).

Utilizing carbohydrate biopolymers, several nanocomposite adsorbents for wastewater treatment have been developed. The effectiveness of extracting inorganic pollutants from aqueous solutions was investigated using these adsorbents. Toxic metals may be efficiently absorbed by cross-linkers, which dissolve in aqueous solutions of divalent heavy metal ions to assess their polymer absorption capacity. These nanocomposites were used to remove Cd (II), Pb (II), and Zn (II), three very dangerous elements, from water. To improve the effectiveness of heavy metal ion absorption, various functionalization techniques have been applied, such as grafting, blending, or mixing with other nanomaterials that have an extra functional group. The ability of an adsorbent to be recycled depends in part on its mechanical efficiency, which is raised by integrating the second component into the primary polymer chain. The method for removing metal ions from wastewater is inexpensive as long as the adsorbent is recycled (Fouda-Mbanga, Prabakaran and Pillay 2021).

To recover heavy metal ions and benzene fumes, (Yarkulov *et al.* 2022) developed diacetate cellulose–silicon bio-nanocomposite adsorbent (DACSBNC). The observed findings validated the following: (i) the DACSBNC's adsorption capacitance for Cd (II), Hg^{2+}, and Pb (II) ions was proven to be 12.23, 13.87, and 31.40 mg/g, respectively; and (ii) the DACSBNC's sorption capacitance for benzene vapors was 0.5618 mmol/g. For the extraction of heavy hazardous metal ions such as Cd (II), Hg^{2+}, and Pb (II) from galvanic aqueous solutions, the researched DACSBNC materials have been suggested as potential sorbents.

To develop a porous matrix with balanced surface characteristics, silica from rice husks was treated using the sol-gel method, and cellulose from Nata de Coco was added in the gelling process. Hazardous waste is laboratory waste that pollutes the environment and contains heavy metals such as cadmium, chromium, nickel, and zinc. Adsorption is an efficient and inexpensive method to handle heavy metal waste. The material silica–cellulose was developed and used in this study by (Royanudin, Utomo and Wonorahardjo 2021) as an adsorbent for heavy metals, including cadmium, chromium, nickel, and zinc, in laboratory waste. The removal percentages of cadmium, chromium, nickel, and zinc were 95.09, 58.77, 94.56, 94.56, and 97.50%, respectively. In the study by (Yang *et al.* 2019), the researchers created ferrocene-incorporated mesoporous organosilica nanoparticles, which are a novel inorganic-organic hybrid nanomaterial (MONs).

Organoalkoxysilanes containing ferrocene were synthesized as shown in Figure 2.13a, and the raw material was used directly to synthesize MONs without any purification because 1,10-ferrocene dicarboxylic acid was not involved in the process. The results of the reaction are shown below.

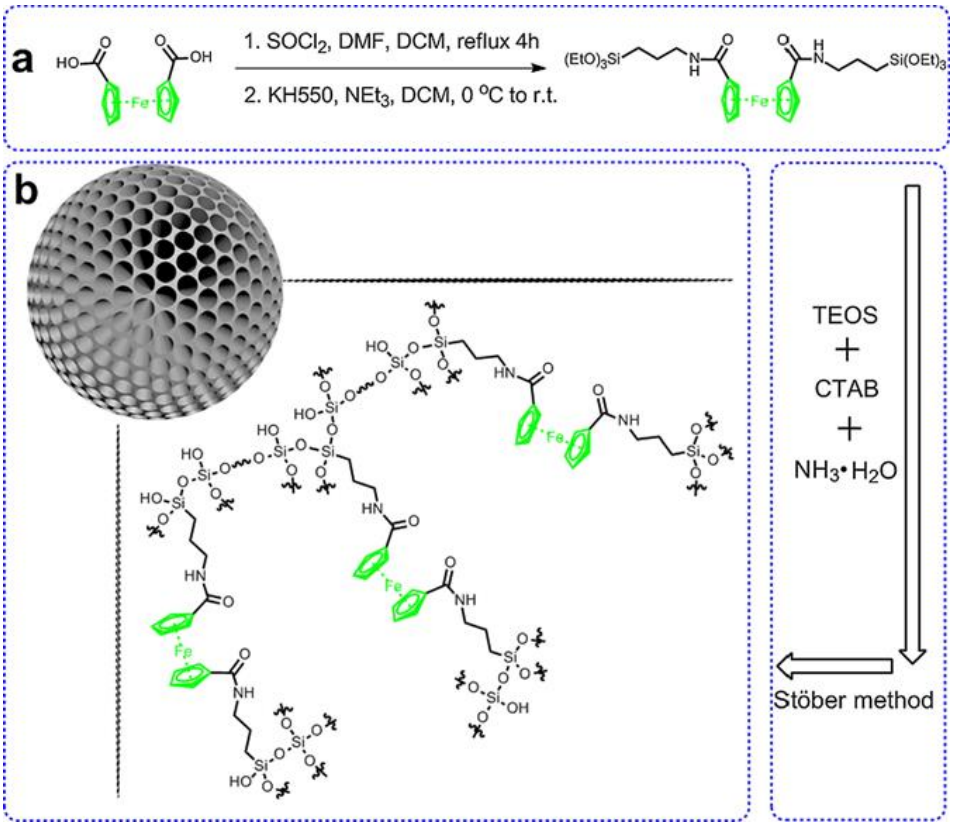

Figure 2.13 (a) Synthetic routes of ferrocene-containing organoalkoxysilanes and (b) schematic illustration of MONs (Yang *et al.* 2019).

The mesoporous structure, significant surface area, and incorporation of the ferrocene group within the framework enabled MONs to exhibit superior adsorption of phosphate anions compared to surface-modified MSNs (SiO_2-Fe) (488 mg/g). Comparative analysis revealed that MONs outperformed MSNs, with ferrocene surface modifications as a more effective absorbent. Additionally, Congo red (CR) and Pb (II) were employed as model pollutants. For the removal of heavy metals, titanium dioxide (TiO_2) and other inorganic nanoparticles were utilized. NanoTiO_2 demonstrated a higher adsorption rate compared to bulk particles (Zito and Shipley 2015). To achieve multiple heavy metal adsorption, (Wang *et al.* 2021) fabricated titanium dioxide

(TiO_2)/rectorite (REC)-trapped cellulose composite nanofibrous mats using electrospinning (See Figure 2.14). The interactions between inorganic adsorbents and cellulose molecules enhanced the mats' thermal stability, surface area, tensile strength, and adsorption capacity.

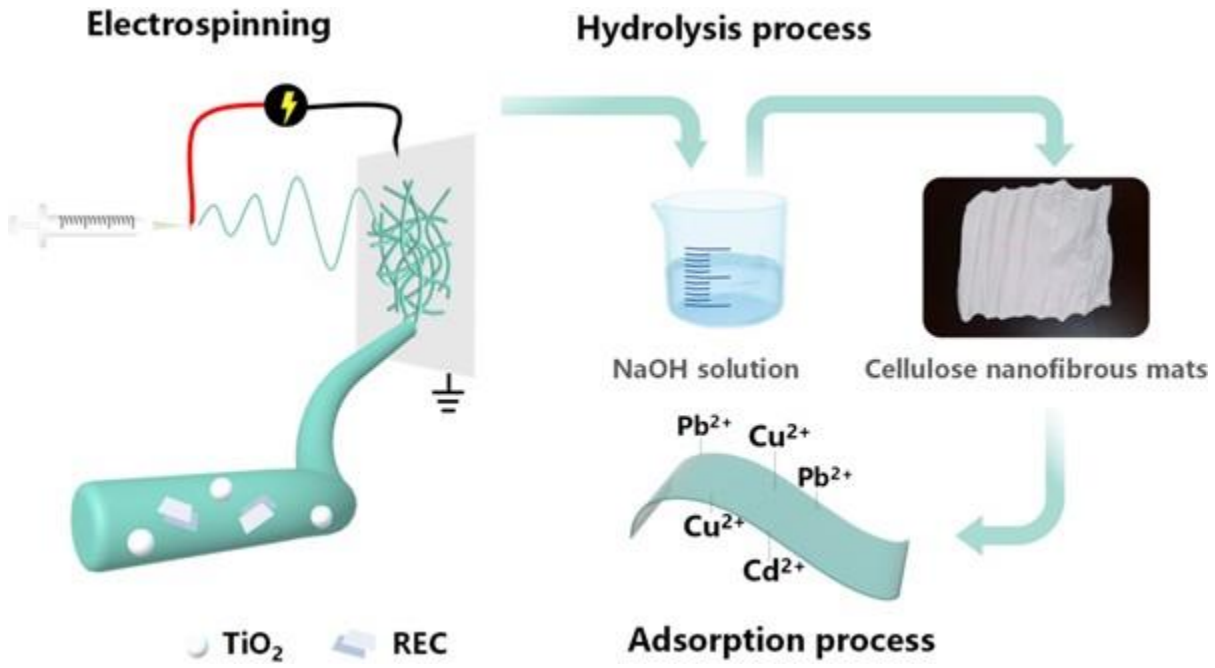

Figure 2.14 The schematic diagram illustrates the process of creating a cellulose membrane through electrospinning of cellulose acetate blended with TiO_2 nanoparticles and rectorite. Subsequently, deacetylation transforms it into pure cellulose, enhancing its absorption properties towards heavy metal ions such as Pb (II), Cu^{2+}, and Cd (II) (Wang *et al.* 2021).

The pseudo-second order model and the Langmuir isotherm model were mostly used in the adsorption of Cd (II) onto cellulose–TiO_2/REC nanofibrous mats. The pH of the solution influenced the multiple adsorptions of Pb (II), Cu^{2+}, and Cd (II) onto composite nanofibrous mats. Cellulose–TiO_2/REC 2:1 nanofibrous mats at pH 6 had the highest total adsorption capacity of 69.81 mg/g. The produced cellulose–TiO_2/REC nanofibrous mats might be employed to extract heavy metals from acidic wastewater. The composite nanofibrous mats successfully captured TiO_2 nanoparticles.

2.3.4 Cellulose–Silica and Amine–Silane Coupling Agents in Absorption of Heavy Metals

There are three common methods of surface modification for cellulose and silica coupling agents in the absorption of heavy metals. Among these includes:

2.3.4.1 Silane Coupling Agents

The functionalization of cellulose through a reaction with organosilanes has frequently been utilized to enhance its characteristics. The impact of substitutions before coupling with silanes on improving the dispersions of the functional groups that act as the adsorption sites for aqueous arsenate has barely been explored (Es-Haghi *et al.* 2014; Lucia *et al.* 2020). Adsorbents with excellent adsorption performance toward heavy metal ions and other contaminants can be produced by adding coordination groups comprising coordination atoms, such as -OH, -COOH, -C-O, -C=N, $-NH_2$, -NH, -C-S, -C=S, -S-S, and -S=O, to cellulose-based adsorbents.

A novel cross-linked polymer known as cellulose acetate aminosilane (CAAS) was created by (Bisla, Kawamura and Yoshitake 2022) using acetylated microcrystalline cellulose and 3-(2-aminoethylamino) propyltrimethoxysilane (AEAPTMS) (See Figure 2.15). The acetyl group probably encourages the formation of a polymer structure that facilitates aqueous ion diffusion during their adsorption.

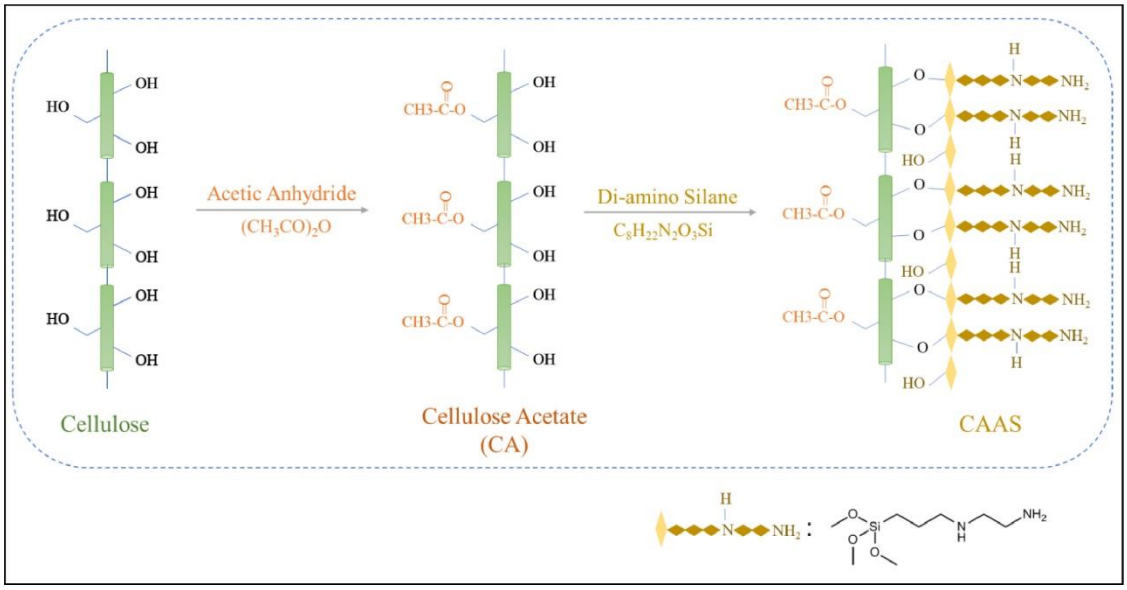

Figure 2.15 Schematic illustration for the preparation of CAAS (Bisla, Kawamura and Yoshitake 2022).

In a pH range of 2 to 10, a sizable amount of arsenate was adsorbed by CAAS, suggesting that the presence of both amine and acetyl groups broadens the adsorption's pH range. The Langmuir isotherm and pseudo-second order kinetic models fit the adsorption data well. The adsorption reached 455 mg/g, demonstrating a remarkable capability for the cellulose polymers treated with aminosilane.

(Shaheen, Radwan and El-Wakeel 2022) created a novel and cost-effective bio-based adsorbent capable of simultaneously removing an anionic dye and a hazardous metal (See Figure 2.16). They utilized 3-aminopropyltriethoxysilane (APTES-CA) to modify porous cellulose acetate (CA) microspheres synthesized through a double emulsion (W/O/W)–solvent evaporation method. According to the adsorption investigation, APTES modification increased the effectiveness of adsorption for RB19 and Pb (II). According to the kinetic investigation, APTES-CA adsorbs RB19 and Pb (II) by several processes, specifically chemisorption for RB19 and physisorption for Pb (II). A good efficiency of APTES-CA towards Pb (II) was demonstrated by the theoretical Langmuir monolayer saturation capacity (180 mg/g).

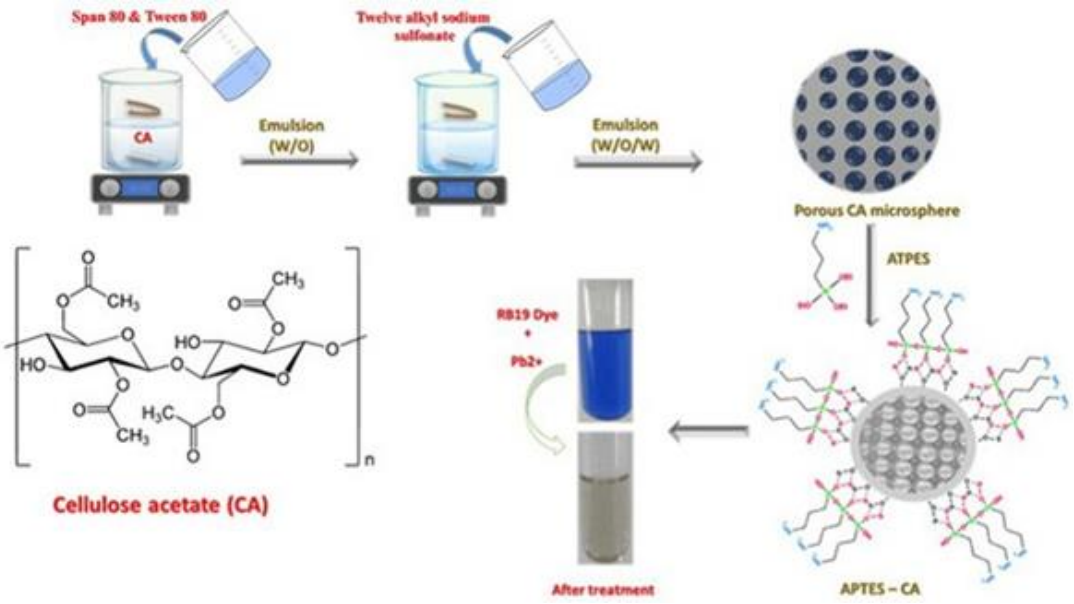

Figure 2.16 Schematic diagram for APTES-CA synthesis pathway and Reactive blue 19 (RB19) and Pb (II) adsorption (Shaheen, Radwan and El-Wakeel 2022).

2.3.4.2 Thiol Functionalization

Through the addition of extra binding sites provided by functional groups containing sulphur, thiol functionalization increases the adsorption capacity for heavy metals. Because of their considerable affinity for metal ions, these groups make it easier to remove them from aqueous solutions. (Dang-Bao *et al.* 2023) produced thiol-functionalized cellulose nanocrystals through chemical hydrolysis of cellulose, followed by autocatalytic esterification with thioglycolic acid. Their study involved assessing the adsorption properties of these nanomaterials for divalent copper ions in water using isotherm and kinetic analyses. The thiol-functionalized cellulose nanocrystals demonstrated a notably enhanced adsorption capacity compared to unmodified cellulose, achieving 4.244 mg/g at pH 5 and room temperature.

A cellulose nanofiber membrane that has been thiol-functionalized and is capable of successfully adsorbing heavy metal ions is described by (Choi *et al.* 2020) (See Figure 2.17). As a result of the deacetylation of electrospun cellulose acetate nanofibers and the subsequent esterification of a thiol precursor molecule, thiol was added to the surface of cellulose nanofibers.

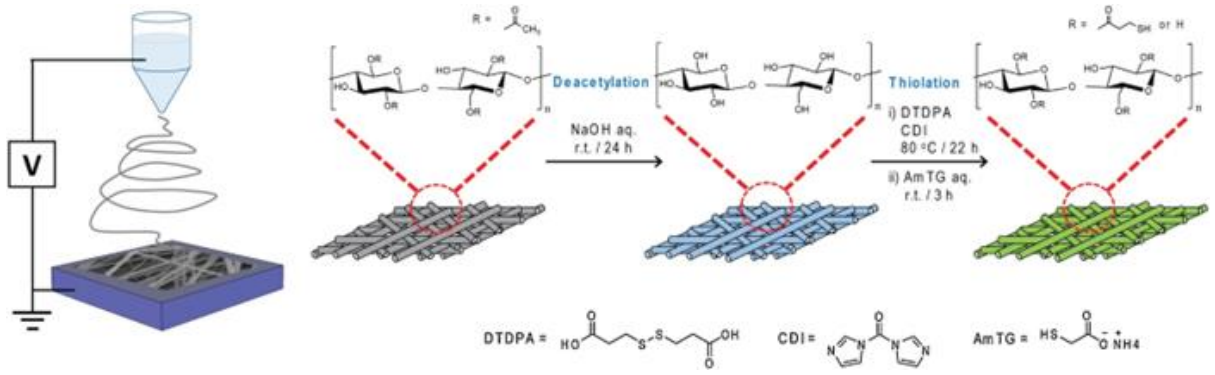

Figure 2.17 A schematic representation illustrating the fabrication process of a thiol-functionalized cellulose nanofiber membrane (Choi *et al.* 2020).

The Langmuir isotherm provided a good description of adsorption capacity as a function of adsorbate concentration, indicating that metal ions form a surface monolayer with a homogeneous distribution of adsorption energy. Cu^{2+}, Cd (II), and Pb (II) ions have maximum adsorption capabilities of 49.0, 45.9, and 22.0 mg/g in the Langmuir isotherm, respectively (See Figure 2.18). According to the time-dependent adsorption capacities, which were consistent with a pseudo-second order kinetic model, chemisorption of each doubly charged metal ion takes place when there are two thiol groups present on the surface.

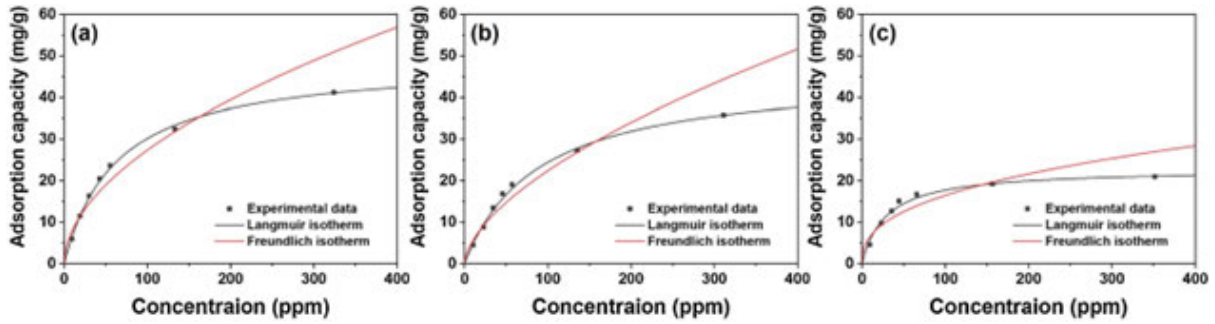

Figure 2.18 Isotherms displaying the adsorption of (a) Cu(II), (b) Cd(II), and (c) Pb(II) ions onto TC nanofibers, along with the fitting outcomes using Langmuir (represented by black solid line) and Freundlich (represented by red solid line) isotherm models (Choi *et al.* 2020).

2.3.4.3 Amino Acid Grafting

In this method, amino acid molecules are attached to the surfaces of cellulose and silica materials. Amino acids possess functional groups like amino (-NH_2) and carboxyl (-COOH) groups, which can engage heavy metal ions through coordination and complexation reactions. The grafting of amino acids enhances the selectivity and effectiveness of adsorption by modifying the surface chemistry of the materials. In order to improve the adsorptive removal of Cd (II) and Pb (II) from aqueous solutions, chelating celluloses functionalized with the four amino acids cysteine, histidine, aspartic acid, and methionine (as named Cys-CL, His-CL, Asp-CL, and Met-CL) were prepared by (Chen *et al.* 2022) through a Schiff base reaction (See Figure 2.19). These materials were then investigated by various means of characterization. Because it has many active binding sites and uses complexation of its thiol, imine, and carboxyl groups with both metal ions as the adsorption mechanism, the Cys-CL stood out among the others for its excellent adsorptive capabilities for the improved adsorption of the Cd (II) and Pb (II) ions.

Using the radiation approach for Pd (II) capture, four environmentally friendly amino acids (arginine, histidine, methionine, and cysteine) were used to change cellulose microspheres (designated as ArgR, HisR, MetR, and CysR). Their excellent specificity for Pd (II) was demonstrated by batch studies, which were in good agreement with the pseudo second order kinetic and Langmuir models. Notably, at 143.47 mg/g, CysR showed the highest maximal adsorption capacity. Moreover, CysR demonstrated remarkable resilience to high salt concentrations, while MetR demonstrated strong resistance to acidic environments. These altered microspheres successfully removed traces of Pd from PCB leachate in real-world applications (Peng *et al.* 2022) (See Figure 2.20).

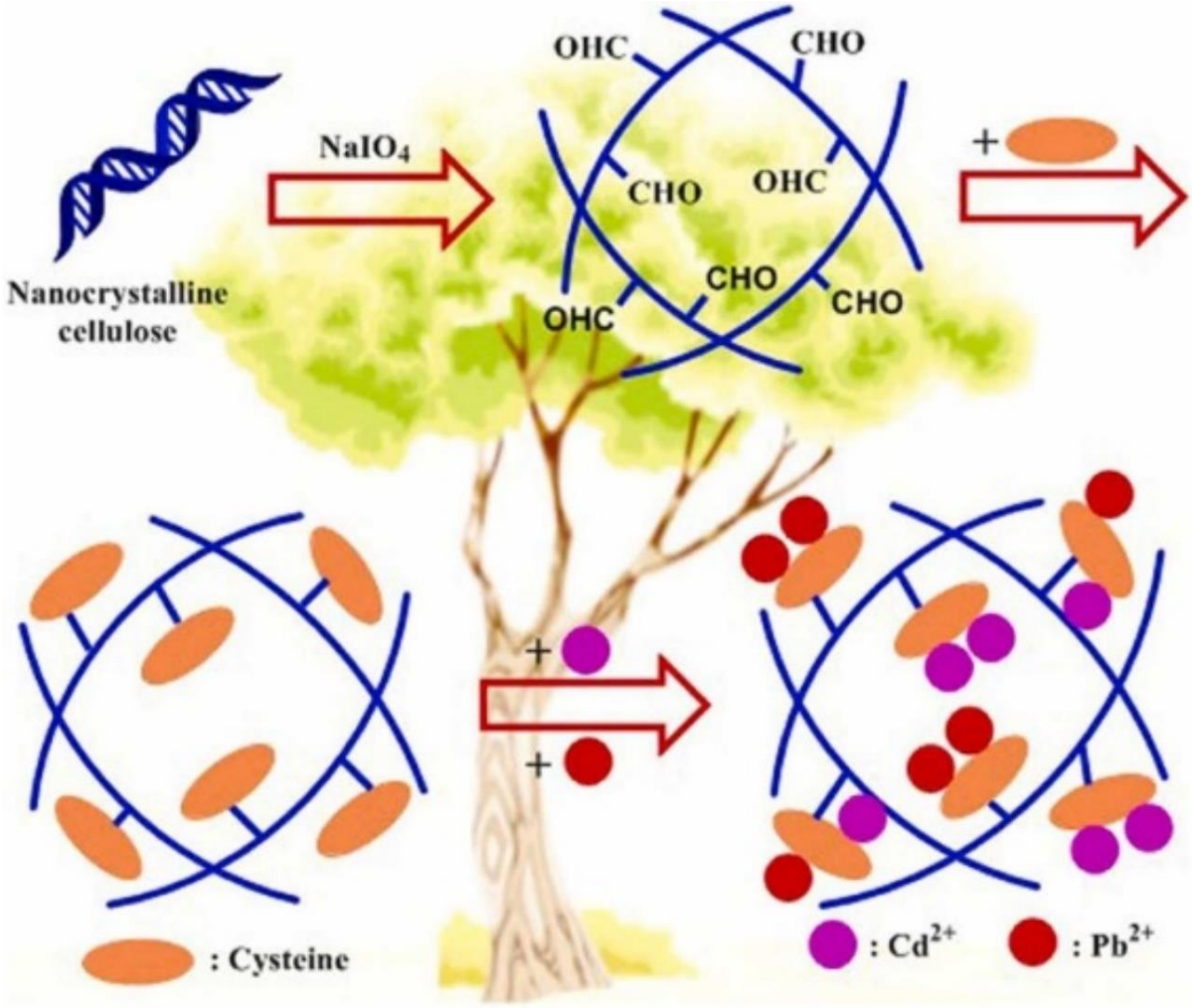

Figure 2.19 Synthesis of chelating celluloses functionalized with amino acid (cysteine) and heavy metals adsorption (Chen *et al.* 2022).

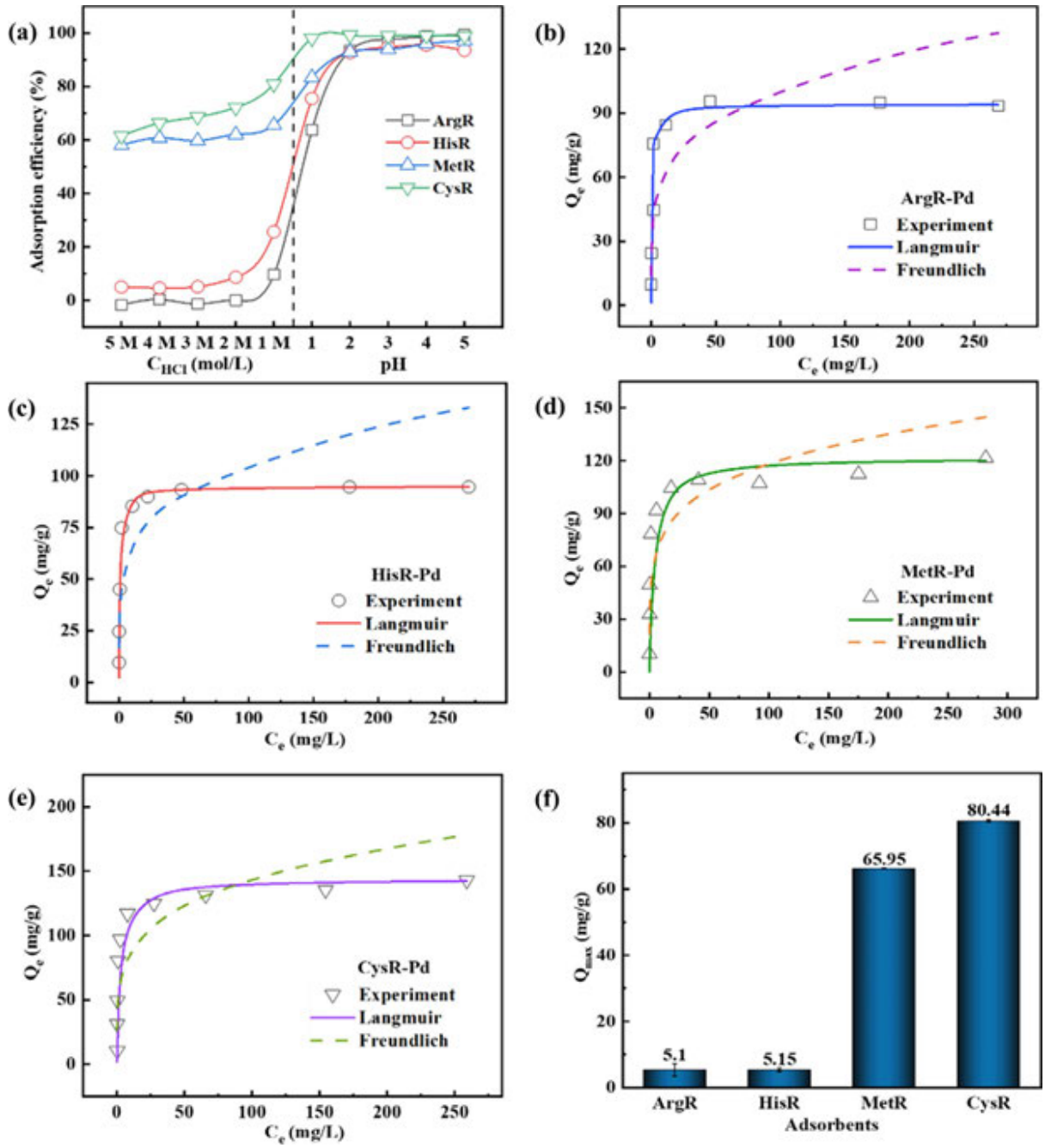

Figure 2.20 **Effect of pH on adsorption efficiency of Pd(II) (a) (C0 = 100 mg/L, adsorbent mass = 10 mg, volume = 10 mL, T = 30 ℃); Experimental isotherms of ArgR (b), HisR (c), MetR (d), and CysR (e) (adsorbent mass = 10 mg, pH = 2, V = 10 mL, T = 30 ℃ , t = 24 h); The maximum adsorption capacity of Pd(II) on amino acid resins at 5 mol/L HCl concentration (f) (C0 = 100 mg/L, adsorbent mass = 10 mg, volume = 10 mL, T = 30 ℃) (Peng *et al.* 2022).**

The study on the reaction of hydroxy groups with diethylenetriaminepentaacetic acid (DPTA)-modified amino silane shows the usage of a silane containing both carboxy and amine for the chemical modification of cellulose (Shen *et al.* 2022) (See Figure 2.21).

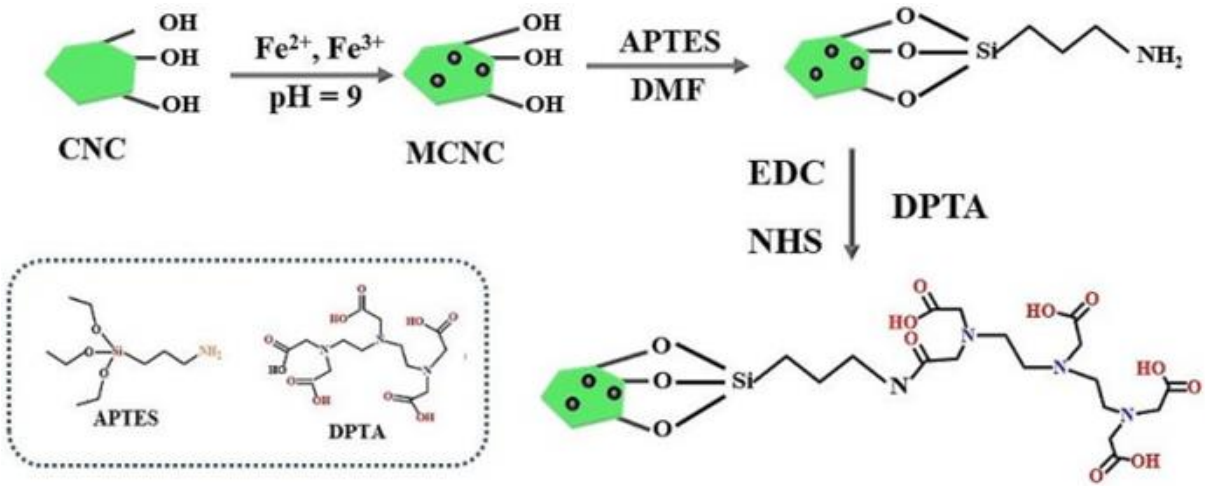

Figure 2.21 Schematic representation of the preparation of MCNC-DPTA (Shen *et al.* 2022).

Higher temperatures were discovered to facilitate adsorption, with maximum Pb (II) adsorption capacities of 424.78, 424.67, and 440.0 mg/g being obtained at 293.3, 298.3, and 303.3 K, respectively. This material's adsorption behaviour was investigated, and the results show that the natural initial pH of the aqueous Pb (II) solution was optimal for the adsorption process. Investigations were made on the isotherm and kinetic parameters for Pb (II) adsorption by MCNC-DPTA. The Langmuir isotherm model and pseudo-second order model were thought to better represent the adsorption process of Pb (II) by MCNC-DPTA due to the greater fitting coefficients. One of the most serious environmental issues that has generated a great deal of worry in recent decades is copper contamination of water. To remove Cu^{2+} from aqueous solutions, (Gao *et al.* 2022) treated cellulose in two steps with N-[3-(trimethoxysilyl)propyl]ethylenediamine (KH-792) and diethylenetriaminepentaacetic acid (DTPA) (See Figure 2.22).

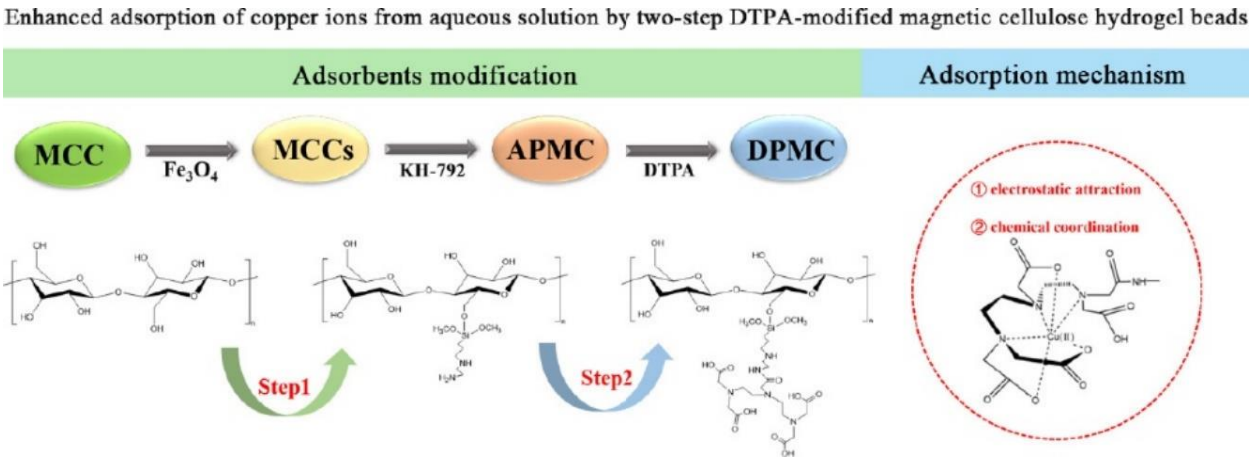

Figure 2.22 Cu (II) adsorption process and related mechanism (Gao *et al.* 2022).

DPMC had more Cu (II) adsorption capacity than MCCs and APMC, with a maximum adsorption capacity of 298.62 mg/g at pH 6. The equilibrium adsorption data were well represented by the Langmuir model, and the adsorption process was found to fit better with the pseudo-second order kinetic model, indicating that monolayer chemical adsorption dominated the process. To remove Cu (II) from aqueous media, the DPMC composite exhibits great potential as an adsorbent.

2.4 Results

Table 2.1 summarizes the type of heavy metal ions and the capacity removal in mg/g and/or percentage reported in the literature.

Table 2.1 Removal of metal ions using adsorbents.

Adsorbent Types	Heavy Metal ions	Capacity Removal (mg/g)	Percentage Removal (%)	References
Natural fiber and heavy metal adsorption capacity				
Banana fibre needle-felted fabric	Pb (II) and Zn (II)	-	95.5 & 98	(Ariharasudhan *et al.* 2022b)
Banana peel	Cd (II)	-	98.146	(Afolabi, Musonge and Bakare 2021)
TCNF	Cu^{2+}	> 60	-	(Mautner *et al.* 2019)
SEBF-CX	Pb (II) and Cd (II)	99.0099 & 67.3401	-	(Sheng *et al.* 2018)
IMI-GMA	Cu^{2+}, Pb (II), and Zn (II)	71.6, 84.2 & 60.1	-	(Selambakkannu *et al.* 2018)
PP/SF/BF fibre and CS/SF/BF fibre	Cd (II)	304 & 419	-	(Alaswad *et al.* 2020)
GCFP	Cd (II)	approximately 128	98	(Abdelkhalek *et al.* 2022)
AC/CB/MCC	Cu^{2+} and As^{2+}	423.55 & 422.9	-	(Mubarak, Zayed and Ahmed 2022)
HTA-BC	Cr (VI)	534.8	-	(Su *et al.* 2022)

Modified cellulose with an Amino acetic acid group	Cu^{2+} and Pb (II)	80.3 & 266.7	-	(Hu *et al.* 2022)
Silica and heavy metal adsorption capacity				
SHNPs	Cd (II), Ni^{2+} and Pb (II)	0.54, 13.48 & 8.87	-	(Di Natale, Gargiulo and Alfè 2020)
SRL SNPs, SOL SNPs, and OSL SNPs	Pb (II) and Cu^{2+}	140.06 & 149.25; 338.55 & 179.45; & 334.7 & 274.02	-	(Sachan, Ramesh and Das 2021)
Silica nanoparticles with 1-hydroxy-2-acetonaphthone	Cu^{2+}, Hg^{2+}, Zn (II), and Ni^{2+}	68.630, 50.942, 45.126, & 40.420	-	(Al-Wasidi *et al.* 2022a)
NZVI-SH-HMS	Pb (II) and Cd (II)	487.8 & 330.0	-	(Li *et al.* 2021)
Silica aerogel	Pd^{2+}	689.65	-	(Parale *et al.* 2023)
Mesoporous silica and chitosan-coated magnetite nanoparticles	Pb (II) and Cd (II)	150.33 &126.26	-	(Amin *et al.* 2023)

Silica with 4,6-diacetylresorcinol	Pb (II), Cu^{2+}, $Co^{2+,}$ and Ni^{2+}	107.066, 89.767, 80.580, & 70.972	-	(Al-Wasidi *et al.* 2022b)
Cellulose, silica nanoparticles, and heavy metal adsorption (Cd, Pb, Cr)				
DACSBNC	Cd (II), Hg^{2+}, and Pb (II)	12.23, 13.87, & 31.40	-	(Yarkulov *et al.* 2022)
Silica-cellulose	cadmium metal, chromium metal, nickel metal, and zinc metal	-	95.09, 58.77, 94.56, & 97.50	(Royanudin, Utomo and Wonorahardjo 2021)
cellulose-TiO_2/REC nanofibrous	Multiple adsorptions of Pb (II), Cu^{2+}, and Cd (II)	69.81	-	(Wang *et al.* 2021)
Cellulose and silica coupling agents in the absorption of heavy metals				
CAAS	As^{4+}	455	-	(Bisla, Kawamura and Yoshitake 2022)
APTES-CA	Pb (II)	180	-	(Shaheen, Radwan and El-Wakeel 2022)
Thiol-functionalized cellulose nanocrystals	Cu^{2+}	4.244	-	(Dang-Bao *et al.* 2023)

Thiol-functionalized cellulose nanofiber	Cu^{2+}, Cd (II), and Pb (II)	49.0, 45.9, & 22.0	-	(Choi *et al.* 2020)
Cys-CL	Cd (II) and Pb (II)	130.7 & 180.9		(Chen *et al.* 2022)
CysR	Pb (II)	143.47	-	(Peng *et al.* 2022)
MCNC-DPTA	Pb (II)	440.0	-	(Shen *et al.* 2022)
DPMC	Cu^{2+}	298.62	-	(Gao *et al.* 2022)

2.5 Discussion

The effectiveness of adsorbents in heavy metal removal is a crucial aspect of environmental remediation, with natural-fiber-based, silica-based, and cellulose–silica coupling agents demonstrating notable performance in various studies (Table 1). The Cd (II) and Pb (II) ions were shown to be adsorbed at 130.7 and 180.9 mg/g by the Cys-CL, respectively. All these studies demonstrated the Cys-CL's potential to remove Cd (II) and Pb (II) ions from water as an effective adsorbent. The Langmuir and pseudo-second order models accurately predicted the spontaneous and endothermic character of the adsorption of both metal ions by the Cys-CL. The Cys-CL has a high potential for the adsorptive removal of Cd (II) and Pb (II) from aqueous solutions due to its good adsorptive properties and recyclability.

Banana stem fibers, needle-felted fabric, and banana peel have shown high removal percentages for heavy metal ions such as Pb (II), Zn (II), and Cd (II) (Afolabi, Musonge and Bakare 2021; Ariharasudhan *et al.* 2022b). These natural-fiber-based materials offer several advantages, including their biodegradability, abundance, and low cost. The fibrous structure of these materials provides ample surface area for adsorption, while their inherent properties make them environmentally friendly options for heavy metal remediation in soil and water bodies (Sharma and Agrawal 2005). Silica nanoparticles and silica aerogels have exhibited remarkable adsorption capacities for a wide range of heavy metal ions, including Pb (II), Cu^{2+}, and Pd^{2+} (Al-Wasidi *et al.* 2022b; Parale *et al.* 2023). The high surface area and porous structure of silica-based materials contribute to their excellent adsorption properties, making them suitable for applications in industrial wastewater treatment and groundwater purification. Additionally, the stability of silica-based adsorbents under varying environmental conditions enhances their potential for long-term use in heavy metal removal processes.

Furthermore, coupling cellulose and silica with different functional groups, such as thiol-functionalized cellulose nanofiber and MCNC-DPTA, has demonstrated promising adsorption capacities for various heavy metal ions (Choi *et al.* 2020; Shen *et al.* 2022). These hybrid materials combine the advantages of both cellulose and silica, including abundant availability, low cost, and

favourable adsorption properties. The synergistic effects resulting from the combination of cellulose and silica further enhance the adsorption capacity and selectivity of these materials, making them suitable for tailored solutions in diverse environmental remediation scenarios.

2.5.1 Potential Applications in Real-World Scenarios

The diverse range of adsorbents offers opportunities for their application in real-world scenarios, including industrial wastewater treatment, agricultural runoff remediation, and groundwater purification. Natural-fiber-based adsorbents can be utilized in agricultural settings to mitigate heavy metal contamination in soil and water bodies, thereby promoting sustainable agriculture practices (Sharma and Agrawal 2005). Silica-based materials hold promise for industrial applications due to their high adsorption capacities and stability under varying environmental conditions, making them suitable for large-scale heavy metal removal processes (Parale *et al.* 2023). Cellulose and silica coupling agents offer customizable adsorption properties, allowing for tailored solutions to specific environmental remediation challenges, including point-source and non-point-source pollution (Choi *et al.* 2020).

2.5.2 Implications for Future Research Directions

Further research is needed to optimize the synthesis methods and functionalization techniques of adsorbents to enhance their adsorption capacities and selectivity for specific heavy metal ions. Exploring novel hybrid materials and surface modification strategies could lead to the development of more efficient adsorbents with improved performance and stability. Long-term studies evaluating the ecological impacts and sustainability of adsorbent-based remediation strategies are essential for assessing their viability in large-scale applications. Collaborative efforts between researchers, industry stakeholders, and policymakers are necessary to translate laboratory findings into practical solutions for addressing heavy metal pollution on a global scale.

2.6 Conclusions

Due to their characteristics, cellulose membranes could be used to lower the high cost of efficient application methods for water treatment. Due to its low cost, high removal efficiency, adaptable working conditions, selectivity, and good stability to remove heavy metal ions, adsorption is a promising approach that has attracted interest. Cellulose has a great affinity for substances with hydroxyl functional groups and is highly reactive with water. Additionally, cellulose contains hydroxyl groups (-OH), which are polar and hydrophilic (like water). The surface-located hydroxyl functional groups (-OH) of cellulose are essential for the adsorption of heavy metals. The ratio of metal/binding sites determines the adsorbent's capacity for adsorption, which explains how much adsorbent to use. The positively charged heavy metal ions and the OH functional groups of the cellulose adsorbents form hydrogen bonds, which lead to the establishment of adsorption. However, the lack of reactive functional groups and poor thermal and chemical resistance are disadvantages for cellulose. The most effective method of action for enhancing the performance of composites is the introduction of silica (SiO_2) into cellulose membranes, which provides design flexibility, permeation performance, durability enhancement, thermal stability, and increases its surface hydrophilicity.

A previous research investigation found that a silica–cellulose composite outperformed cellulose alone and silica alone in terms of hydrophilicity, water content, permeability, thermal stability, and the removal of heavy metal ions. Due to the presence of silanols (Si-OH), which are hydrophilic and have numerous reactive sites, on the surface of silica particles, the researchers found that adding silica to cellulose did not sufficiently modify it to bind to heavy metal ions. As a result, silane coupling agents ($Si(OR)_3$) are mainly utilized for silica surface modification. They can combine an organic polymer (cellulose) with inorganic substances like silica nanoparticles. To improve the structure of nanomaterials for the removal of heavy metals, the previous work showed that surface modification was performed on amines ($-NH_2$), thiols (-SH), carboxylic (-COOH), and methyl ($-CH_3$) groups. Previous studies have mostly shown that the adsorption process is best described by a pseudo-second order kinetic model.

Overall, the findings from this comprehensive review shed light on the critical role of adsorbents in mitigating heavy metal pollution, a pressing environmental issue with far-reaching implications. The significance of this review lies in its synthesis of current research, which offers a holistic understanding of the strengths and limitations of different adsorbents. By highlighting the promising performance of natural-fiber-based materials, silica-based compounds, and hybrid cellulose–silica agents, this review presents a roadmap for the development of effective and sustainable solutions for heavy metal remediation.

Moreover, this review underscores the importance of continued research efforts to optimize adsorbent synthesis methods, assess their environmental impact, and explore novel hybrid materials. Such endeavours are essential for translating laboratory findings into practical applications, ultimately contributing to the preservation of water quality, protection of ecosystems, and safeguarding of public health. In essence, this review serves as a valuable resource for advancing the field of heavy metal remediation, guiding future research directions, and facilitating the development of innovative adsorption technologies with real-world applications. Through collaborative efforts and interdisciplinary approaches, the insights gleaned from this review can pave the way for effective strategies to address heavy metal pollution and create a more sustainable future for generations to come.

2.7 References

Abdelkhalek, A., Ali, S. S., Sheng, Z., Zheng, L. and Hasanin, M. 2022. Lead removal from aqueous solution by green solid film based on cellulosic fiber extracted from the banana tree, doped in polyacrylamide. Fibers and Polymers, 23 (5): 1171-1181.

Abdelrahman, E. A., Abou El-Reash, Y., Youssef, H. M., Kotp, Y. H. and Hegazey, R. 2021. Utilization of rice husk and waste aluminum cans for the synthesis of some nanosized zeolite, zeolite/zeolite, and geopolymer/zeolite products for the efficient removal of Co (II), Cu (II), and Zn (II) ions from aqueous media. Journal of hazardous materials, 401: 123813.

Abdelrahman, E. A., Alharbi, A., Subaihi, A., Hameed, A. M., Almutairi, M. A., Algethami, F. K. and Youssef, H. M. 2020. Facile fabrication of novel analcime/sodium aluminum silicate hydrate

and zeolite Y/faujasite mesoporous nanocomposites for efficient removal of Cu (II) and Pb (II) ions from aqueous media. Journal of Materials Research and Technology, 9 (4): 7900-7914.

Abouzeid, R. E., Khiari, R., El-Wakil, N. and Dufresne, A. 2018. Current state and new trends in the use of cellulose nanomaterials for wastewater treatment. Biomacromolecules, 20 (2): 573-597.

Afolabi, F. O., Musonge, P. and Bakare, B. F. 2021. Evaluation of Lead (II) Removal from Wastewater Using Banana Peels: Optimization Study. Polish Journal of Environmental Studies, 30 (2)

Alaswad, S. O., Lakshmi, K. B., Sudha, P., Gomathi, T. and Arunachalam, P. 2020. Toxic heavy metal cadmium removal using chitosan and polypropylene-based fiber composite. International journal of biological macromolecules, 164: 1809-1824.

Al-Wasidi, A. S., Naglah, A. M., Saad, F. A. and Abdelrahman, E. A. 2022a. Modification of silica nanoparticles with 1-hydroxy-2-acetonaphthone as a novel composite for the efficient removal of Ni (II), Cu (II), Zn (II), and Hg (II) ions from aqueous media. Arabian Journal of Chemistry, 15 (8): 104010.

Al-Wasidi, A. S., Naglah, A. M., Saad, F. A. and Abdelrahman, E. A. 2022b. Modification of silica nanoparticles with 4, 6-diacetylresorcinol as a novel composite for the efficient removal of Pb (II), Cu (II), Co (II), and Ni (II) ions from aqueous media. Journal of Inorganic and Organometallic Polymers and Materials, 32 (6): 2332-2344.

Amin, K. F., Gulshan, F., Asrafuzzaman, F., Das, H., Rashid, R. and Hoque, S. M. 2023. Synthesis of mesoporous silica and chitosan-coated magnetite nanoparticles for heavy metal adsorption from wastewater. Environmental Nanotechnology, Monitoring & Management, 20: 100801.

Ariharasudhan, S., Chandrasekaran, P., Dhinakaran, M., Rameshbabu, V., Sundaresan, S., Natarajan, S. and Arunraj, A. 2022. Study of banana/cotton blended nonwoven fabric for lead and zinc adsorption. In: Proceedings of AIP Conference Proceedings. AIP Publishing LLC, 170008.

Barreto, A., Costa, M., Sombra, A., Rosa, D., Nascimento, R., Mazzetto, S. and Fechine, P. 2010. Chemically modified Banana stem fibers: structure, dielectrical properties and biodegradability. Journal of Polymers and the Environment, 18: 523-531.

Bhagat, S., Gedam, V. V. and Pathak, P. 2020. Adsorption/desorption, kinetics and equilibrium studies for the uptake of Cu (II) and Zn (II) onto Banana Peel. International Journal of Chemical Reactor Engineering, 18 (3): 20190109.

Bhatnagar, A., Hogland, W., Marques, M. and Sillanpää, M. 2013. An overview of the modification methods of activated carbon for its water treatment applications. Chemical Engineering Journal, 219: 499-511.

Bisla, V., Kawamura, I. and Yoshitake, H. 2022. Cross-linked cellulose acetate aminosilane (CAAS) for aqueous arsenic (V) adsorption. Carbohydrate Polymer Technologies and Applications, 4: 100259.

Carpenter, A. W., de Lannoy, C.-F. and Wiesner, M. R. 2015. Cellulose nanomaterials in water treatment technologies. Environmental science & technology, 49 (9): 5277-5287.

Cheah, C., Yue, C. S. and Ting, A. S. Y. 2021. Effects of heat and chemical pretreatments of banana peels for metal removal in single and multimetal systems. Water, Air, & Soil Pollution, 232: 1-14.

Chen, Y., Wang, X., Hao, D., Ding, Y. and Fan, H. 2022. Chelating cellulose functionalized with four amino acids: A comparative study on the enhanced adsorptive removal of cadmium and lead ions. Colloids and Surfaces A: Physicochemical and Engineering Aspects, 650: 129599.

Choi, H. Y., Bae, J. H., Hasegawa, Y., An, S., Kim, I. S., Lee, H. and Kim, M. 2020. Thiol-functionalized cellulose nanofiber membranes for the effective adsorption of heavy metal ions in water. Carbohydrate polymers, 234: 115881.

d'Halluin, M., Rull-Barrull, J., Bretel, G., Labrugère, C., Le Grognec, E. and Felpin, F.-X. 2017. Chemically modified cellulose filter paper for heavy metal remediation in water. ACS Sustainable Chemistry & Engineering, 5 (2): 1965-1973.

Dang-Bao, T., Nguyen, T.-M.-C., Hoang, G.-H., Lam, H.-H., Phan, H.-P. and Tran, T.-K.-A. 2023. Thiol-surface-engineered cellulose nanocrystals in favor of copper ion uptake. Polymers, 15 (11): 2562.

Di Natale, F., Gargiulo, V. and Alfè, M. 2020. Adsorption of heavy metals on silica-supported hydrophilic carbonaceous nanoparticles (SHNPs). Journal of hazardous materials, 393: 122374.

Dong, X. and Ge, Q. 2019. Metal ion-bridged forward osmosis membranes for efficient pharmaceutical wastewater reclamation. ACS applied materials & interfaces, 11 (40): 37163-37171.

Es-Haghi, H., Mirabedini, S., Imani, M. and Farnood, R. 2014. Preparation and characterization of pre-silane modified ethyl cellulose-based microcapsules containing linseed oil. Colloids and Surfaces A: Physicochemical and Engineering Aspects, 447: 71-80.

Fouda-Mbanga, B., Prabakaran, E. and Pillay, K. 2021. Carbohydrate biopolymers, lignin-based adsorbents for removal of heavy metals (Cd2+, Pb2+, Zn2+) from wastewater, regeneration and reuse for spent adsorbents including latent fingerprint detection: A review. Biotechnology Reports, 30: e00609.

Gao, J., Zhang, L., Liu, S. and Liu, X. 2022. Enhanced adsorption of copper ions from aqueous solution by two-step DTPA-modified magnetic cellulose hydrogel beads. International journal of biological macromolecules, 211: 689-699.

Gao, W., Liang, H., Ma, J., Han, M., Chen, Z.-l., Han, Z.-s. and Li, G.-b. 2011. Membrane fouling control in ultrafiltration technology for drinking water production: A review. Desalination, 272 (1-3): 1-8.

García Raurich, J., Martínez Roldán, T. and Monagas Asensio, P. 2020. Obtaining a bioadsorbent from orange peel suitable for batch and continous treatment. International Journal of Environmental & Agriculture Research (IJOEAR), 6 (2): 50-61.

Gharai, M. and Venugopal, R. 2016. Modeling of flotation process—An overview of different approaches. Mineral Processing and Extractive Metallurgy Review, 37 (2): 120-133.

Gupta, A. D., Kirti, N., Katiyar, P. and Singh, H. 2023. A critical review on three-dimensional cellulose-based aerogels: synthesis, physico-chemical characterizations and applications as adsorbents for heavy metals removal from water. Cellulose, 30 (6): 3397-3427.

Hao, S., Verlotta, A., Aprea, P., Pepe, F., Caputo, D. and Zhu, W. 2016. Optimal synthesis of amino-functionalized mesoporous silicas for the adsorption of heavy metal ions. Microporous and Mesoporous Materials, 236: 250-259.

Hojjati-Najafabadi, A., Mansoorianfar, M., Liang, T., Shahin, K. and Karimi-Maleh, H. 2022. A review on magnetic sensors for monitoring of hazardous pollutants in water resources. Science of the Total Environment, 824: 153844.

Hu, T., Hu, X., Tang, C. and Liu, D. 2022. Adsorbent grafted on cellulose by in situ synthesis of EDTA-like groups and its properties of metal ion adsorption from aqueous solution. Cellulose, 29 (2): 941-952.

Huzaisham, N. A., Marsi, N., Rus, A. Z. M., Masrol, S. R., Mahmood, S., Main, N. M., Fodzi, M. H. M., Singam, R. A. and Thana, P. 2020. Application of waste banana peels for wastewater treatment: a Review. Journal of Computational and Theoretical Nanoscience, 17 (2-3): 596-602.

Ince, M. and Ince, O. K. 2017. An overview of adsorption technique for heavy metal removal from water/wastewater: a critical review. International Journal of Pure and Applied Sciences, 3 (2): 10-19.

Ismanto, A., Hadibarata, T., Widada, S., Indrayanti, E., Ismunarti, D. H., Safinatunnajah, N., Kusumastuti, W., Dwiningsih, Y. and Alkahtani, J. 2023. Groundwater contamination status in Malaysia: level of heavy metal, source, health impact, and remediation technologies. Bioprocess and Biosystems Engineering, 46 (3): 467-482.

Jiang, J.Q. 2015. The role of coagulation in water treatment. Current Opinion in Chemical Engineering, 8: 36-44.

Jilal, I., El Barkany, S., Bahari, Z., Sundman, O., El Idrissi, A., Abou-Salama, M., Romane, A., Zannagui, C. and Amhamdi, H. 2018. New quaternized cellulose based on hydroxyethyl cellulose (HEC) grafted EDTA: synthesis, characterization and application for Pb (II) and Cu (II) removal. Carbohydrate polymers, 180: 156-167.

Joo, S. H. and Tansel, B. 2015. Novel technologies for reverse osmosis concentrate treatment: A review. Journal of Environmental Management, 150: 322-335.

Kalia, S., Kaith, B. and Kaur, I. 2009. Pretreatments of natural fibers and their application as reinforcing material in polymer composites—a review. Polymer Engineering & Science, 49 (7): 1253-1272.

Karim, Z., Hakalahti, M., Tammelin, T. and Mathew, A. P. 2017. In situ TEMPO surface functionalization of nanocellulose membranes for enhanced adsorption of metal ions from aqueous medium. RSC advances, 7 (9): 5232-5241.

Khulbe, K. and Matsuura, T. 2018. Removal of heavy metals and pollutants by membrane adsorption techniques. Applied Water Science, 8: 1-30.

Li, S., Li, S., Wen, N., Wei, D. and Zhang, Y. 2021. Highly effective removal of lead and cadmium ions from wastewater by bifunctional magnetic mesoporous silica. Separation and Purification Technology, 265: 118341.

Li, X., Tabil, L. G. and Panigrahi, S. 2007. Chemical treatments of natural fiber for use in natural fiber-reinforced composites: a review. Journal of Polymers and the Environment, 15: 25-33.

Lucia, A., Bacher, M., van Herwijnen, H. W. and Rosenau, T. 2020. A direct silanization protocol for dialdehyde cellulose. Molecules, 25 (10): 2458.

Maksoud, M. A., Elgarahy, A. M., Farrell, C., Ala'a, H., Rooney, D. W. and Osman, A. I. 2020. Insight on water remediation application using magnetic nanomaterials and biosorbents. Coordination Chemistry Reviews, 403: 213096.

Malik, D., Jain, C. and Yadav, A. K. 2017. Removal of heavy metals from emerging cellulosic low-cost adsorbents: a review. Applied Water Science, 7: 2113-2136.

Malik, S., Kishore, S., Shah, M. P. and Kumar, S. A. 2022. A comprehensive review on nanobiotechnology for bioremediation of heavy metals from wastewater. Journal of Basic Microbiology, 62 (3-4): 361-375.

Mautner, A., Kobkeatthawin, T. and Bismarck, A. 2017. Efficient continuous removal of nitrates from water with cationic cellulose nanopaper membranes. Resource-Efficient Technologies, 3 (1): 22-28.

Mautner, A., Kwaw, Y., Weiland, K., Mvubu, M., Botha, A., John, M. J., Mtibe, A., Siqueira, G. and Bismarck, A. 2019. Natural fibre-nanocellulose composite filters for the removal of heavy metal ions from water. Industrial Crops and Products, 133: 325-332.

Mei, Y. and Tang, C. Y. 2018. Recent developments and future perspectives of reverse electrodialysis technology: A review. Desalination, 425: 156-174.

Mohammad, A. W., Teow, Y., Ang, W., Chung, Y., Oatley-Radcliffe, D. and Hilal, N. 2015. Nanofiltration membranes review: Recent advances and future prospects. Desalination, 356: 226-254.

Mubarak, M. F., Ragab, A. H., Hosny, R., Ahmed, I. A., Ahmed, H. A., El-Bahy, S. M. and El Shahawy, A. 2021. Enhanced performance of chitosan via a novel quaternary magnetic nanocomposite chitosan/grafted halloysitenanotubes@ ZnγFe3O4 for uptake of Cr (III), Fe (III), and Mn (II) from wastewater. Polymers, 13 (16): 2714.

Mubarak, M. F., Zayed, A. M. and Ahmed, H. A. 2022. Activated Carbon/Carborundum@ Microcrystalline Cellulose core shell nanocomposite: Synthesis, characterization and application for heavy metals adsorption from aqueous solutions. Industrial Crops and Products, 182: 114896.

Nasef, M. M. and Ujang, Z. 2012. Introduction to ion exchange processes. Ion Exchange Technology I: Theory and Materials: 1-39.

Parale, V. G., Choi, H., Kim, T., Phadtare, V. D., Dhavale, R. P., Lee, K.Y., Panda, A. and Park, H.H. 2023. One pot synthesis of hybrid silica aerogels with improved mechanical properties and

heavy metal adsorption: Synergistic effect of in situ epoxy-thiol polymerization and sol-gel process. Separation and Purification Technology, 308: 122934.

Peng, L., Zhang, M., Dong, Z., Qi, W., Zhai, M. and Zhao, L. 2022. Efficient and selective adsorption of Pd (II) by amino acid-functionalized cellulose microspheres and their applications in palladium recovery from PCBs leaching solution. Separation and Purification Technology, 301: 122037.

Radjenovic, J. and Sedlak, D. L. 2015. Challenges and opportunities for electrochemical processes as next-generation technologies for the treatment of contaminated water. Environmental science & technology, 49 (19): 11292-11302.

Rajendran, S., Priya, A., Kumar, P. S., Hoang, T. K., Sekar, K., Chong, K. Y., Khoo, K. S., Ng, H. S. and Show, P. L. 2022. A critical and recent developments on adsorption technique for removal of heavy metals from wastewater-A review. Chemosphere, 303: 135146.

Rana, V., Bandyopadhyay, S. and Maiti, S. K. 2022. Bioadsorbents for Industrial Wastewater Treatment. In: Encyclopedia of Green Materials. Springer, 1-11.

Rangaraj, S. and Venkatachalam, R. 2017. A lucrative chemical processing of bamboo leaf biomass to synthesize biocompatible amorphous silica nanoparticles of biomedical importance. Applied Nanoscience, 7: 145-153.

Rovani, S., Santos, J. J., Corio, P. and Fungaro, D. A. 2018. Highly pure silica nanoparticles with high adsorption capacity obtained from sugarcane waste ash. ACS omega, 3 (3): 2618-2627.

Royanudin, M., Utomo, Y. and Wonorahardjo, S. 2021. The application of silica-cellulose material as heavy metal adsorbent on laboratory wastewater. In: Proceedings of AIP Conference Proceedings. AIP Publishing LLC, 030123.

Šabanović, E., Memić, M., Sulejmanović, J. and Selović, A. 2020. Simultaneous adsorption of heavy metals from water by novel lemon-peel based biomaterial. Polish journal of chemical technology, 22 (1): 46-53.

Sachan, D., Ramesh, A. and Das, G. 2021. Green synthesis of silica nanoparticles from leaf biomass and its application to remove heavy metals from synthetic wastewater: A comparative analysis. Environmental Nanotechnology, Monitoring & Management, 16: 100467.

Selambakkannu, S., Othman, N. A. F., Bakar, K. A., Shukor, S. A. and Karim, Z. A. 2018. A kinetic and mechanistic study of adsorptive removal of metal ions by imidazole-functionalized polymer graft Banana stem fibers. Radiation Physics and Chemistry, 153: 58-69.

Sgriccia, N., Hawley, M. and Misra, M. 2008. Characterization of natural fiber surfaces and natural fiber composites. Composites Part A: Applied Science and Manufacturing, 39 (10): 1632-1637.

Shaheen, T. I., Radwan, E. K. and El-Wakeel, S. T. 2022. Unary and binary adsorption of anionic dye and toxic metal from wastewater using 3-aminopropyltriethoxysilane functionalized porous cellulose acetate microspheres. Microporous and Mesoporous Materials, 338: 111996.

Sharma, H. K., Sofi, I. R. and Wani, K. A. 2018. Low-cost absorbents, techniques, and heavy metal removal efficiency. In: Biostimulation Remediation Technologies for Groundwater Contaminants. IGI Global, 50-79.

Sharma, R. K. and Agrawal, M. 2005. Biological effects of heavy metals: an overview. Journal of environmental Biology, 26 (2): 301-313.

Shen, J., Jiang, F., Wang, N., Ouyang, X. k. and Jin, M.-c. 2022. Diethylenetriaminepentaacetic acid (DPTA)-modified magnetic cellulose nanocrystals can efficiently remove Pb (II) from aqueous solution. Journal of Polymers and the Environment, 30 (4): 1344-1354.

Sheng, Z., Shen, Y., Dai, H., Pan, S., Ai, B., Zheng, L., Zheng, X. and Xu, Z. 2018. Physicochemical characterization of raw and modified banana pseudostem fibers and their adsorption capacities for heavy metal Pb^{2+} and Cd^{2+} in water. Polymer Composites, 39 (6): 1869-1877.

Solyman, S. M. and Ahmed, H. A. 2022. Treatment of industrial dye effluent by photo-catalytic process using modified Egyptian Bentonite. Egyptian Journal of Chemistry, 65 (4): 333-340.

Sörme, L. and Lagerkvist, R. 2002. Sources of heavy metals in urban wastewater in Stockholm. Science of the Total Environment, 298 (1-3): 131-145.

Su, K., Zhao, D., Lu, A., Zhong, C., Shen, X.-C. and Ruan, C. 2022. One-pot green synthesis of poly (hexamethylenediamine-tannic acid)-bacterial cellulose composite for the reduction, immobilization, and recovery of Cr (VI). Journal of Environmental Chemical Engineering, 10 (1): 107026.

Syeda, H. I. and Yap, P.S. 2022. A review on three-dimensional cellulose-based aerogels for the removal of heavy metals from water. Science of the Total Environment, 807: 150606.

Van der Bruggen, B., Vandecasteele, C., Van Gestel, T., Doyen, W. and Leysen, R. 2003. A review of pressure-driven membrane processes in wastewater treatment and drinking water production. Environmental progress, 22 (1): 46-56.

Vasileva-Tcankova, R. S. 2022. Global Ecological Problems of Modern Society. Acta Scientifica Naturalis, 9 (2): 63-86.

Wang, C., Zhan, Y., Wu, Y., Shi, X., Du, Y., Luo, Y. and Deng, H. 2021. TiO_2/rectorite-trapped cellulose composite nanofibrous mats for multiple heavy metal adsorption. International journal of biological macromolecules, 183: 245-253.

Wang, J. and Chen, C. 2009. Biosorbents for heavy metals removal and their future. Biotechnology advances, 27 (2): 195-226.

Wang, L. K., Vaccari, D. A., Li, Y. and Shammas, N. K. 2005. Chemical precipitation. In: Physicochemical treatment processes. Springer, 141-197.

Wang, P., Du, M., Zhu, H., Bao, S., Yang, T. and Zou, M. 2015. Structure regulation of silica nanotubes and their adsorption behaviors for heavy metal ions: pH effect, kinetics, isotherms and mechanism. Journal of hazardous materials, 286: 533-544.

Worch, E. 2012. Adsorption technology in water treatment. de Gruyter Berlin.

Yang, S., Chen, S., Fan, J., Shang, T., Huang, D. and Li, G. 2019. Novel mesoporous organosilica nanoparticles with ferrocene group for efficient removal of contaminants from wastewater. Journal of colloid and interface science, 554: 565-571.

Yarkulov, A., Umarov, B., Rakhmatkarieva, F., Kattaev, N., Akbarov, K. and Berdimurodov, E. 2022. Diacetate cellulose-silicon bionanocomposite adsorbent for recovery of heavy metal ions and benzene vapours: An experimental and theoretical investigation. Biointerface Research in Applied Chemistry-Open-Access Journal, 12: 2862-2880.

Youssef, H. M., Shah, R. K., Algethami, F. K., Hegazey, R., Naglah, A. M., Al-Omar, M. A., Alluhaybi, A. A., Alherbish, H. A., Mabrouk, E. and Abdelrahman, E. A. 2021. Facile hydrothermal procedure for the synthesis of sodium aluminum silicate hydrate/analcime and analcime for effective removal of manganese (II) ions from aqueous solutions. Journal of Inorganic and Organometallic Polymers and Materials, 31: 1035-1046.

Zhao, X. and Liu, C. 2019. Efficient removal of heavy metal ions based on the selective hydrophilic channels. Chemical Engineering Journal, 359: 1644-1651.

Zito, P. and Shipley, H. J. 2015. Inorganic nano-adsorbents for the removal of heavy metals and arsenic: a review. RSC advances, 5 (38): 29885-29907.

Chapter Three

Amine-functionalized cellulose-silica composites for the remediation of hexavalent chromium (Cr (VI)) in contaminated water

This chapter has been published as:

Mayenzeke Trueman Mazibuko, Stanley Chibuzor Onwubu, Phumlane Selby Mdluli, Vimla Paul, Mokhena Clement Teboho, Mokhothu Thabang, 2024. Amine-functionalized cellulose-silica composites for the remediation of hexavalent chromium (Cr IV) in contaminated water. Results in Chemistry, 11, p.101796. https://doi.org/10.1016/j.rechem.2024.101796

3.1 Abstract

Adsorption method for Hexavalent chromium (Cr (VI) removal from domestic and industrial wastewater is widely desirable due to public health concerns of the heavy metal. The purpose of this study was to investigate the evaluation of Cr (VI) adsorption using a novel adsorbent: amine-functionalized cellulose-silica composite derived from Banana stem fibers. We employed the in-situ sol–gel method to create cellulose-silica silane functionalized composites, analyzing them through different characterization techniques such as Attenuated total reflectance- Fourier transform infrared spectroscopy (ATR-FTIR), X-ray Diffraction Analysis (XRD), thermogravimetric analysis (TGA)/differential thermogravimetric (DTG), Brunauer–Emmett–Teller (BET), Scanning electron microscopy (SEM), and transmission electron microscopy (TEM) techniques. ATR-FTIR depicted key organic constituents in raw banana pseudo-stem fibers (BF) and the formation of Si–O bonds in BC–SiO_2 composite and further enhanced by the grafting of N-[3-(trimethoxysilyl)propyl ethylenediamine (DAPTMS) onto the BC-SiO_2 surface in BC-SiO_2-DAPTMS. XRD and TGA analyses revealed changes in crystallinity and thermal stability, while BET analysis showcased altered surface area and pore characteristics in BC-SiO_2-DAPTMS (2%). SEM and TEM imaging provided visual evidence of structural modifications and improved dispersion in BC-SiO_2-DAPTMS composites. The impact of composite weight, contact time, and pH on Cr (VI) removal rates was examined, revealing optimal performance at slightly acidic pH 4 value (80.7 %) and enhanced efficiency with increased contact time of 65 min (86.66 %),

composite weight of 1 g (82.62 %), and initial concentration was for 0.8 mg/l (80 %). The kinetics and isotherms analyzed using pseudo-second order (PSO) and pseudo-first order (PFO) models highlight the composite's efficiency. The Freundlich model was found to better fit the adsorption isotherm data, while the PSO model described the kinetics more accurately. These insights contribute to optimizing the BC-SiO_2-DAPTMS (2%) composite for efficient Cr (VI) ion removal in water treatment applications.

Keywords: Hexavalent chromium (Cr (VI)) Adsorption, Adsorption isotherms, Bleach Cellulose, Silica, Composites, Adsorption kinetics

3.2 Introduction

Hexavalent chromium (Cr (VI)) is a highly toxic heavy metal pollutant commonly found in industrial activities such as metal plating, leather tanning, and textile dyeing processes. It is well-known for its carcinogenicity and adverse effects on human health (Sarin, Singh and Pant 2006; Prasad *et al.* 2021). Classified as a Group (1) carcinogen by the International Agency for Research on Cancer (IARC), alongside cadmium, Cr (VI) is also listed as a priority substance on the Agency for Toxic Substances and Disease Registry's (ATSDR) Substances Priority List (SPL) (I.A.R.C 2021; A.T.S.D.R 2022). The World Health Organization (WHO) has set the allowable limit for chromium in drinking water at 0.05 mg/L, underscoring its hazardous nature (W.H.O 2017). Additionally, the National Toxicology Program (NTP) identifies chromium as a known human carcinogen (N.T.P 2016).

Chromium exists in various valence states, with Cr (III) and Cr (VI) being the most common and stable forms (Mukherjee *et al.* 2012). Cr (VI) is particularly concerning due to its carcinogenic properties and extensive industrial applications, which often lead to its transformation from Cr (III) in wastewater (Islam *et al.* 2023). Cr (VI) salts exhibit higher solubility compared to Cr (III) salts, making them moderately mobile in water (Rakhunde, Deshpande and Juneja 2012). The major forms of Cr (VI) in aqueous solutions include chromate and dichromate, both of which possess strong oxidative and soluble properties (Zhang and Tian 2020; Chen and Tian 2021).

Traditionally, Cr (VI) ions are removed through chemical treatments that reduce Cr (VI) to Cr (III), precipitating it as $Cr(OH)_3$. Modern methods, such as membrane separation, ion exchange, and hexavalent chromium reduction techniques, reflect advancements in environmental remediation technologies (Terry 2004; Alvarez-Ayuso and Nugteren 2005; Li, Li and Yang 2016; Sun *et al.* 2017), reflecting advancements in environmental remediation technologies. Adsorption processes have gained significant attention as efficient and cost-effective methods for Cr (VI) removal due to their high adsorption capacities and ease of operation (Madhubashani *et al.* 2021). Composite materials, particularly those based on cellulose and silica matrices, have shown great potential in heavy metal adsorption because of their abundant availability, eco-friendliness, and tunable surface properties (Gupta *et al.* 2023). Amine functionalization of cellulose-silica composites has been explored as a strategy to enhance their adsorption capabilities for heavy metals (Hong *et al.* 2015). The introduction of amine groups onto the composite surface increases the affinity for metal ions through complexation and ion exchange mechanisms, thereby improving adsorption efficiency (Bisla, Kawamura and Yoshitake 2022).

Previous studies have investigated the synthesis and characterization of amine-functionalized cellulose-silica composites and their application in heavy metal removal. Cellulose/silica carrier particles functionalized with tetraethylenepentamine (SiO_2@Cel-TEPA) were successfully used by Yousif and colleagues for the detection and removal of copper (II) ions in contaminated waters (Yousif *et al.* 2019). The synthesized SiO_2@Cel-TEPA material showed high sensitivity to Cu (II) ions even at trace concentrations and maintained functionality for reuse and recycling without significant performance degradation. Similarly, (Jamroz *et al.* 2019) studied the adsorption performance of amino-silanized cellulose membranes for selectively removing hexavalent chromium ions. They emphasized the role of surface amine functional groups in enhancing adsorption efficiency and that the adsorption capacity correlates with the number of protonated amino groups on the membrane surface. Ali et al. investigated the use of Artemisia monosperma plant powder impregnated with trimethyloctadecylammonium bromide (TMOA-Br) as an eco-friendly and cost-effective adsorbent for the removal of hexavalent chromium (Cr (VI)) from contaminated groundwater. They reported that modified powder showed efficient/selective adsorption towards the hazardous Cr(VI) ions (Ali *et al.* 2021). Similarly, Alrowaili et al.

successfully fabricated silver-imprinted Titania/silica nanospheres ($Ag@TiO_2/SiO_2$) and employed them for photocatalytic wastewater purification under visible light. Their study found a significant increase in pollutant degradation efficiency (Alrowaili *et al.* 2020). More recently, Alshammari et al. investigated the adsorption performance of hexavalent chromium (Cr (VI)) from aqueous solutions using α-Fe_2O_3 (hematite)-coated hydroxy magnesium silicate (HMS) as an adsorbent. The study systematically examined adsorption behaviour by varying parameters such as contact time, pH, initial metal concentration, and temperature. The results indicated that Cr (VI) adsorption onto the α-Fe_2O_3/HMS composite fit well with the Langmuir isotherm model, suggesting monolayer adsorption (Alshammari *et al.* 2023).

Low-cost adsorbents derived from industrial or agricultural waste streams have received increased attention (Romero-Cano, Gonzalez-Gutierrez and Baldenegro-Perez 2016). Agricultural by-products are being widely used for adsorption with or without modification. Particularly, Banana stem fibers are widely available globally as agricultural waste from banana cultivation (Abdelkhalek *et al.* 2022). Banana stem fibers are environmentally friendly and possess important attributes such as low density, light weight, and low cost (Abdel-Khalek, Hamed and Hasheesh 2021). This waste, consisting of leaves, stems, and rhizomes, is left in the field for natural degradation for months after fruit harvesting and can be utilized in different applications, including cellulose production and heavy metal adsorption from water (Bagali, Gowrishankar and Roy 2017; Huzaisham and Marsi 2020; Abdel-Khalek, Hamed and Hasheesh 2021).

However, there is a gap in the literature regarding the functionalization of cellulose with silica extracted from agricultural waste like Banana stem fibers. This study aims to address this gap by conducting an experimental investigation focused on the evaluation of Cr (VI) adsorption using a novel adsorbent: amine-functionalized cellulose-silica composite derived from Banana stem fibers. We employed the in-situ sol–gel method to create cellulose-silica silane functionalized composites, utilizing N-[3-(trimethoxysilyl)propyl ethylenediamine (DAPTMS) as an amine-based silane coupling agent and tetraethoxysilane (TEOS) as the silica precursor. This composite can serve as an effective heavy metal adsorbent, with chromium (Cr (VI)) chosen due to its high toxicity. We assessed several parameters, such as contact time, pH, concentration, and absorbent

dosage, on the adsorption properties. Additionally, we performed equilibrium and kinetic studies to evaluate different adsorption conditions. The outcomes of this study are expected to contribute to the development of efficient adsorbents for Cr (VI) removal from contaminated water sources, with potential applications in wastewater treatment and environmental remediation.

3.3 Materials and methods

Samples of banana pseudo-stems without any disease symptoms were collected from a Nanda farm, South Africa. Potassium hydroxide (KOH) and sodium hypochlorite (NaOCl) were purchased from Associated Chemical Enterprises Pty Ltd (ACE) (South Africa, Johannesburg). N-[3- (trimethoxysilyl)propyl 97 % (DAPTMS), ethanol (C_2H_6O), and tetraethoxysilane (TEOS) with a density of 0.933 g/ml, glycerol (99.5 %, and 1,5-diphenylcarbazide were all purchased from Sigma-Aldrich. Deionised water (18.2 MΩcm specific resistance) was collected from the Aqua MAX-Basic 360 Series water purification system. Potassium dichromate AR ($K_2Cr_2O_7$) was purchased from Minema Chemicals (Gauteng, Clockwork Tower Road, South Africa). All chemicals and reagents were of analytical grade and ready to use.

3.3.1 Bleach cellulose extraction

Banana stem fibers, pseudo stem, were collected from Nanda farm, South Africa were directly chopped to about 2 cm in length. They were then air-dried at 100℃ overnight in a Scientific Lab Oven – 2000 Series. Next, the dried stems were ground into a fine powder using a Chetak Mixer Grinder heavy-duty machine with a stainless-steel jar and blades. The resulting dry samples were stored in sealed plastic bags at room temperature. For the treatment process, as depicted in schematic 1, 500 g of Banana stem fibers underwent two cycles of treatment with 2 % sodium hydroxide (NaOH) and potassium hydroxide (KOH) solutions, each lasting an hour, in a 5-liter beaker at 100 ℃ (Figure 4.1). After each treatment, the fibers were thoroughly rinsed with deionized water until reaching a neutral pH. Subsequently, the fibers were treated with a 2 % sodium hypochlorite (NaOCl) bleaching solution for an additional hour at 100℃ to extract the cellulose. The entire treatment process, including treatments and rinsing steps, lasted three hours.

After bleaching, the bleached cellulose (BC) was rinsed again with deionized water to neutralize the pH and dried overnight at room temperature.

3.3.2 Synthesis of amine functionalized cellulose-silica composite

The composite material was synthesized following a modified approach to introduce amine functional groups onto the cellulose-silica matrix. The in-situ sol–gel method was employed to create cellulose-silica silane functionalized composites, utilizing N-[3-(trimethoxysilyl) propyl ethylenediamine (DAPTMS) as an amine-based silane coupling agent and tetraethoxysilane (TEOS) as the silica precursor. The synthesis of BC-SiO_2-DAPTMS composites followed a specific procedure: BC/SiO_2 (w/w) at a 1:1 ratio was initially added. To synthesize SiO_2 nanoparticles within cellulose structures, TEOS, H_2O, ethanol, and NaOH catalyst were combined in a 1:4:4:3.52 mol ratio. The sequence of addition was BC first, followed by TEOS, H_2O, ethanol, and NaOH catalyst, each in the specified ratio, for three hours. Afterward, a 2 % concentration of the amine-based silane coupling agent was added. The reaction mixtures underwent mechanical stirring and were heated to 80℃ for an additional 3 h, completing a total reaction time of 6 h.

A 10 % glycerol solution was prepared by combining 10 mL of glycerol and 90 mL of deionized water. Glycerol was added to improve the adhesion properties of the composite material, promoting better bonding between the components, such as cellulose, silica, and DAPTMS, leading to a more cohesive and stable structure. A BC-SiO_2-DAPTMS composite: glycerol (1:10), the BC-SiO_2-DAPTMS composite was measured out, and the appropriate amount of 10 % aqueous glycerol solution was poured into a glass beaker (using 10 ml of 10 % glycerol solution for every 1.0 g of BC-SiO_2-DAPTMS composite). The mixture was stirred with a glass rod, then a magnetic stirrer bar was employed to thoroughly blend the mixture on a hot plate set at 100 ℃ until it achieved complete homogenization. Finally, to complete the cross-linking of the composite, which resembled a dry paste-like dough, was transferred and allowed to dry in an oven at 120 ℃ for 48 h.

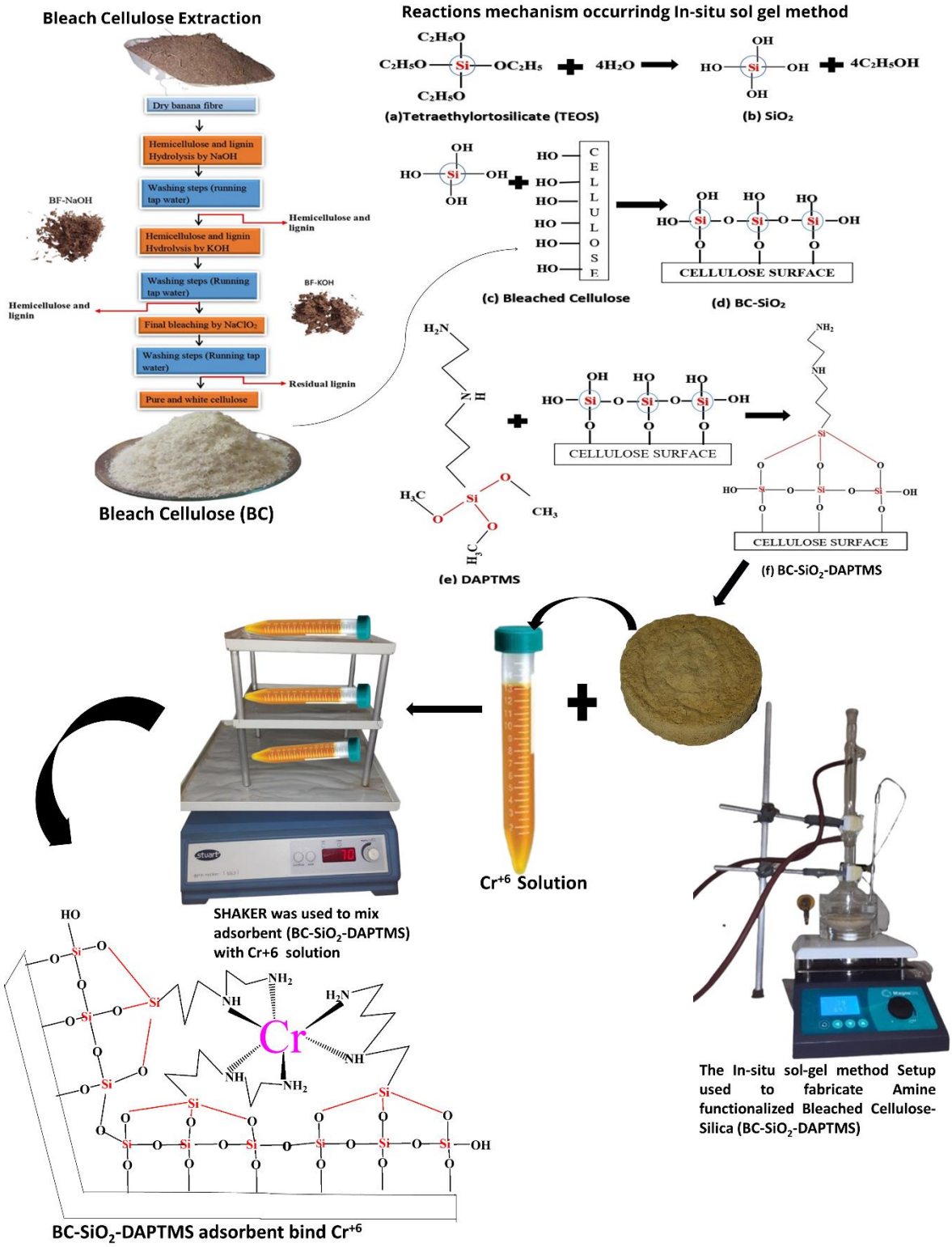

Figure 23.1 Schematic diagram of the extraction of cellulose from banana stem fibre, and the reaction mechanism occurring in-situ gel method.

3.3.3 Characterization techniques

The morphology and chemical composition of the prepared samples were analysed using a Tescan Vega 3 scanning electron microscope (SEM) equipped with an Oxford X-MaxN energy dispersive X-ray spectrometer (EDS). Attenuated total reflectance- Fourier transform infrared spectroscopy (ATR-FTIR) spectra of BF, BC, commercial cellulose (CC), silica (SiO_2), BC-SiO_2, and BC-SiO_2-DAPTMS were obtained using a Perkin Elmer Spectrum System (Perkin Elmer FTIR spectrometer Frontier). The samples were analysed over a range of 400 – 4000 cm^{-1}, and all the spectra were averaged over 16 scans.

The crystal structures of the cellulose were determined with a D8 Bruker AXS Discover diffractometer with CuKα (1.5418 Å) radiation. Powder X-ray diffraction patterns for structure and phase identification were carried out using a Bruker D8 Advance diffractometer equipped with a graphite monochromatic filter operated at 40 kV and 40 mA (Billerica, M.A., USA). The radiation source was CuKα with a λ of 1.5406 nm. The percentage crystallinity (%Cr) was calculated from Equation 3.1 below (Sohaimy and Isa 2020):

$$\%Crystallinity = \left(\frac{\text{Area Crystilline peaks}}{\text{Total Area Crystilline}}\right) \times 100\% \qquad (3.1)$$

Where the area crystalline and area amorphous are the crystalline and amorphous intensities at 2θ scale close to 22° and 15° respectively.

The thermal degradation of synthesized BC-SiO_2-DAPTMS was done using the thermogravimetric analyzer. TGA is a thermos-analytical technique in which changes in weight are measured as a function of increasing temperatures. TGA analysis was performed in the following parameters: thermal analyser at a heating rate of 10 ℃ /min in a flow rate of nitrogen gas: 20 ml/min and a final temperature range from 25 to 600 ℃.

3.3.4 Batch adsorption experiments

Batch adsorption experiments were conducted to evaluate the adsorption capacity of the composite for Cr (VI) removal. The experimental setup, initial concentration of Cr (VI), contact time, pH, and temperature conditions are described. The study employed the diphenylcarbazide method for quantifying hexavalent chromium (Cr (VI)) ions, using 1,5-diphenylcarbazide (DPC) as a complex-forming reagent with chromium ions, detectable via spectrophotometry. Calibration standards were prepared by creating a stock solution of 200 ppm $K_2Cr_2O_7$, from which 125 ppm and 5 ppm standard solutions were derived. These standards were used to calibrate the spectrophotometer for subsequent analysis.

The adsorption efficiency of hexavalent chromium (Cr (VI)) ions using BC-SiO_2-DAPTMS (2%) was investigated under various operational variables. Adsorption tests were conducted in plastic centrifuge tubes with varying amounts of adsorbents and Cr (VI) solutions at different concentrations, agitated using a rotating rocker, and separated using a centrifuge. The effect of initial metal ion concentration, adsorbent dose, and pH on adsorption efficiency was systematically studied by adjusting parameters and analysing samples via spectrophotometry. Additionally, the effect of contact time on Cr (VI) adsorption onto BC-SiO_2-DAPTMS was investigated by varying the mixing durations and analyzing the resulting solutions spectrophotometrically. The analysis of Cr (VI) adsorption kinetics and isotherms on the composite material aims to comprehend the adsorption mechanism and capacity. Experimental data is fitted with kinetic models and isotherm equations. The quantity of Cr (VI) absorbed per unit of adsorbent (Qt) is calculated using the Equation 3.2:

$$Q_t = (C_i - C_t) \times \left(\frac{V}{M}\right) \tag{3.2}$$

The Cr (VI) removal percentage (R % is determined using the Equation 3.3:

$$R\% = \left(\frac{C_i - C_t}{C_i}\right) \times 100\% \tag{3.3}$$

Here, C_i represents the initial concentration, C_t represents the concentration at time, V represents the volume of the solution (l), and *M* represents the mass (g) of the added sorbent. All experiments were repeated three times under the same conditions, and the average values were recorded to minimize experimental uncertainties.

3.3.4.1 Equilibrium experiment

20 ml of Cr (VI) aqueous solutions with concentrations ranging from 0.1 to 1.0 mg/L were placed individually in 50 ml plastic centrifuge tubes. The pH was adjusted to neutral using NaOH and HCl. 0.5 g of BC- SiO_2-DAPTMS adsorbents was added to each tube for equilibrium studies. The solutions were mixed in a shaker at 21℃ for 30 min at 70 rpm and centrifuged for 5 min to separate the solids from the liquids. This was followed by transferring 5 ml of each standard into 15 ml plastic tubes for spectrophotometric analysis. To gain insights into how adsorbents remove metal ions from water, different adsorption isotherm models (Langmuir and Freundlich) were examined to understand how metal ions interact with the adsorbent. Each isotherm model has specific constants that describe the surface properties and how well the adsorbent attracts ions (Freundlich 1906; Langmuir 1916).

3.3.4.1.1 Langmuir model.

The Langmuir Model applies to adsorption where a monolayer forms on the surface with a limited number of evenly distributed sites. It's represented by Equation 3.4:

$$\frac{C_{eq}}{q_{eq}} = \frac{1}{Kq_{max}} + \frac{C_{eq}}{q_{max}} \quad (3.4)$$

Here, q_{eq} is the amount of Cr (VI) adsorbed when equilibrium is reached, C_{eq} is the equilibrium concentration in the solution, q_{max} is the maximum adsorption capacity, and K is the adsorption equilibrium constant. Plotting C_{eq}/q_{eq} against C_{eq} yields a straight line with a slope of $1/q_{max}$ and an intercept of $1/Kq_{max}$.

3.3.4.1.2 Freundlich model.

The Freundlich Model, derived from adsorption on a heterogeneous surface, accounts for non-identical and/ or non-uniform binding sites according to Equation 3.5:

$$lnq_{eq} = lnK_F + \frac{1}{n} lnC_{eq} \quad (3.5)$$

Here, K_F represents adsorption capacity, and n indicates adsorption intensity. Plotting lnq_{eq} against lnC_{eq} helps determine K_F and $1/n$.

3.3.4.2 Kinetic experiment

For kinetic experiments, various sorption models under different conditions were used to study the sorption mechanism. Specifically, the pseudo-first order and pseudo-second order models were employed to understand how Cr (VI) adsorbs onto BC-SiO_2-DAPTMS (2%). 20 ml of 0.7 mg/L Cr (VI) aqueous solutions was transferred into a 50 ml plastic centrifuge tube using a pipette. The pH was adjusted to neutral using NaOH and HCl. 0.5 g of BC-SiO_2-DAPTMS adsorbents was added to each tube for equilibrium studies. The tubes were centrifuged at room temperature (21°C) for 5–65 min at 70 rpm to separate the solid from the liquid, followed by transferring 5 ml of each standard into 15 ml plastic tubes for spectrophotometric analysis. To find out how Cr (VI) adsorbs onto BC-SiO_2-DAPTMS, pseudo-first-order and pseudo-second- order models were explored. (Lagergren 1898) introduced a linear pseudo-first order kinetic model, described as follows. The integrated form of the model is given by Equation 3.6:

$$log(q_{eq} - q_t) = logq_{eq} - \frac{k_1}{2.303} t \quad (3.6)$$

In this equation, q_t represents the amount of Cr (VI) adsorbed at time t (minutes), q_{eq} is the amount of Cr (VI) adsorbed at equilibrium, and k_1 is the rate constant for pseudo-first-order adsorption. This model can also be presented linearly to describe adsorption kinetics.

The pseudo-second order reaction (Ho and McKay 1999) Equation 3.7 can be expressed in its integrated linear form as:

$$\frac{t}{q_t} = \frac{1}{k_2\, q_{eq}^2} + \frac{1}{q_{eq}} t \qquad (3.7)$$

Here, k_2 represents the rate constant for pseudo-second order Cr (VI) adsorption. By plotting t/q_t against t, a linear relationship is observed. This linear correlation allows the determination of q_{eq} and k_2 from the slope and intercept of the plot, respectively, if the second-order kinetic equation is applicable.

3.4 Results and discussion

3.4.1 Characterization of composite material

Characterization results, including SEM images, FTIR spectra, and surface area analysis, provide insights into the structural and functional properties of the amine-functionalized cellulose-silica composite.

3.4.1.1 ATR-FTIR analysis

ATR-FTIR analysis was employed to assess structural changes in banana pseudo-stem fiber before and after chemical treatment. Figure 3.2(a) illustrates the IR spectra of various samples, including raw banana pseudo-stem fibers (BF), alkali-treated fibers (BF-KOH and BF-NaOH), while Figure 3.2(b) illustrates the bleached cellulose (BC) and commercial cellulose (CC). In the BF spectrum, characteristic peaks were observed at 3500 cm^{-1} (OH stretching), 2918 cm^{-1} and 2851 cm^{-1} (aliphatic C–H stretching), 1594 cm^{-1} (aromatic C–C stretching), and 1700 cm^{-1} (C–O group), representing organic constituents like lignin, cellulose, and α-cellulose in plant fibers (Selambakkannu *et al.* 2018). The addition of silica (SiO_2) to BC resulted in the formation of Si–O bonds in the cellulose chain, broadening the OH band at 3500 cm^{-1} due to hydrogen bonding with silica nanoparticles (Figure 3.2(c)). This indicates strong chemical interactions between BC

and SiO_2. Moreover, the incorporation of DAPTMS into BC-SiO_2 led to the formation of new peaks in the FTIR spectrum, confirming the grafting of DAPTMS onto the BC-SiO_2 surface's OH functional group (Figure 3.2(d)). This grafting process involved multiple steps, including physisorption, hydrolysis, dehydration, condensation, and covalent bond formation. The resulting BC-SiO_2- DAPTMS composite exhibited increased Si-O–Si bond formation and a new N–H peak at 769 cm^{-1}, indicating successful preparation and enhanced heavy metals adsorption capabilities due to increased hydrogen bonding (Ullah *et al.* 2016; Azarshin, Moghadasi and A Aboosadi 2017).

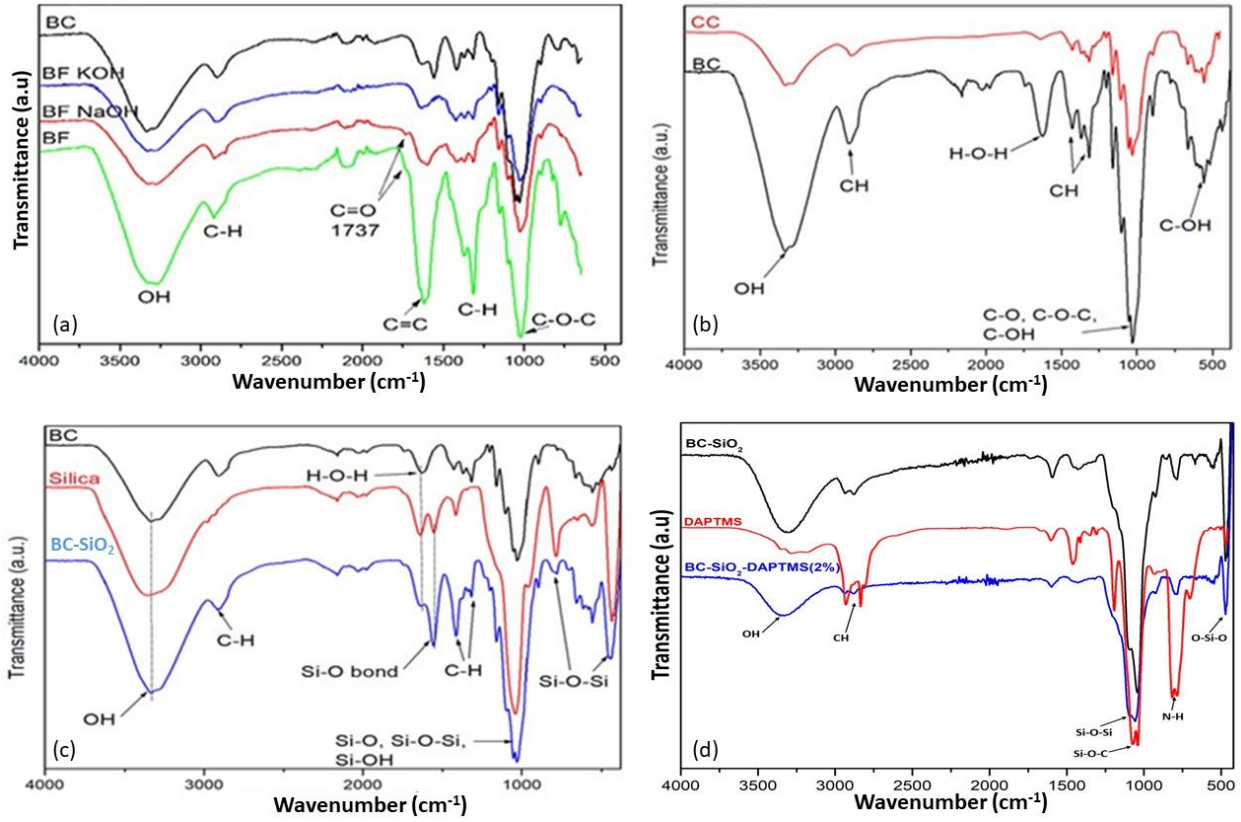

Figure 3.2 ATR-FTIR spectra of (a) BF, BF-NaOH, BF-KOH, & bleached cellulose (BC), (b) BC and CC, (c) Bleached Cellulose-Silica (BC-SiO_2), Silica (SiO_2), & BC, and (d) BC-SiO_2, DAPTMS, & BC-SiO_2-DAPTMS (2%).

3.4.1.2 XRD analysis

The XRD diffractograms of bleached cellulose (BC) in Figure 3.3 exhibit well-defined peaks at 2θ = 15°, 22°, and 34°, corresponding to the crystallographic planes (101), (002), and (040) of the typical cellulose I structure (Mohd *et al.* 2016; Khanjanzadeh *et al.* 2018; Helmiyati and Suci 2019). Amorphous silica greatly diminishes the crystallinity of cellulose by disrupting its orderly chain structure. Cellulose is composed of both crystalline and amorphous regions, with the crystalline areas being highly structured. The introduction of amorphous silica interferes with the regular arrangement of cellulose chains, leading to a reduction in overall crystallinity. However, the composite maintained the BC's characteristic peaks, signifying minimal alteration to the BC's crystalline structure. Barud *et al.* found similar outcomes and highlighted that the introduction of silica nanoparticles does not appear to impact the crystal structure of cellulose (Barud *et al.* 2008).

This is observed in BC-SiO_2 and BC-SiO_2-DAPTMS (2%) composites, which exhibit lower crystallinity compared to pure bleached cellulose (BC). The addition of amorphous silica increases the amorphous phase within the composite, as silica itself lacks a crystalline structure. For instance, the crystallinity in Table 3.1 was calculated using Equation (3.1). The crystallinity index declined from 98.8851 % in pure BC to 97.8845 % in BC-SiO_2. Moreover, the surface hydroxyl groups of silica form hydrogen bonds with cellulose, further disrupting the crystalline structure. Silica particles also act as a physical barrier, preventing proper alignment of cellulose chains and further increasing the amorphous content. Functionalizing silica with DAPTMS (N-[3-(Trimethox ysilyl)propyl]ethylenediamine) reduced the crystallinity even further, as seen in BC-SiO_2-DAPTMS (2%), where the crystallinity drops to 93.0234 %. The DAPTMS groups created additional interactions between cellulose and silica, leading to greater disruption. Mohd reported similar findings regarding the influence of amino silane modification on nano-crystalline cellulose (Mohd *et al.* 2016). This reduction in crystallinity affected the mechanical and adsorption properties of the composite. Lower crystallinity enhanced the flexibility and boosted adsorption capacity, as more amorphous regions provided additional active sites for metal ion adsorption. While the material may lose some mechanical strength, its improved adsorption properties make it highly effective for applications such as heavy metal remediation.

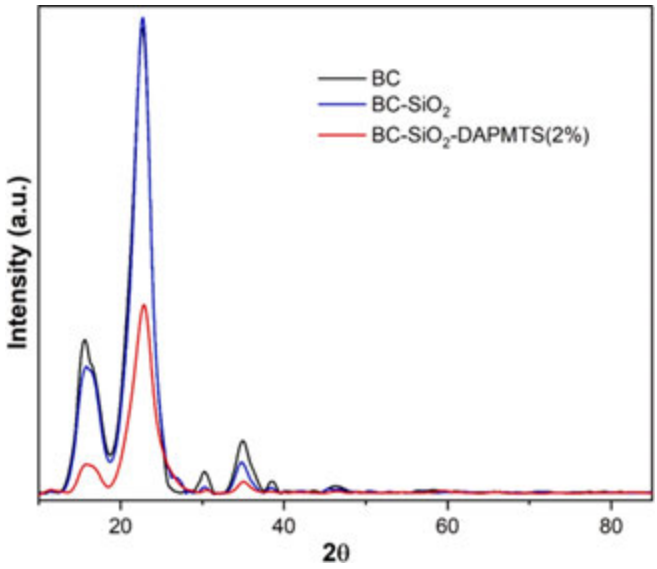

Figure 3.3 X-ray diffractograms of BC, BC-SiO_2, BC-SiO_2–DAPTMS (2%).

Table 3.1 Crystallinity index of BC, BC-SiO_2, BC-SiO_2-DAPTMS (2%).

Samples	Percentage Crystallinity (%)
BC	98.9
BC-SiO_2	97.9
BC-SiO_2-DAPTMS (2%)	93.0

3.4.1.3 Thermogravimetric analysis (TGA) analysis

Thermogravimetric analysis (TGA) and Differential Scanning Calorimetry (DSC) curves were employed to evaluate the thermal characteristics of bleached cellulose (BC), silica (SiO_2), BC-SiO_2 composite, and BC-SiO_2-DAPTMS composites with a 2 % concentration of the amine silane coupling agent (Figure 3.4a and b). The TGA curves of BC, BC-SiO_2, and BC-SiO_2-DAPTMS displayed similar decomposition patterns, following the typical stages of cellulose thermal degradation. Considering the initial weight loss is not the result of chemical degradation, it is usually not included in the degradation stages. It is only in charge of the evaporation of volatiles and adsorbed moisture. Thus, two primary chemical degradation stages are represented by the three

mass loss zones that are shown. BC exhibited two degradation stages, including depolymerization and glycosyl unit decomposition, with notable weight loss at higher temperatures due to cellulose chain decomposition (Kumar *et al.* 2014; Lin and Zhou 2017). The addition of SiO_2 to BC notably enhanced thermal stability, with BC< BC-SiO_2 < BC-SiO_2-DAPTMS (2%).

Analysis of the DSC curves revealed distinct thermal degradation peaks for BC, BC-SiO_2, and BC-SiO_2-DAPTMS (2%), representing different thermal processes such as bonded water evaporation and molecular fragment removal. BC-SiO_2 exhibited a well-separated second peak, indicating improved thermal stability over BC alone. Incorporating DAPTMS into BC-SiO_2 increased hydrogen bond formation, enhancing thermal stability compared to BC-SiO_2 alone (Tang *et al.* 2017). The interaction of DAPTMS with BC-SiO_2 further improved thermal stability, demonstrated by the higher peak temperature in BC-SiO_2-DAPTMS (2%), highlighting the significance of additives like silica and DAPTMS in enhancing cellulose-based composites' thermal properties for industrial applications.

The thermal gravimetric analysis (TGA) of the composites BC-SiO_2, BC-SiO_2-DAPTMS (2%) provided valuable insights into their thermal stability and degradation behaviour in Table 3.2. For the BC-SiO_2 composite, the first degradation stage, occurring between 25 and 150 ℃, resulted in a 14.18 % mass loss, which can be attributed to the evaporation of absorbed moisture and loosely bound water in the cellulose-silica matrix. The second stage, from 150 to 400 ℃, showed a significant mass loss of 53.04 %, reflecting the decomposition of the cellulose polymeric chains. The third stage, between 400 and 600 ℃, led to a 16.20 % mass loss, indicating the breakdown of remaining organic matter. The residual ash content at 600 ℃, primarily representing silica, was 15.83 %. In the BC-SiO_2-DAPTMS (2%) composite, the initial mass loss was reduced to 8.55 %, suggesting that DAPTMS functionalization lowers moisture content. The second stage exhibits a 41.92 % mass loss, attributed to the decomposition of both the cellulose matrix and DAPTMS functional groups. The final mass loss was 15.85 %, and the ash content, significantly higher at 33.23 %, reflected an increased silica content due to the DAPTMS coating. Overall, the ash content, representing the residue at 600 ℃, increased as the DAPTMS content rises, indicating enhanced thermal stability and a higher inorganic (silica) content. The increased residue correlates

with the functionalization level, suggesting that the DAPTMS coating contributes to both thermal stability and structural integrity, essential for applications like heavy metal adsorption. Thus, the DAPTMS-modified composites, particularly those with higher DAPTMS concentrations, demonstrate improved stability, making them more suitable for demanding environmental applications such as heavy metal remediation.

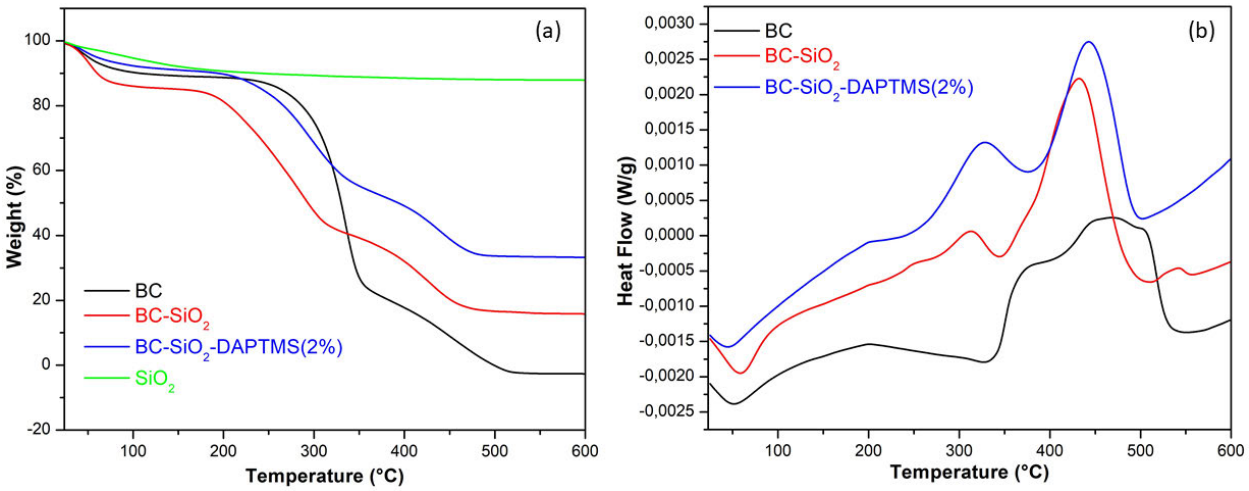

Figure 3.4 Presents the following: (a) TGA curves for Silica (SiO_2), BC, BC-SiO_2, and BC-SiO_2-DAPTMS (2%), (b) Differential Scanning Calorimetry (DSC) thermogram comparison of BC, BC-SiO_2, and BC-SiO_2-DAPTMS (2 %).

Table 2.2 Mass Loss at each degradation stage and Ash Content for BC-SiO_2 and BC-SiO_2-DAPTMS (2%).

Temperature (°C)		Weight (%)		Calculations (%)		
BC-SiO_2						
Initial	**Final**	**Initial**	**Final**	**Mass loss (At each degradation point)**		**Ash content (Residue at 600°C)**
25	150	99.25	85.07	14.18	1st stage	
150	400	85.07	32.03	53.04	2nd stage	15.83
400	600	32.03	15.83	16.20	3rd stage	
BC-SiO_2-DAPTMS (2%)						
Initial	**Final**	**Initial**	**Final**	**Mass loss at each degradation point**		**Ash content (Residue at 600°C)**
25	150	99.55	91.0	8.55	1st stage	
150	400	91.0	49.08	41.92	2nd stage	33.23
400	600	49.08	33.23	15.85	3rd stage	

3.4.1.4 BET analysis

The BET analysis reveals crucial insights into surface properties and porosity, vital for understanding adsorption capabilities. Studying bleached cellulose (BC) and its composites with silica (SiO_2) and amine silane coupling agent (DAPTMS) highlights significant changes in surface area and pore characteristics, suggesting potential enhancements in adsorption capacity. The isotherm curves in Figure 3.5 for the samples displayed type III isotherms, indicative of mesoporous structures, notably seen in SiO_2, BC-SiO_2, and BC-SiO_2-DAPTMS (2%) samples with pore widths between 2 and 50 nm. In contrast, BC alone exhibits a macroporous structure with pore widths exceeding 50 nm, depicting multi-layer adsorption without an initial monolayer, emphasizing the material's porous nature. In Table 3.3, BC shows a low BET surface area of 0.172 m /g, despite a large pore size of 143 nm, indicating limited adsorption surface availability yet a porous structure. Pure SiO_2 boasts a significantly higher BET surface area of 6.0627 m^2/g, suggesting a larger adsorption surface with smaller pores (8.9871 nm) and higher pore volume

(0.01607 cm^3/g). The BC-SiO_2 composite exhibits an increased BET surface area of 1.2662 m^2/g, indicating improved surface area due to silica nanoparticle addition, albeit lower than pure SiO_2. Incorporating DAPTMS into BC-SiO_2 at a 2 % concentration boosts the BET surface area to 2.3924 m^2/g, approaching that of pure SiO_2, while modifying pore structure. Overall, the addition of silica and DAPTMS enhances surface area and alters pore characteristics in bleached cellulose composites, crucial for applications like heavy metal remediation. Senthamaraikannan and Kathiresan conducted a study that found the alkali-treated fibers had a greater specific surface area compared to untreated fibers. This suggests an enhancement in the hydrophobic nature of the treated fibers (Senthamaraikannan and Kathiresan 2018).

The porosity distribution plot (Figure 3.5b) shows that BC primarily exhibits macroporous structures, with pore diameters ranging from 263.14 nm to 87.51 nm. These larger pores facilitate rapid fluid and molecule transport but result in a lower surface area for adsorption. As a result, BC is well-suited for applications requiring high flow rates, although its larger pore sizes limit its adsorption capacity compared to materials with mesopores. In contrast, silica (SiO_2) is characterized by mesoporous structures, with pore diameters between 2 nm and 50 nm. This mesoporous nature significantly enhances SiO_2′s adsorption potential, offering a high surface area for capturing contaminants like heavy metals. The presence of some macropores further aids in the rapid transport of fluids, complementing its adsorption efficiency. When BC and SiO_2 are combined to form a composite material, the resulting structure incorporates both mesopores and macropores, with pore diameters ranging from 12.97 nm to 256.30 nm. This combination allows the composite to leverage the fast transport capabilities of BC's macropores and the high surface area of SiO_2′s mesopores, enhancing its overall adsorption capacity for heavy metals. The introduction of an amine-functionalized silane coupling agent, specifically DAPTMS (2 %), further modifies this composite by enhancing mesoporosity while retaining some macroporous characteristics, with pore sizes ranging from 100 Å to 2600 Å. Functionalization with DAPTMS improves the composite's adsorption efficiency by increasing its interaction with metal ions, particularly Cr (VI). The mesoporous structure maximizes the available adsorption sites, while the amine groups increase selectivity and binding capacity for heavy metals.

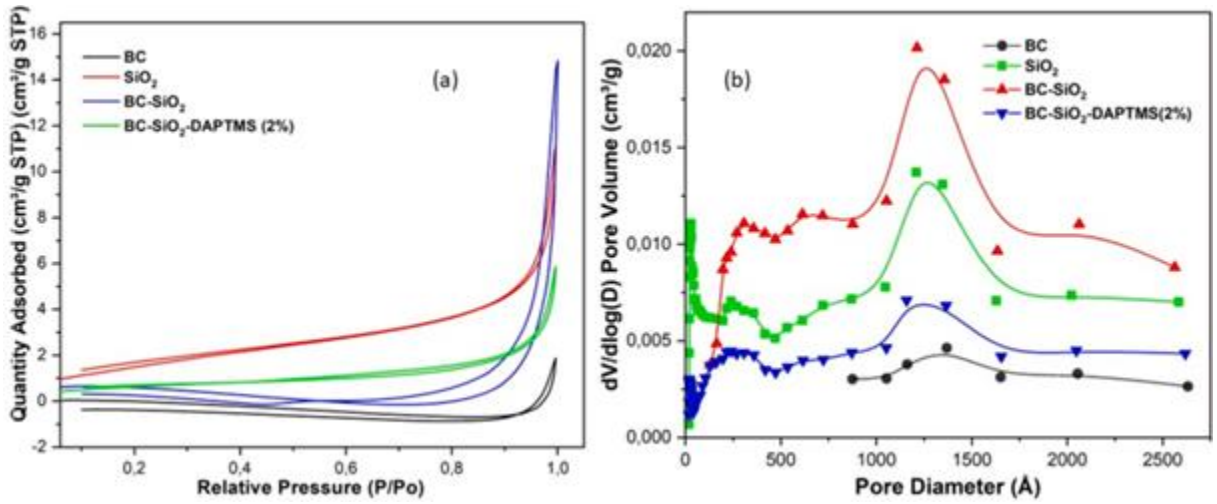

Figure 3.5 Nitrogen adsorption–desorption isotherms (a) pore size distribution (b) for BC, SiO_2, BC- SiO_2, BC-SiO_2-DAPTMS (2%).

Table 3.3 Summary of BET analysis data.

Samples	BET Surface area (m^2/g)	Pore Size (nm)	Pore Volume (cm^2/g)
BC	0.172	143	0.00201
SiO_2	6.0627	8.99	0.01607
BC-SiO_2	1.2662	47	0.01445
BC-SiO_2-DAPTMS (2%)	2.3924	12.94	0.008034

In summary, the incorporation of BC, SiO_2, and DAPTMS in a composite material optimizes both surface area and transport properties, leading to improved adsorption performance, particularly for heavy metal removal. The functionalization with DAPTMS further enhances the composite's selectivity and binding efficiency, making it a highly effective adsorbent in water treatment applications.

3.4.1.5 SEM analysis

SEM imaging of BC reveals its typical fibrous and irregular structure, with relatively smooth surfaces and occasional roughness due to natural cellulose fiber variations (Figure 3.6(a–c)). Chen et al. conducted a study on cellulose, where scanning electron microscopy (SEM) images revealed smooth and clean surfaces without pores on the cellulose material (Chen *et al.* 2011). When SiO_2 nanoparticles are introduced (Figure 3.6(d–f)), they appear spherical and form clusters or individual attachments on BC fibers in BC-SiO_2 composites (Figure 3.6(g–i)). However, these particles cannot create a film-type structure due to phase separation issues. In BC-SiO_2-DAPTMS composites (Figure 3.6(i–j)), SEM analysis shows a more uniform distribution of silica nanoparticles on BC fibers, indicating improved compatibility and bonding facilitated by DAPTMS. This leads to a more organized arrangement of nanoparticles, reducing agglomeration and enhancing dispersion within the composite. Yang et al. modified the surface of SiO_2 nanoparticles, and the SEM image showed a distinctive spherical morphology (Yang *et al.* 2019).

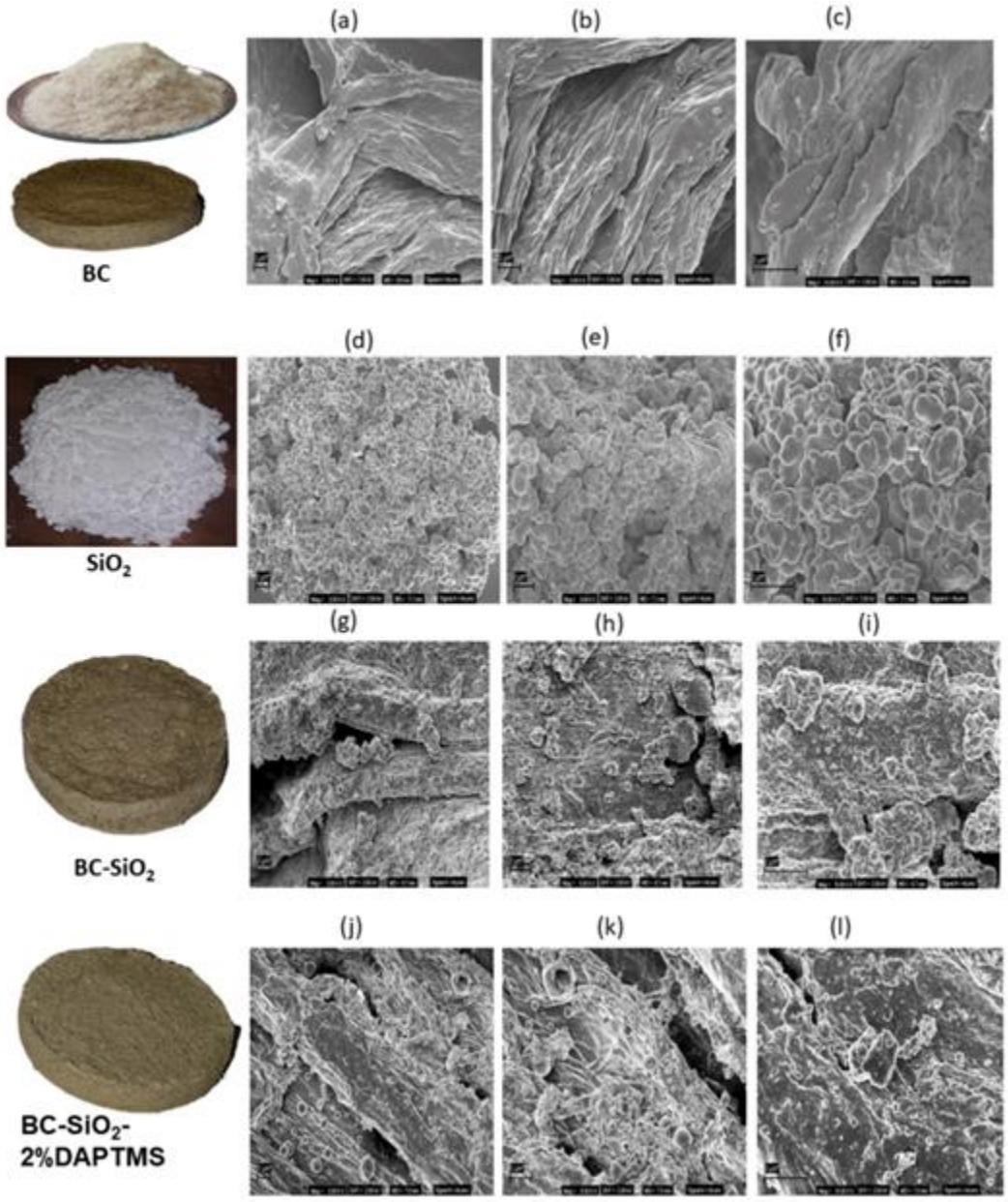

Figure 3.6 Presents a series of SEM images showing different magnifications (3.00 KX, 5.00 KX, and 10.00 KX) for various samples: SEM images of BC (a–c) at different magnifications; SEM images of SiO_2 nanoparticles (d–f) at different magnifications; SEM images of BC-SiO_2 composites (g–i) at different magnifications; SEM images of BC-SiO_2-DAPTMS (2%) composites (j–l) at different magnifications.

3.4.1.6 TEM analysis

TEM analysis of BC confirms its fibrous nature, displaying well-defined cellulose fibrils and pores at the nanoscale (Figure 3.7(a–b)). In the absence of silica or other additives, BC forms a homogeneous cellulose matrix. When silica nanoparticles are added, TEM analysis shows spherical particles distributed homogeneously on the reduced SiO_2, with sizes ranging from 64.7 to 516 nm (Figure 3.8). Figure 3.7(c–d) further explains the distribution of silica within the composite, revealing integration between cellulose fibrils and potentially within pores. This integration creates a heterogeneous structure with enhanced surface roughness due to the presence of nanoparticles. TEM images of BC-SiO_2-DAPTMS composites highlight the impact of the amine silane coupling agent (Figure 3.7(e–f)). It reveals the formation of chemical bonds between DAPTMS, cellulose, and silica, promoting covalent bond formation at suitable temperatures. This enhances bonding and dispersion, resulting in a more stable and structured composite with tailored surface properties and improved structural integrity.

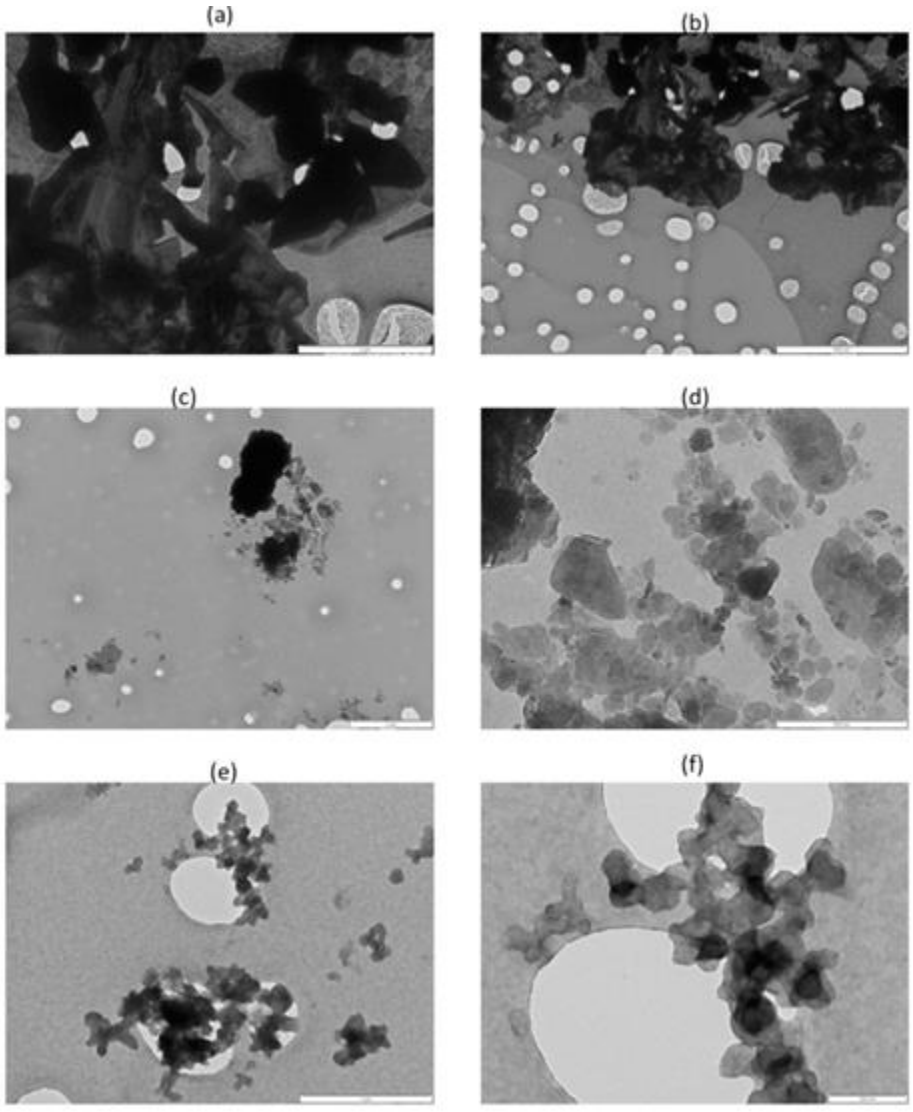

Figure 3.7 Presents TEM images of various samples: BC at magnifications of (a) 2 µm and (b) 500 nm; BC-SiO_2 at magnifications of (c) 2 µm and (d) 500 nm; BC-SiO_2-DAPTMS (2 %) at magnifications of (e) 1 µm, and (f) 200 nm.

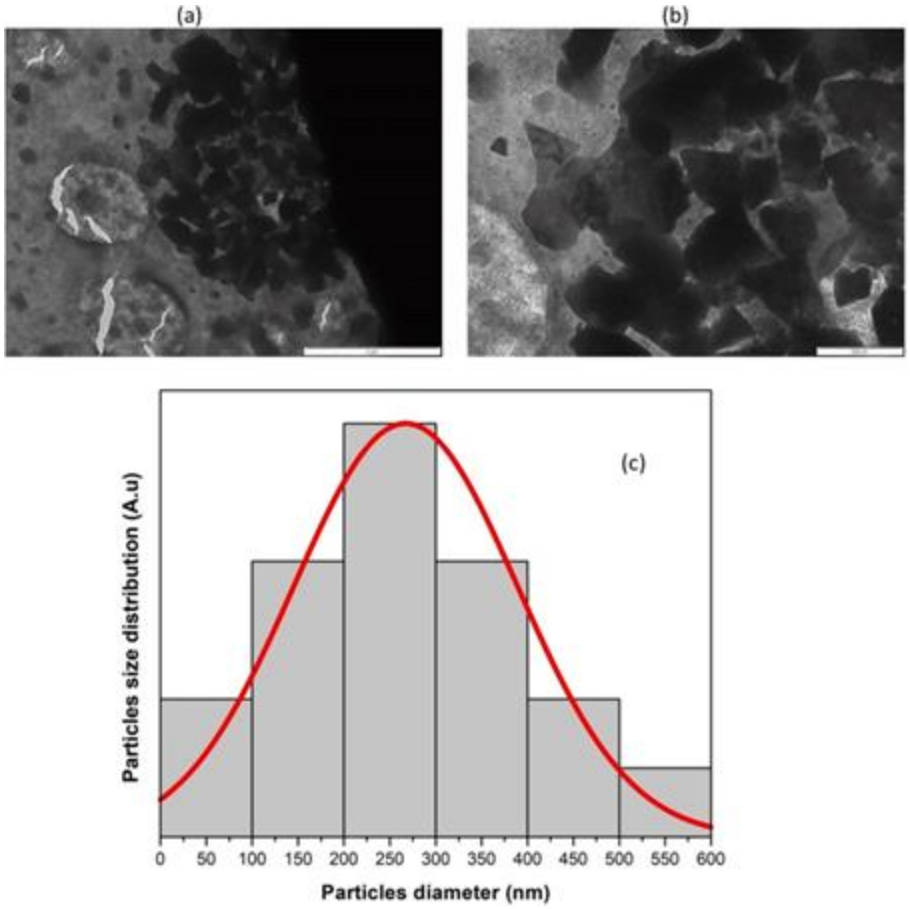

Figure 3.8 Depicts TEM images of the synthesized silica (SiO_2), including images at magnifications of (a) 2 µm and (b) 500 nm. Additionally, it presents the size distribution of the synthesized silica (SiO_2) nanoparticles.

3.4.2 Adsorption kinetics and isotherms

The effect of different operating conditions on the removal rate of Cr (VI) ions using BC-SiO_2-DAPTMS (2%) composite is presented in Fig. 3.10 (a–d).

3.4.2.1 Effect of the initial concentration

Figure 3.9(a) illustrates the influence of initial Cr (VI) ion concentrations on the removal rate within a concentration range from 0.1 to 1.0 mg/L and pH 7 in 20 ml of Cr (VI) solution and an adsorbent dose of 0.5 g in a period of 30 min. The results show a positive correlation between the

initial Cr (VI) concentration and the removal percentage by the BC-SiO_2-DAPTMS (2%) composite. Starting at 0.1 mg/L, the removal rate begins at approximately 60.87 % and steadily increases with higher concentrations. At 0.8 mg/L, the removal rate peaks at nearly 80 %, indicating a strong adsorption capacity. However, at 1.0 mg/L, the removal rate slightly drops to around 76.19 %. This trend suggests that the adsorbent is effective over a range of concentrations but may exhibit saturation or encounter competitive adsorption effects at higher concentrations. Despite this, the observed removal rates demonstrate the composite's efficiency in removing Cr (VI) ions from solutions, showcasing its potential for practical applications in water treatment. Further exploration of adsorption kinetics and equilibrium behaviour at varying concentrations could offer deeper insights into the adsorption mechanisms, aiding in optimizing the process for specific Cr (VI) ion concentrations encountered in real-world scenarios. As the initial concentration of chromium (VI) increased, the removal percentage also increased until reaching the equilibrium adsorption capacity, after which the percentage remained relatively stable over time. This phenomenon can be attributed to the rise in the number of chromium (VI) ions competing for the available binding sites on the surface of the adsorbent (Wang, Li and Tao 2009).

3.4.2.2 Effect of the adsorbent dose

Figure 3.9(b) shows the removal of Cr (VI) by the BC-SiO_2-DAPTMS (2%) composite at different weights (0.05–1.1 g). The experiment was carried out using 20 ml of 0.7 mg/L of Cr (VI) solution at pH 7 for 30 min. The results demonstrate a consistent pattern of increasing removal percentages as the weight of the BC-SiO_2-DAPTMS (2%) composite rises. Starting at 0.05 g, the removal efficiency is 79.45 %. At 0.1 g, the efficiency increases slightly to 80.14 %. The increase in removal efficiency is minimal at these low doses, suggesting that a small dose of this adsorbent may not provide sufficient active sites to achieve significant pollutant removal. At doses below 100 mg, adsorbent capacity is limited, and significant improvements in removal efficiency typically require higher doses to provide more active sites for the pollutant. With incremental increases in weight from 0.2 g to 1.1 g, the removal percentages steadily climb, peaking at 82.62 % for both 1 g and 1.1 g of the composite. This trend implies a direct correlation between the adsorption capacity of the composite and the amount used. Greater composite weight equates to more active sites for Cr

(VI) ions, enhancing adsorption efficiency. Minor deviations in removal percentages across different weights (e.g., 0.1 to 0.9 g) could stem from experimental variability or slight variations in available surface area and active sites for adsorption. This underscores the need to optimize composite dosage for practical Cr (VI) ion removal applications. While higher doses yield higher removal rates, there's a threshold where further increases may not significantly boost efficiency. Thus, selecting an optimal dosage based on desired removal rates and economic viability is crucial for the effective utilization of the BC-SiO_2-DAPTMS (2%) composite in Cr (VI) ion remediation. It can be concluded that increasing the dosage of the adsorbent enhances the removal efficiency of Cr (VI) from the solution. This is due to the increased number of available adsorption sites on the adsorbent surface resulting from the increased dosage, thus leading to improved removal efficiency. These findings are consistent with similar results reported by multiple researchers (Rengaraj *et al.* 2003; Ofomaja 2008; Wang, Li and Tao 2009).

3.4.2.3 Effect of pH

Figure 3.9(c) shows the effect of solution pH on the removal rate of Cr (VI) ions by the BC-SiO_2-DAPTMS (2%) composite, which changed in the range from 2 to 10. This experiment was performed within 30 min at a Cr (VI) concentration of 0.7 mg/L and an adsorbent dose of 0.5 g. As pH levels rise, the positive charge on the membrane's surface decreases, affecting Cr (VI) ion adsorption. The removal efficiency of Cr (VI) ions is significantly influenced by pH variations. At extremely acidic conditions (pH 1), the removal rate is about 53.76 %, indicating moderate adsorption capacity. However, with increasing pH, the removal rate notably improves, peaking at pH 4 with a remarkable removal rate of 80.70 %. This pH-dependent behaviour highlights the BC-SiO_2-DAPTMS composite's optimal adsorption performance under slightly acidic conditions. Beyond pH 4, the removal rate gradually declines, reaching 48.46 % at pH 10, indicating reduced efficiency under highly alkaline conditions. The observed pH dependency mirrors the composite's surface charge and the speciation of Cr (VI) ions at different pH levels. A positive surface charge at lower pH values favours adsorption of negatively charged Cr (VI) ions, while higher pH values result in negative surface charges, reducing adsorption efficiency due to repulsion. Therefore, controlling pH is crucial for optimizing the adsorption process using the BC-SiO_2-DAPTMS (2%)

composite for Cr (VI) ion removal, with pH 4 being optimal for high removal rates. In a related study by Jamroz et al., amino-salinized cellulose membranes were developed for selectively adsorbing Cr (VI) ions, showing effective adsorption at pH 4 within 300 min (Jamroz *et al.* 2019).

The speciation of Cr (VI) ions, encompassing forms like $Cr_2O_7^{2-}$, CrO_4^{2-}, H_2CrO_4, and $HCrO_4^-$, undergoes significant changes based on pH levels in water. This phenomenon is illustrated in the thermodynamic Eh-pH diagram (Pourbaix Diagram, Fig. 3.9(e)), highlighting the importance of pH in chromium's redox chemistry. Under highly acidic conditions (pH < 1) and elevated Eh levels, Cr (VI) predominantly exists as chromic acid (H_2CrO_4), known for its strong oxidizing characteristics. In the pH range of 1.0–6.0, the stable form is the anionic species $HCrO_4^-$, particularly at higher Eh values. Beyond pH 6.0, Cr (VI) is mainly present as CrO_4^{2-}. Importantly, the solubility of Cr (VI) species remains high across varying pH ranges (Barrera-Díaz, Lugo-Lugo and Bilyeu 2012; Dhal *et al.* 2013; Jobby *et al.* 2018). At trace levels of Cr (VI), the concentration of dichromate species ($Cr_2O_7^{2-}$) remains low due to chemical equilibria, specifically the equilibrium involving protonated species: $2HCrO_4^- \rightleftharpoons Cr_2O_7^{2-} + H_2O$. In acidic solutions, the protonated amino groups on the membrane's surface play a crucial role in electrostatic interactions with anionic Cr (VI) species. Additionally, hydrogen bond interactions occur between functional groups (e.g., Si–OH and $-NH_3^+$) of the membrane and $HCrO_4^-$ (Kumar, Kakan and Rajesh 2013; Araghi, Entezari and Chamsaz 2015). The relatively weak adsorption of Cr (VI) at very low pH values is attributed to its reduction to Cr (III), represented as $HCrO_4^- + 7H^+ + 3e^- \rightarrow Cr^{3+} + 4H_2O$ (Chen *et al.* 2017). This reduction leads to a positively charged membrane surface, which repels positively charged Cr (VI) ions, hindering adsorption.

3.4.2.4 Effect of the contact time

The effect of contact time on the removal rate of Cr (VI) ions by the BC-SiO_2-DAPTMS (2%) is depicted in Figure 3.9(d). An experiment was performed in the time range of 5–75 min at pH 7, 0.7 mg/L of Cr (VI), and an adsorbent dose of 0.5 g. The removal percentage of Cr (VI) ions exhibits a consistent upward trend with increasing time, reflecting the time-dependent adsorption capacity of the BC-SiO_2-DAPTMS composite. Initially, at 5 min, the removal rate stands at 53.27

%, showcasing the rapid adsorption kinetics of the composite material. As the contact time prolongs, the removal efficiency experiences a substantial enhancement. For instance, within 30 min, the removal percentage escalates to 81.21 %, indicating a significant boost in adsorption efficiency within the initial half-hour period. This upward trajectory persists, with the removal rate peaking at 86.66 % after 65 min. This trend underscores the role of longer contact times in achieving higher removal rates, a common phenomenon in adsorption processes where immediate equilibrium or saturation of active sites is not attained. These findings underscore the importance of optimizing contact time to achieve maximum removal efficiency. Longer contact durations facilitate enhanced interaction between the adsorbent and the target ions, resulting in more effective adsorption. Understanding this time-dependent behaviour is pivotal in designing efficient adsorption processes and establishing optimal operational parameters for practical applications, such as water treatment or remediation of Cr (VI) contaminated environments. Das et al. conducted a study that revealed a similar trend, where the percentage of adsorption increases with contact time. Once equilibrium is reached, the percentage remains relatively stable over time (Das *et al.* 2000).

3.4.2.5 Point of zero charge

The experimental data reveal that the point of zero charge (pHpzc) for the BC-SiO_2-DAPTMS (2%) adsorbent is approximately 8.04 in Figure 3.9 (f). This is the pH at which the surface has no net charge, which significantly impacts its behavior in different aqueous environments. When the solution's pH is below 8.04, the surface becomes positively charged, enhancing the adsorption of negatively charged species such as Cr (VI) ions, typically present as chromate anions (CrO_4^{2-} or $HCrO_4^-$), due to electrostatic attraction. Conversely, when the pH exceeds 8.04, the surface charge turns negative, leading to repulsion of negatively charged ions, reducing the adsorption efficiency for these species. The data suggest that around pH 8.04, the adsorbent exhibits minimal electrostatic interactions. Therefore, for maximum adsorption of anionic metals like Cr (VI), the pH should ideally be maintained below the pHpzc, where the adsorbent is positively charged. In contrast, cationic heavy metals would be better adsorbed at pH levels above 8.04, where the adsorbent surface becomes negatively charged. The pHpzc of BC-SiO_2-DAPTMS (2%) is

relatively high compared to other adsorbents such as activated carbon or raw cellulose, which usually have pHpzc values between 4 and 7. This higher pHpzc is likely due to the functionalization of the composite with DAPTMS (N-[3-(trimethoxysilyl) propyl]ethylenediamine), which introduces amine groups, shifting the pHpzc upward. These amine groups ($–NH_2$) play an essential role in the adsorption process by accepting protons at lower pH levels, making the surface more positively charged and better suited for adsorbing anionic metals. In real-world applications, particularly for the removal of hexavalent chromium (Cr (VI)) from wastewater, the pH of the solution is typically acidic (below pH 7), which is beneficial for adsorbents with higher pHpzc values like BC-SiO_2-DAPTMS (2%). In these conditions, the positively charged adsorbent surface can effectively attract Cr (VI) species. However, it is essential to avoid working at pH values above 8, as the adsorbent's efficiency may decrease due to the repulsion of negatively charged Cr (VI) ions.

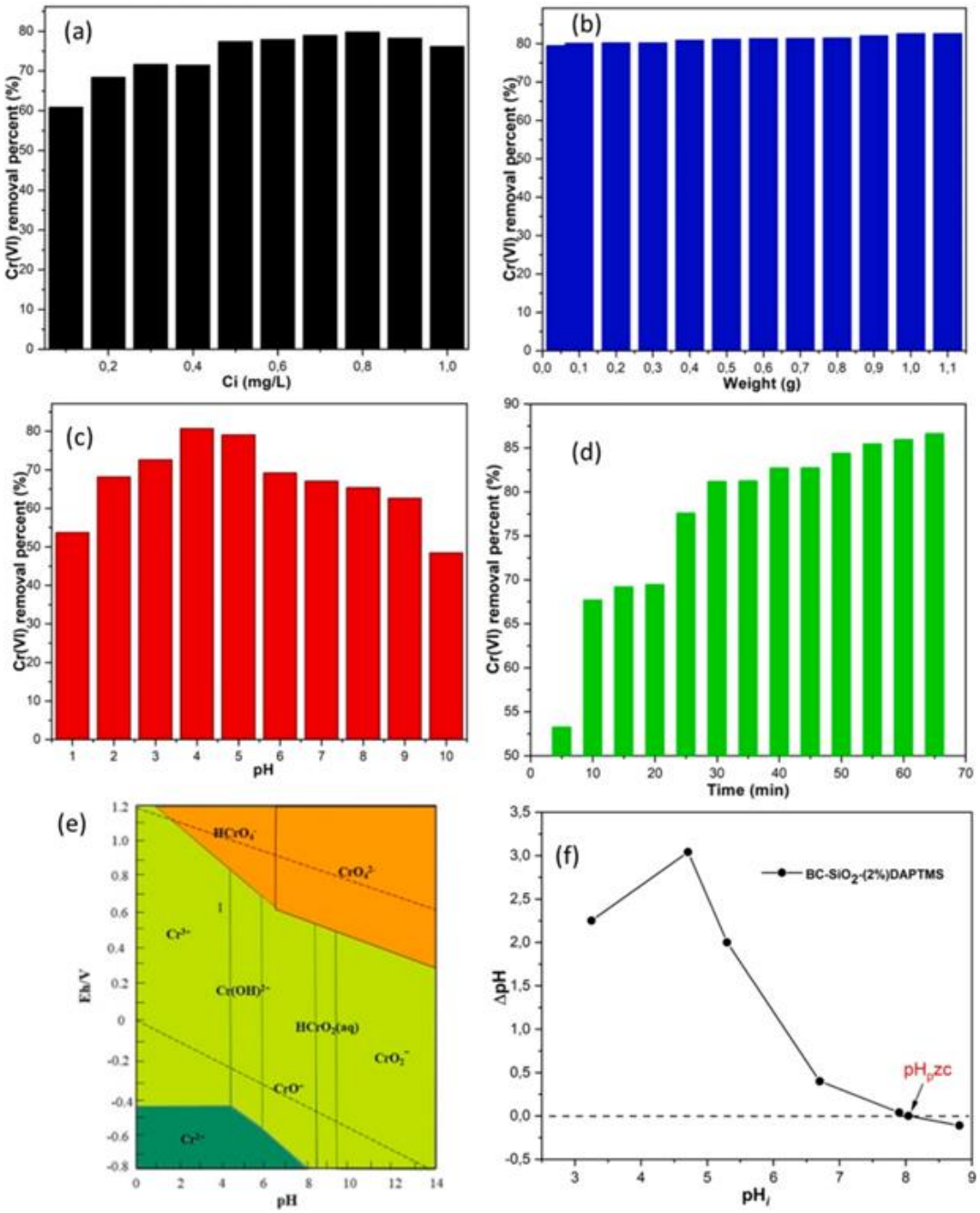

Figure 3.9 **Effect of different operating conditions on the Cr (VI) removal percent; (a) effect of the initial concentration, (b) effect of the adsorbent dose, (c) effect of pH, (d) effect of the contact time, and (e) Eh-pH phase diagram for chromium (Chen and Tian 2021), and (f) point of Zero Charge (PZC) of BC-SiO_2-DAPTMS (2%),**

3.4.3 Equilibrium study

The R^2 comparison table evaluates the goodness-of-fit (R^2) for different regression types of the Langmuir and Freundlich adsorption isotherms concerning Cr (VI) ions, providing insights into their alignment with experimental data (Table 3.4). For the Langmuir model, both linear and non-linear regressions were employed. The linear regression yielded a low R^2 value of 0.37035, indicating a weak fit with the linear Langmuir model. Conversely, the non-linear regression improved slightly with an R^2 value of 0.51091, yet it still lacked strong accuracy in representing the adsorption behaviour solely through the Langmuir model (Figure 3.10a and b). In contrast, the Freundlich model, utilizing both linear and non-linear regressions, exhibited notably higher R^2 values (Figure 3.10c and d). The linear regression for the Freundlich isotherm showed a substantial improvement with an R^2 value of 0.81838, indicating a good fit with the linear Freundlich model. Similarly, the non-linear regression produced a strong R^2 value of 0.81600, confirming the suitability of the Freundlich model in describing Cr (VI) ions' adsorption behaviour. Overall, the comparison underscores the superior fitting performance of the Freundlich model over the Langmuir model for Cr (VI) ions' adsorption.

The higher R^2 values for both linear and non-linear regressions of the Freundlich model signify its accuracy and reliability in representing the experimental data, emphasizing its practical applicability in describing the adsorption process accurately. Chakraborty et al. analyzed the equilibrium isotherms concerning the removal of Cr (VI) using the Langmuir, Freundlich, and Temkin isotherm models. The experimental data were effectively described by the Freundlich isotherm model (Chakraborty *et al.* 2021).

Table 3.4 Comparison of Adsorption isotherm parameters (Langmuir and Freundlich) for the metal ions adsorption onto BC-SiO_2-DAPTMS (2%).

Adsorption isotherm of Cr (VI)	Regression types	R^2
Langmuir	linear	0.37035
	Non-linear	0.51091
Freundlich	linear	0.81838
	Non-linear	0.81600

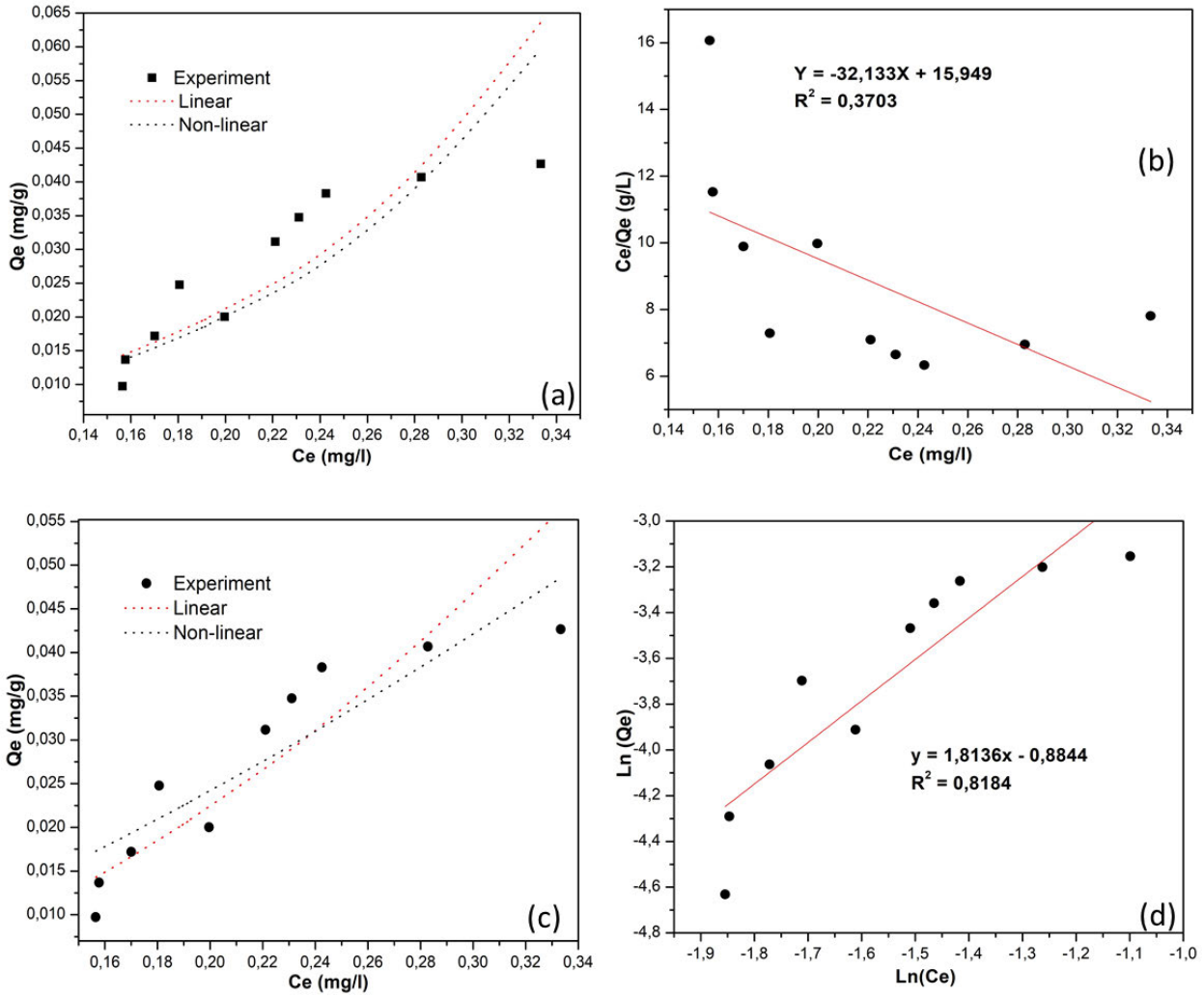

Figure 3.10 (a) Langmuir (linear & non-linear), (b) Langmuir (linear), (c) Freundich (linear & non-linear) and (d) Freundich (linear) adsorption isotherm for adsorption of Cr (VI) ion solutions (0,1 – 1,0 ppm) onto BC-SiO_2- DAPTMS (2 %) at neutral pH (7).

3.4.4 Kinetic study

The study employed both the pseudo-first order and pseudo-second- order adsorption kinetic models to investigate the adsorption kinetics, as illustrated in Figure 3.11. Table 3.5 illustrates the adsorption kinetics of Cr (VI) ions on BC-SiO_2-DAPTMS (2%) using linear and non-linear pseudo-second order (PSO) models, along with linear and non-linear pseudo-first order (PFO)

models. The accompanying R^2 values indicate how well each model fits the experimental data, with higher R^2 values indicating a better fit. The linear PSO model demonstrated an exceptionally high R^2 value of 0.9994, suggesting an almost perfect fit and accurately describing the adsorption kinetics of Cr (VI) ions on the composite material. The non-linear PSO model also exhibited a high R^2 value of 0.9838, indicating a very good fit and confirming the effectiveness of the PSO model in capturing the adsorption kinetics (Figure 3.11(a) and (c)). In contrast, the PFO models showed comparatively lower R^2 values. The linear PFO model had an R^2 value of 0.9640, indicating a good but weaker fit than the PSO models. However, the non-linear PFO model showed a higher R^2 value of 0.9717, suggesting a better fit than the linear PFO model but still lower than the PSO models (Figure 3.11b and d). Overall, the R^2 comparison highlights the superior performance of the PSO models over the PFO models in describing the adsorption kinetics of Cr (VI) ions on BC-SiO_2-DAPTMS (2%). The exceptionally high R^2 value of the linear PSO model signifies its superior ability to accurately predict the adsorption process, making it the preferred model for studying the adsorption kinetics of Cr (VI) ions on this composite material. Su et al. conducted a study similar to ours, and their findings revealed that the adsorption behaviour towards Cr (VI) exhibited higher regression coefficients for the pseudo-second order kinetic parameters (Su *et al.* 2022). The proposed kinetic model, which follows the pseudo-second order (PSO) model, is influenced by several factors that contribute to its accuracy in describing the adsorption process of Cr (VI) ions onto the BC-SiO_2-DAPTMS (2 %) composite. This includes surface area and active sites, reduction in crystallinity, functional group interactions, adsorbate-adsorbent Interaction, and time dependence. Taken together, these factors contribute to the composite's adsorption behaviour, making the PSO model a more accurate representation of the kinetics compared to the pseudo-first-order model.

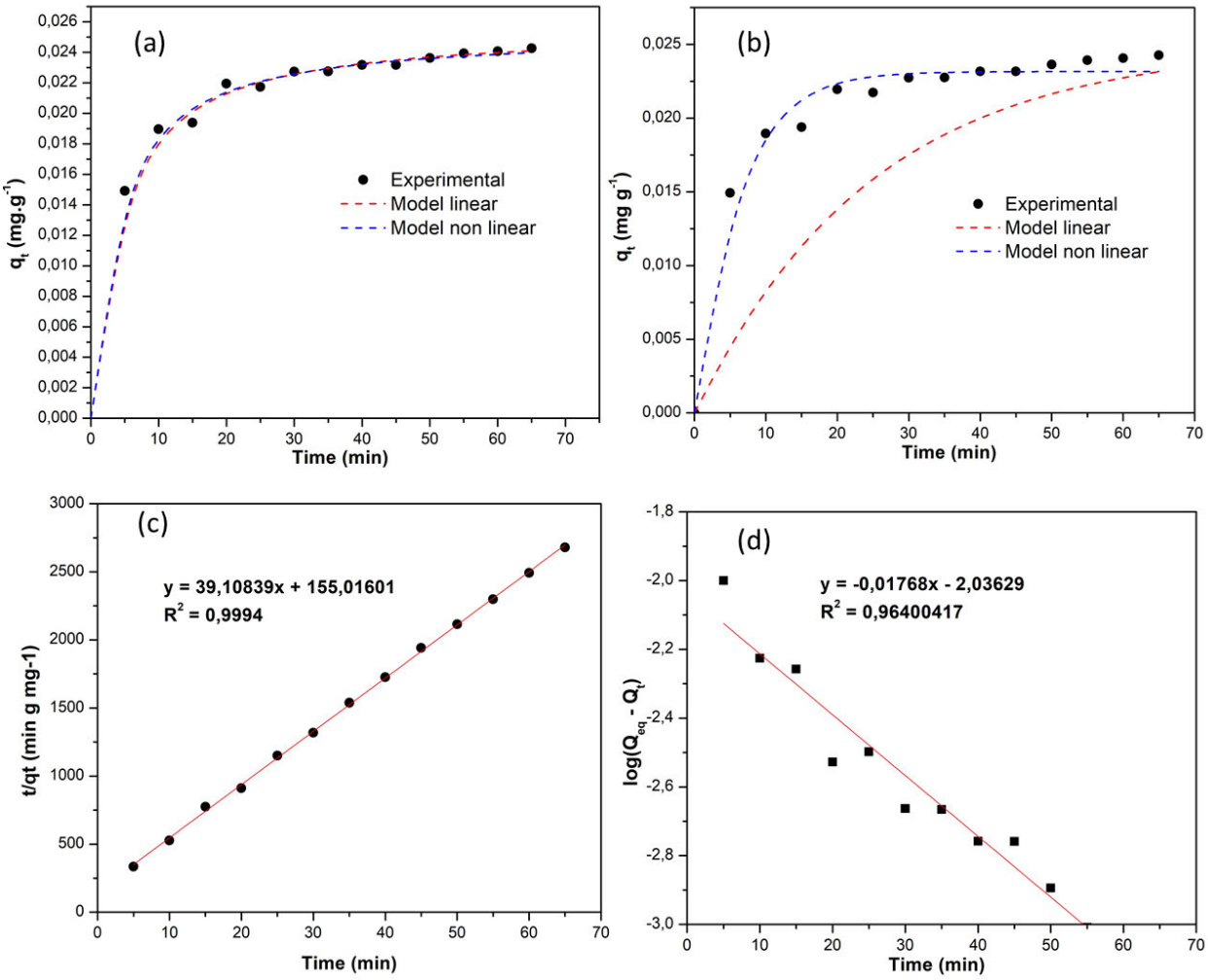

Figure 3.11 Pseudo-first-order (PFO) and pseudo-Second order (PSO) plot for the adsorption of Cr (VI) ion solutions (5–65 min) onto BC-SiO_2-DAPTMS (2 %: (a) PSO linear and non-linear plot for BC-SiO_2-DAPTMS (2 % composite, (b) PFO linear and non-linear plot for BC-SiO_2-DAPTMS (2%) composite, (c) PSO linear plot for BC- SiO_2-DAPTMS (2 % composite, and (d) PFO linear plot for BC-SiO_2-DAPTMS (2 % composite at neutral pH (7) over time intervals ranging from 5 to 65 min.

Table 3.5 Adsorption kinetics of Cr (VI) on (on or with) BC-SiO_2-DAPTMS (2 %; linear and non-linear pseudo-second (PSO) order model, and linear and non-linear pseudo-first (PFO) order model, and R^2 comparison.

PSO	**R^2**
Linear	0,9994
Non-linear	0,9838
PFO	R^2
Linear	0,9640
Non-linear	0,9717

3.5 Conclusion

This study offers significant insights into the structural, thermal, and adsorption characteristics of bleached cellulose (BC), BC-SiO_2, and BC-SiO_2-DAPTMS (2 %) composites, highlighting their potential for environmental applications, especially in heavy metal clean-up. XRD analysis shows that although the incorporation of amorphous silica and DAPTMS disrupts cellulose crystallinity, the fundamental cellulose structure remains mostly intact. This decrease in crystallinity increases the adsorption capacity of the composite by expanding the amorphous regions, which offer additional active sites for heavy metal ion uptake. TGA results underscore the enhanced thermal stability of the composites, particularly with DAPTMS, making them suitable for high temperature uses. Additionally, BET surface area analysis reveals that the addition of silica and DAPTMS improves surface area and alters pore structures, greatly enhancing the composite's adsorption performance. The BC-SiO_2-DAPTMS (2%) composite demonstrates considerable potential for Cr (VI) ion adsorption from aqueous solutions. The pseudo-second order (PSO) model fits the adsorption kinetics better than the pseudo-first order (PFO) model, confirming the composite's efficacy in modelling the adsorption process. The Freundlich isotherm model provides a better fit compared to the Langmuir model, indicating its practical usefulness for predicting adsorption

behaviour. Experimental findings show that increasing the composite dosage enhances Cr (VI) removal by providing more adsorption sites, although efficiency levels off after a certain amount. Optimal adsorption occurs at pH 4, where surface charge interactions facilitate Cr (VI) uptake, with contact time and concentration also playing crucial roles in adsorption effectiveness. Overall, the BC-SiO_2-DAPTMS (2%) composite stands out as a highly effective adsorbent for Cr (VI) remediation, offering excellent adsorption capacity, kinetic performance, and robustness across diverse conditions. These results establish a strong basis for future research focused on optimizing operational parameters and scaling up for practical water treatment applications.

3.6 References

A.T.S.D.R. 2022. *The ATSDR 2022 Substance Priority List*. Retrieved from https://www.atsdr.cdc.gov/spl/#2019spl

Abdel-Khalek, A. A., Hamed, A. and Hasheesh, W. S. 2021. Does the adsorbent capacity of orange and banana peels toward silver nanoparticles improve the biochemical status of Oreochromis niloticus? *Environmental Science and Pollution Research*, 28: 33445-33460.

Abdelkhalek, A., Ali, S. S., Sheng, Z., Zheng, L. and Hasanin, M. 2022. Lead removal from aqueous solution by green solid film based on cellulosic fiber extracted from banana tree doped in polyacrylamide. *Fibers and Polymers*, 23 (5): 1171-1181.

Ali, H. M., Essawy, A. A., Elnasr, T. A. S., Aldawsari, A. M., Alsohaimi, I., Hassan, H. M. and Abdel-Farid, I. B. 2021. Selective and efficient sequestration of Cr (VI) in ground water using trimethyloctadecylammonium bromide impregnated on Artemisia monosperma plant powder. *Journal of the Taiwan Institute of Chemical Engineers*, 125: 122-131.

Alrowaili, Z. A., Alsohaimi, I. H., Betiha, M. A., Essawy, A. A., Mousa, A. A., Alruwaili, S. F. and Hassan, H. M. 2020. Green fabrication of silver imprinted titania/silica nanospheres as robust visible light-induced photocatalytic wastewater purification. *Materials Chemistry and Physics*, 241: 122403.

Alshammari, M. S., Ahmed, I., Alsharari, J. S., Alsohaimi, I. H., Al-Muaikel, N. S., Alraddadi, T. S. and Hasanin, T. H. 2023. Adsorption of Cr (VI) using α-Fe2O3 coated hydroxy magnesium

silicate (HMS): isotherm, thermodynamic and kinetic study. *International Journal of Environmental Analytical Chemistry*, 103 (10): 2223-2239.

Alvarez-Ayuso, E. and Nugteren, H. 2005. Purification of chromium (VI) finishing wastewaters using calcined and uncalcined Mg-Al-CO3-hydrotalcite. *Water Research*, 39 (12): 2535-2542.

Araghi, S. H., Entezari, M. H. and Chamsaz, M. 2015. Modification of mesoporous silica magnetite nanoparticles by 3-aminopropyltriethoxysilane for the removal of Cr (VI) from aqueous solution. *Microporous and Mesoporous Materials*, 218: 101-111.

Azarshin, S., Moghadasi, J. and A Aboosadi, Z. 2017. Surface functionalization of silica nanoparticles to improve the performance of water flooding in oil wet reservoirs. *Energy Exploration & Exploitation*, 35 (6): 685-697.

Bagali, S. S., Gowrishankar, B. S. and Roy, A. S. 2017. Optimization, kinetics, and equilibrium studies on the removal of lead (II) from an aqueous solution using banana pseudostem as an adsorbent. *Engineering*, 3 (3): 409-415.

Barrera-Díaz, C. E., Lugo-Lugo, V. and Bilyeu, B. 2012. A review of chemical, electrochemical and biological methods for aqueous Cr (VI) reduction. *Journal of hazardous materials*, 223: 1-12.

Barud, H. d. S., Assunção, R., Martines, M., Dexpert-Ghys, J., Marques, R., Messaddeq, Y. and Ribeiro, S. 2008. Bacterial cellulose–silica organic–inorganic hybrids. *Journal of Sol-Gel Science and Technology*, 46: 363-367.

Bisla, V., Kawamura, I. and Yoshitake, H. 2022. Cross-linked cellulose acetate aminosilane (CAAS) for aqueous arsenic (V) adsorption. *Carbohydrate Polymer Technologies and Applications*, 4: 100259.

Chakraborty, R., Verma, R., Asthana, A., Vidya, S. S. and Singh, A. K. 2021. Adsorption of hazardous chromium (VI) ions from aqueous solutions using modified sawdust: kinetics, isotherm and thermodynamic modelling. *International Journal of Environmental Analytical Chemistry*, 101 (7): 911-928.

Chen, J. and Tian, Y. 2021. Hexavalent chromium reducing bacteria: mechanism of reduction and characteristics. *Environmental Science and Pollution Research*, 28: 20981-20997.

Chen, W., Yu, H., Liu, Y., Chen, P., Zhang, M. and Hai, Y. 2011. Individualization of cellulose nanofibers from wood using high-intensity ultrasonication combined with chemical pretreatments. *Carbohydrate polymers*, 83 (4): 1804-1811.

Chen, W., Zhang, X., Mamadiev, M., Zhao, C., Wang, Z. and Xu, H. 2017. Synthesis of interstratified graphene/montmorillonite composite material through organics-pillared, delamination and co-stacking and its application in hexavalent chromium removal from aqueous solution. *Advanced Powder Technology*, 28 (2): 521-533.

Das, D. D., Mahapatra, R., Pradhan, J., Das, S. N. and Thakur, R. S. 2000. Removal of Cr(VI) from Aqueous Solution Using Activated Cow Dung Carbon. *J Colloid Interface Sci*, 232 (2): 235-240.

Dhal, B., Thatoi, H., Das, N. and Pandey, B. 2013. Chemical and microbial remediation of hexavalent chromium from contaminated soil and mining/metallurgical solid waste: a review. *Journal of hazardous materials*, 250: 272-291.

Freundlich, H. M. F. 1906. Over the adsorption in solution. *J. Phys. chem*, 57 (385471): 1100-1107.

Gupta, A. D., Kirti, N., Katiyar, P. and Singh, H. 2023. A critical review on three-dimensional cellulose-based aerogels: synthesis, physico-chemical characterizations and applications as adsorbents for heavy metals removal from water. *Cellulose*, 30 (6): 3397-3427.

Helmiyati, H. and Suci, R. 2019. Nanocomposite of cellulose-ZnO/SiO2 as catalyst biodiesel methyl ester from virgin coconut oil. In: Proceedings of *AIP Conference Proceedings*. AIP Publishing LLC, 020063.

Ho, Y.S. and McKay, G. 1999. Pseudo-second order model for sorption processes. *Process biochemistry*, 34 (5): 451-465.

Hong, G.W., Ramesh, S., Kim, J.-H., Kim, H.-J. and Lee, H.-S. 2015. Synthesis and properties of cellulose-functionalized POSS-SiO2/TiO2 hybrid composites. *Journal of Nanoscience and Nanotechnology*, 15 (10): 8048-8054.

Huzaisham, N. A. and Marsi, N. 2020. Utilization of banana (Musa paradisiaca) peel as bioplastic for planting bag application. *International Journal of Advanced Research in Engineering and Technology (IJARET)*, 11 (4)

I.A.R.C. , 2021. *Monographs on the identification of carcinogenic hazards to humans*. Retrieved from: https://monographs.iarc.who.int/list-of-classifications

Islam, M. M., Mohana, A. A., Rahman, M. A., Rahman, M., Naidu, R. and Rahman, M. M. 2023. A comprehensive review of the current progress of chromium removal methods from aqueous solution. *Toxics*, 11 (3): 252.

Jamroz, E., Kocot, K., Zawisza, B., Talik, E., Gagor, A. and Sitko, R. 2019. A green analytical method for ultratrace determination of hexavalent chromium ions based on micro-solid phase extraction using amino-silanized cellulose membranes. *Microchemical Journal*, 149: 104060.

Jobby, R., Jha, P., Yadav, A. K. and Desai, N. 2018. Biosorption and biotransformation of hexavalent chromium [Cr (VI)]: a comprehensive review. *Chemosphere*, 207: 255-266.

Khanjanzadeh, H., Behrooz, R., Bahramifar, N., Gindl-Altmutter, W., Bacher, M., Edler, M. and Griesser, T. 2018. Surface chemical functionalization of cellulose nanocrystals by 3-aminopropyltriethoxysilane. *International journal of biological macromolecules*, 106: 1288-1296.

Kumar, A., Negi, Y. S., Choudhary, V. and Bhardwaj, N. K. 2014. Characterization of cellulose nanocrystals produced by acid-hydrolysis from sugarcane bagasse as agro-waste. *J. Mater. Phys. Chem*, 2 (1): 1-8.

Kumar, A. S. K., Kakan, S. S. and Rajesh, N. 2013. A novel amine impregnated graphene oxide adsorbent for the removal of hexavalent chromium. *Chemical Engineering Journal*, 230: 328-337.

Lagergren, S. 1898. About the theory of so-called adsorption of soluble substances.

Langmuir, I. 1916. The constitution and fundamental properties of solids and liquids. Part I. Solids. *Journal of the American chemical society*, 38 (11): 2221-2295.

Li, L., Li, Y. and Yang, C. 2016. Chemical filtration of Cr (VI) with electrospun chitosan nanofiber membranes. *Carbohydrate polymers*, 140: 299-307.

Lin, B. and Zhou, S. 2017. Poly (ethylene glycol)-grafted silica nanoparticles for highly hydrophilic acrylic-based polyurethane coatings. *Progress in Organic Coatings*, 106: 145-154.

Madhubashani, A., Giannakoudakis, D. A., Amarasinghe, B., Rajapaksha, A. U., Kumara, P. T. P., Triantafyllidis, K. S. and Vithanage, M. 2021. Propensity and appraisal of biochar performance in removal of oil spills: A comprehensive review. *Environmental Pollution*, 288: 117676.

Mohd, N. H., Ismail, N. F. H., Zahari, J. I., Fathilah, W., Kargarzadeh, H., Ramli, S., Ahmad, I., Yarmo, M. A. and Othaman, R. 2016. Effect of aminosilane modification on nanocrystalline cellulose properties. *Journal of Nanomaterials*, 2016

Mukherjee, S., Sushma, V., Patra, S., Barui, A. K., Bhadra, M. P., Sreedhar, B. and Patra, C. R. 2012. Green chemistry approach for the synthesis and stabilization of biocompatible gold nanoparticles and their potential applications in cancer therapy. *Nanotechnology*, 23 (45): 455103.

N.T.P. , 2016. *Report on Carcinogens, fourteenth edition, Department of Health and Human Services* retrieved from https://ntp.niehs.nih.gov/go/roc14

Ofomaja, A. E. 2008. Sorptive removal of Methylene blue from aqueous solution using palm kernel fibre: Effect of fibre dose. *Biochemical Engineering Journal*, 40 (1): 8-18.

Prasad, S., Yadav, K. K., Kumar, S., Gupta, N., Cabral-Pinto, M. M., Rezania, S., Radwan, N. and Alam, J. 2021. Chromium contamination and effect on environmental health and its remediation: A sustainable approaches. *Journal of Environmental Management*, 285: 112174.

Rakhunde, R., Deshpande, L. and Juneja, H. 2012. Chemical speciation of chromium in water: a review. *Critical reviews in environmental science and technology*, 42 (7): 776-810.

Rengaraj, S., Joo, C. K., Kim, Y. and Yi, J. 2003. Kinetics of removal of chromium from water and electronic process wastewater by ion exchange resins: 1200H, 1500H and IRN97H. *Journal of hazardous materials*, 102 (2-3): 257-275.

Romero-Cano, L. A., Gonzalez-Gutierrez, L. V. and Baldenegro-Perez, L. A. 2016. Biosorbents prepared from orange peels using Instant Controlled Pressure Drop for Cu (II) and phenol removal. *Industrial Crops and Products*, 84: 344-349.

Sarin, V., Singh, T. S. and Pant, K. 2006. Thermodynamic and breakthrough column studies for the selective sorption of chromium from industrial effluent on activated eucalyptus bark. *Bioresource technology*, 97 (16): 1986-1993.

Selambakkannu, S., Othman, N. A. F., Bakar, K. A., Shukor, S. A. and Karim, Z. A. 2018. A kinetic and mechanistic study of adsorptive removal of metal ions by imidazole-functionalized polymer graft Banana stem fibers. *Radiation Physics and Chemistry*, 153: 58-69.

Senthamaraikannan, P. and Kathiresan, M. 2018. Characterization of raw and alkali treated new natural cellulosic fiber from Coccinia grandis. L. *Carbohydrate polymers*, 186: 332-343.

Sohaimy, M. I. H. A. and Isa, M. I. N. M. 2020. Natural inspired carboxymethyl cellulose (CMC) doped with ammonium carbonate (AC) as biopolymer electrolyte. *Polymers*, 12 (11): 2487.

Su, K., Zhao, D., Lu, A., Zhong, C., Shen, X.-C. and Ruan, C. 2022. One-pot green synthesis of poly (hexamethylenediamine-tannic acid)-bacterial cellulose composite for the reduction,

immobilization, and recovery of Cr (VI). *Journal of Environmental Chemical Engineering*, 10 (1): 107026.

Sun, J., Zhang, Z., Ji, J., Dou, M. and Wang, F. 2017. Removal of Cr6+ from wastewater via adsorption with high-specific-surface-area nitrogen-doped hierarchical porous carbon derived from silkworm cocoon. *Applied Surface Science*, 405: 372-379.

Tang, C., Li, X., Li, Z. and Hao, J. 2017. Interfacial hydrogen bonds and their influence mechanism on increasing the thermal stability of nano-SiO2-modified meta-aramid fibres. *Polymers*, 9 (10): 504.

Terry, P. A. 2004. Characterization of Cr ion exchange with hydrotalcite. *Chemosphere*, 57 (7): 541-546.

Ullah, M. W., Ul-Islam, M., Khan, S., Kim, Y. and Park, J. K. 2016. Structural and physico-mechanical characterization of bio-cellulose produced by a cell-free system. *Carbohydrate polymers*, 136: 908-916.

W.H.O., 2017. *Guidelines for drinking-water quality*. Retrieved from https://www.who.int/publications/i/item/9789241549950

Wang, X. S., Li, Z. Z. and Tao, S. R. 2009. Removal of chromium (VI) from aqueous solution using walnut hull. *Journal of Environmental Management*, 90 (2): 721-729.

Yang, S., Chen, S., Fan, J., Shang, T., Huang, D. and Li, G. 2019. Novel mesoporous organosilica nanoparticles with ferrocene group for efficient removal of contaminants from wastewater. *Journal of colloid and interface science*, 554: 565-571.

Yousif, A. M., Zaid, O. F., El-Said, W. A., Elshehy, E. A. and Ibrahim, I. A. 2019. Silica Nanospheres-Coated Nanofibrillated Cellulose for Removal and Detection of Copper (II) Ions in Aqueous Solutions. *Industrial & Engineering Chemistry Research*, 58 (12): 4828-4837.

Zhang, R. and Tian, Y. 2020. Characteristics of natural biopolymers and their derivative as sorbents for chromium adsorption: a review. *Journal of Leather Science and Engineering*, 2: 1-15.

Chapter Four

Effect of Varying Concentrations of N-[3-(trimethoxysilyl)propyl]ethylenediamine (4% and 10%) Modified Bleached Cellulose-SiO_2 Composites on Chromium Removal from Wastewater

Manuscript I

This chapter presents a manuscript currently under review in a peer-reviewed journal focusing on environmental science and material chemistry.

Citation (Under Review):

Mazibuko, M.T., Onwubu, S.C., Mokhothu, T.H., Mdluli, P.S., Mokhena, T.C., Paul, V. (2025). Effect of Varying Concentrations of N-[3-(trimethoxysilyl)propyl]ethylenediamine (4% and 10%) Modified Bleached Cellulose-SiO_2 Composites on Chromium Removal from Wastewater.

4.1 Abstract

Hexavalent chromium (Cr (VI)) contamination in water presents significant environmental and health challenges, necessitating the development of efficient and sustainable remediation strategies. This study examines the influence of N-[3-(trimethoxysilyl)propyl]ethylenediamine (DAPTMS) concentrations (4% and 10%) on the adsorption efficiency of bleached cellulose-silica (BC-SiO_2) composites for Cr(VI) removal. The composites were synthesized via an in-situ sol-gel method and characterized using ATR-FTIR, XRD, TGA, BET, SEM, and TEM to evaluate their structural, thermal, and surface properties. Both BC-SiO_2-DAPTMS (4%) and BC-SiO_2-DAPTMS (10%) exhibited excellent Cr (VI) removal capacities, with the 10% composite demonstrating superior performance due to a higher density of functional amine groups. Batch adsorption experiments revealed that the BC-SiO_2-DAPTMS (10%) composite achieved a maximum removal efficiency of 91.29% at pH 3 and equilibrium within 50 minutes, while the BC-SiO_2-DAPTMS (4%) composite attained 97.14% efficiency at 0.3 mg/L Cr (VI) amount. Adsorption behaviour followed the Freundlich isotherm model, indicating heterogeneous surface interactions, and the pseudo-second order kinetic model, which implies a mechanism dominated by chemisorption.

The study underscores that higher DAPTMS concentrations enhance the composites' functional group density, thermal stability, and adsorption capacity, with the 10% formulation consistently

outperforming its 4% counterpart across varying conditions. These findings establish DAPTMS-functionalized BC-SiO_2 composites as scalable, effective, and environmentally sustainable materials for Cr (VI) remediation, providing critical insights for optimizing adsorbent design and operational parameters in water treatment applications targeting heavy metal contamination.

Keywords: Hexavalent chromium (Cr (VI)), Heavy metal remediation, Bleached cellulose-silica composites, N-[3-(trimethoxysilyl)propyl]ethylenediamine (DAPTMS), Adsorption kinetics

4.2 Introduction

The contamination of ecosystems by heavy metals, particularly chromium [Cr (VI)], has become a serious environmental and public health issue due to their persistence and bioaccumulation potential (Pohl 2020). Industrial activities such as metal plating, mining, and manufacturing are key contributors to this pollution, which infiltrates water and soil, compromising food safety and biodiversity (Sharma and Agrawal 2005; Wang and Chen 2009). A common heavy metal in industrial operations like textile production, leather, the process of tanning, and electroplating is chromium. As a result, chromium contamination in wastewater is a significant environmental concern. Trivalent chromium (Cr (III)) and hexavalent chromium (Cr (VI)) are the two main oxidation states of chromium recovered in the environment. Cr (VI) is extremely poisonous, carcinogenic, and persistent in the environment. Therefore, removing Cr (VI) from wastewater is critical to ensuring environmental and human health. Adsorption, chemical precipitation, ion exchange, and membrane filtration are some of the procedures that have been proposed for the removal of chromium. Because of its simplicity and efficiency, adsorption is seen to be among the most cost-effective and efficient techniques (Malik, Jain and Yadav 2017).

Among the materials explored for adsorptive removal of chromium, bio-based composites are gaining attention for their sustainability and effectiveness. Bleached cellulose (BC), a highly porous and fibrous material derived from plant cellulose, is often used as a precursor for the preparation of composite materials (Selvaraj *et al.* 2024). Bleaching enhances the material's porosity and surface properties, making it an effective adsorbent for heavy metals (Johari *et al.*

2016). However, to further improve the adsorption capacity and selectivity of BC, modifications using inorganic materials, such as silica (SiO_2), are commonly employed (Sequeira, Evtuguin and Portugal 2009). Silica is known for its high surface area, chemical stability, and ease of functionalization (Agaba *et al.* 2018), which makes it ideal for composite preparation.

Functionalizing cellulose with silica and amine groups has been shown to significantly enhance adsorption capacity, especially for Cr (VI) ions (Lee *et al.* 2018). N-[3-(trimethoxysilyl)propyl]ethylenediamine (DAPTMS) is a silane coupling agent commonly used to modify silica and other inorganic materials. DAPTMS contains both amino and silane functional groups, which enhance the surface reactivity of silica, enabling stronger interactions with metal ions (Bois *et al.* 2003). The amine groups on DAPTMS provide active sites for binding metal ions, while the silane groups facilitate bonding with the cellulose fibers, enhancing the mechanical and chemical characteristics of the composite material. The concentration of DAPTMS used in the modification process plays a crucial role in determining the composite's performance, as varying amounts of DAPTMS can alter the surface structure, functional group density, and adsorption capacity (Gao *et al.* 2022).

Recent studies have focused on cellulose-based materials for the adsorption of heavy metals from aqueous solutions. Agaba et al. produced silica-cellulose composites by reinforcing precipitated silica agglomerates with cellulose nanofibrils (CNFs), leveraging the silica's large surface area and the mechanical strength and biodegradability of CNFs as adsorbents for Cr (III) (Agaba *et al.* 2018). Taha et al. investigated the effectiveness of tetraethoxysilane (TEOS) and cellulose acetate (CAc) nanofibrous membranes using 3-ureidopropyltriethoxysilane as the coupling reagent. Electrospinning technology was used to create composites with a removal efficacy of 97% and a maximal capacity for adsorption of 19.5 mg/g of Cr(VI) (Taha *et al.* 2012). Tao et al. outlined how to use terminal amino hyperbranched polymer to introduce functional mesoporous silica nanoparticles onto the surface of modified cotton fiber, creating an effective and recyclable cellulose/polymer/silica (HM-cotton) composite adsorbent. In aqueous settings, HM-cotton exhibits significantly better adsorption efficacy for heavy metals, particularly chromium (Tao *et al.* 2017).

Silane coupling agents such as 3-Aminopropylsilane (APS) are frequently used to enhance the interaction between inorganic particles and organic materials (Okhrimenko *et al.* 2017). Three different kinds of silane coupling agents were examined by Wang et al. The thermodynamic characteristics of cellulose improved with nano-SiO_2 were examined after 3-glycidoxypropyltrimethoxy silane KH-560, 3-aminopropyltriethoxy silane KH550, and 3-methacryloyloxypropyltrimethoxy silane KH-570 were grafted onto the surface of nano-SiO_2. A composite model of nano-SiO_2/cellulose was made using the molecular dynamics technique. To further examine the effects of mechanical parameters, hydrogen bonds, free volume, and interaction energy on thermodynamic properties, a Nano-SiO_2/cellulose model grafted with a variety of silane coupling agents was created. Out of the three grafted silane coupling agents, the outcomes indicated that KH-550 was the most effective modification of the nano-SiO_2/cellulose system. More hydrogen bonds were formed in the cellulose system when KH-550 was grafted onto the surface of nano-SiO_2 (Wang *et al.* 2019). Kim et al. used powdered and granular DAPTMS-modified mesoporous silica SBA-15 to adsorb Cr (VI), and it was shown that the composite's affinity for removing Cr (VI) from industrial effluent was enhanced via the existence of amino groups on the silica surface. Batch studies showed that powdered adsorbents effectively removed Cr (VI) from the solution after ten minutes of equilibrium. The largest sorption of Cr (VI) occurred at pH 3, and it was most efficient at lower pH values (Kim *et al.* 2018).

Hexavalent chromium was selectively removed using amino-silanized cellulose membranes, according to research by Jamroz *et al.* 2019. After silica-amino groups were added to the membranes, derivatives with one, two, or three amino groups were produced. Batch adsorption experiments revealed that the membranes showed a preference for Cr (VI) over Cr (III) at pH 4. The ability of the membranes to adsorb increased as the number of amino groups that have been protonated grew, following a sequence cellulose-1N < cellulose-2N < cellulose-3N, with maximum adsorption values of 10.2, 18.1, and 34.7 mg g^{-1}, respectively. The results emphasized the importance of amine functionalization in enhancing adsorption efficiency. However, few studies have explored the preparation of DAPTMS-functionalized silica particles for eliminating heavy metals such as Cr (VI) from water (Yoshitake, Yokoi and Tatsumi 2002).

The purpose of this study is to investigate how different N-[3-(trimethoxysilyl)propyl]ethylenediamine (DAPTMS) concentrations (4% and 10%) affect the efficacy of bleached cellulose-silica (BC-SiO_2) composites in the removal of chromium from wastewater. By modifying the BC-SiO_2 composite with two different concentrations of DAPTMS, the research seeks to determine the optimal concentration for maximizing Cr (VI) removal while maintaining the structural and chemical stability of the composite.

4.3 Materials and Methodology

4.3.1 Materials

Samples of banana pseudo-stems were gathered at South Africa's Inanda Farm. Associated Chemical Enterprises Pty Ltd (ACE) in Johannesburg, South Africa, provided the sodium hypochlorite (NaOCl) and Potassium hydroxide (KOH). Sigma-Aldrich provided the following: glycerol (99.5%), Ethanol (C_2H_6O), Tetraethoxysilane (TEOS, density 0.933 g/mL), N-[3-(trimethoxysilyl)propyl]ethylenediamine (DAPTMS, 97%), Hydrochloric acid (HCl), and 1,5-diphenylcarbazide. The Aqua MAX Basic 360 Series water purification system provided distilled water using a specific resistance of 18.2 MΩ·cm. Minema Chemicals in Gauteng, South Africa, provided Potassium dichromate ($K_2Cr_2O_7$, AR grade), whereas Merck in Durban, South Africa, provided sodium chloride (NaCl). All the reagents and chemicals mentioned above were operationally ready and of analytical quality.

4.3.2 Extraction of cellulose from banana pseudo-stem fibers

The pseudo-stem fibers of bananas were obtained from Nanda Farm in South Africa (see Figure 4.1(a)) and sliced into lengths of around 2 cm. These pieces were placed in a Scientific Lab Oven 2000 Series and allowed to air dry overnight at 100 ℃. After drying, a Chetak Mixer Grinder with a stainless-steel container and blades was used to grind the stems into a fine powder (see Figure 4.1(b)). The final powder was kept at room temperature in airtight plastic bags. According to schematic 1, 500 g of Banana stem fibers were treated twice with 2% solutions of potassium hydroxide (KOH) and sodium hydroxide (NaOH) for an hour each in a 5-liter beaker at 100 ℃.

The fibers were carefully washed with deionized water until their pH was neutral following each treatment. The cellulose was subsequently extracted from the fibers by treating them for an additional hour at 100 ℃ using a bleaching solution containing 2% sodium hypochlorite (NaOCl). Three hours were needed for the complete procedure, including treatments and rinsing. The bleached cellulose (BC) was washed once more after bleaching using distilled water to balance the pH, then left at room temperature to air dehydrated for the whole night (see Figure 4.1(c)).

4.3.3 Amine-functionalized cellulose-silica composite preparation

A modified in-situ sol-gel technique was used to include amine groups into the cellulose-silica matrix and create the cellulose-silica composite functionalized with an amine (BC-SiO_2-DAPTMS). Tetraethoxysilane (TEOS) was employed as the silica precursor, and N-[3-(Trimethoxysilyl)propyl]ethylenediamine (DAPTMS) was employed as the silane coupling agent. A BC:SiO_2 weight ratio of 1:1 was obtained by mixing bleached cellulose (BC) and TEOS with water, Ethanol, and a NaOH catalyst in a molar ratio of 1:4:4:3.52. For three hours, the mixture was agitated to promote the in-situ development of silica nanoparticles inside the cellulose structure. The mixture was then mixed and heated to 80 ℃ for three more hours, increasing the total reaction time to six hours, after which different concentrations of DAPTMS (4 and 10%) were added.

The synthesis was carried out using a reflux setup to control heating and prevent solvent evaporation. Ethanol was chosen as the solvent due to its low boiling point of 78 ℃, and at 80 ℃, the reaction temperature was maintained using a silicone oil bath on a hot plate. The reaction mixture was placed in the round-bottom flask, which was submerged in the oil bath then connected to a water-cooled condenser to recycle evaporated ethanol back into the mixture. This method ensured accurate temperature control, preventing the solvent from boiling over or causing damage to the sample. DAPTMS was introduced after the first three hours, and the reaction proceeded under reflux for an additional three hours, completing the functionalization of the cellulose-silica composite.

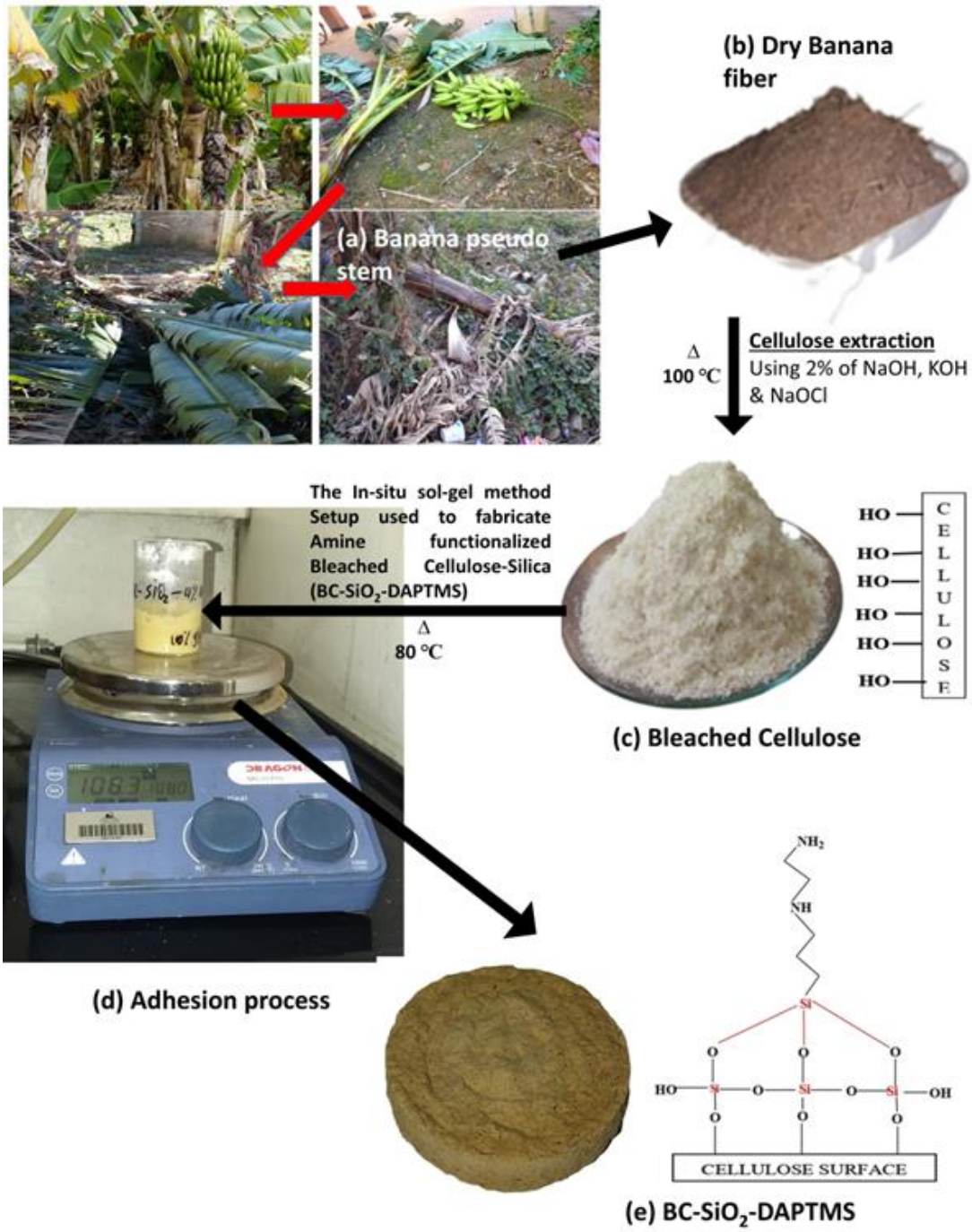

Figure 4.1 **The following steps are described in a schematic illustration: (a) collecting banana pseudo-stems; (b) grinding the fiber into a powder; (c) the experimental process for cellulose extraction from banana pseudo-stem fibers; (d) adhesion of BC-SiO_2-DAPTMS using a 10% glycerol solution; and (e) successful synthesis of the BC-SiO_2-DAPTMS composite.**

4.3.4 Adhesive preparation

Ten milliliters of glycerol and ninety milliliters of deionized water were combined to create a 10% glycerol solution. Glycerol was added to the composite material to enhance its adhesive properties. This strengthened the bond between cellulose, silica, and DAPTMS, resulting in a further solid then cohesive formation. As shown in Figure 1(d), the BC-SiO_2-DAPTMS composite with glycerol (1:10) was mixed with the proper volume of 10% glycerol solution in a glass beaker, using 1.0 g of the composite and 10 mL of the solution. On a hot plate that was set to 100 ℃, the liquid was first stirred with a glass rod and afterwards fully mixed with a magnetic stirrer until it reached a consistent texture. To finish the crosslinking procedure, the resultant dough-like mixture was put in an oven and dried for 48 hours at 120 ℃.

4.3.5 Analysis of pH Point of Zero Charge (pHpzc)

Understanding the pH at the pHpzc is important for comprehending the mechanism of surface adsorption. To determine the pHpzc of the adsorbent, a straightforward solid addition process was employed (Salama *et al.* 2023). This method involved making a 0.1 mol/L NaCl solution, boiling it to remove the dissolved CO_2, letting it cool to room temperature, and then adding either 0.1 mol/L HCl or 0.1 mol/L NaOH to bring the solution's initial pH (pHi) between 1 and 10. Then, 50 mL of the 0.1 mol/L NaCl solution in 100 mL conical flasks was mixed with 0.1 g of the BC-SiO_2-DAPTMS composite (4% or 10%). The mixture was shaken at 150 rpm for 300 minutes at 25 ℃, and the final pH (pH_f) of the solution was noted. The final and initial pH differences (pHf-pHi) were plotted against the beginning pH (pHi) in a graph. The pHpzc was determined as the point where the difference between the final and initial pH (pHf-pHi) was zero for the BC-SiO_2-DAPTMS (4% and 10%) composite.

4.3.6 Characterization Methods Employed

A Tescan Vega 3 Scanning Electron Microscope (SEM) fitted using an Oxford X-MaxN Energy-Dispersive X-ray Spectrometer (EDS) was used to examine the morphology and chemical makeup

of the produced samples. BC-SiO_2-DAPTMS composites (4% and 10%) were analyzed for their spectra using Attenuated Total Reflectance-Fourier Transform Infrared (ATR-FTIR) spectroscopy. Using a Perkin Elmer Spectrum System (Perkin Elmer FTIR Frontier Spectrometer), the study was performed over a 400–4000 cm^{-1} spectral range. Each spectrum was averaged over 16 scans.

A D8 Bruker AXS Discover diffractometer was used to investigate the crystal structures of the cellulose samples using CuKα radiation (λ = 1.5418 Å). A Bruker D8 Advance diffractometer equipped with a graphite monochromatic filter was used to record powder X-ray diffraction (XRD) patterns, which are utilized for structural and phase identification. The device used CuKα radiation with a wavelength of 1.5406 nm and ran at 40 kV and 40 mA (Billerica, MA, USA).

To calculate the percentage crystallinity (%Cr), the following formulas were used (Sohaimy and Isa 2020):

$$\%Crystallinity = \left(\frac{\text{Area Crystilline peaks}}{\text{Total Area Crystilline}}\right) \times 100\% \quad (4.1)$$

On the X-ray diffraction (XRD) scale, the crystalline and amorphous regions are identified by intensity peaks at roughly 2θ angles of 22º and 15º, respectively.

A thermogravimetric analyzer (TGA), which measures weight changes as temperature increases, was used to evaluate the thermal degradation behavior of the synthesized BC-SiO_2-DAPTMS composite. The TGA analysis was conducted under the following conditions: a heating rate of 10℃/min, a nitrogen gas flow rate of 20 mL/min, and a temperature range of 25 – 600 ℃.

4.3.7 Adsorption studies

To assess the composite material's ability to remove Cr (VI), adsorption tests were performed. The experimental setup included specific information about the initial concentrations of Cr (VI), contact time, pH, and temperature. Cr (VI) ions were quantified using the diphenylcarbazide

technique, with 1,5-diphenylcarbazide (DPC) acting as a reagent to form a recognized complex with chromium ions for spectrophotometric analysis. A 200-ppm stock solution of $K_2Cr_2O_7$ was diluted to create 125 ppm and 5 ppm standard solutions, which were then used to calibrate the spectrophotometer for accurate measurements.

The adsorption performance of Cr (VI) ions by BC-SiO_2-DAPTMS (4 and 10%) was examined under different experimental conditions. Plastic centrifuge tubes containing adsorbent and Cr (VI) solutions in varying concentrations were used for the testing. The tubes were shaken with a rotating rocker and separated by centrifugation. The effects of the initial metal ion concentration, the adsorbent dosage, and the pH on adsorption effectiveness were thoroughly assessed by adjusting these parameters and spectrophotometrically analyzing the samples. Additionally, the effect of contact time on Cr (VI) adsorption was studied by varying the mixing periods and measuring the concentration of Cr (VI) in the solutions.

To understand the capacity and adsorption mechanism, the kinetics and isotherms of Cr (VI) adsorption onto the composite material were examined. The adsorption quantity per unit mass of the adsorbent (Qt) was determined using Equation (4.2), with experimental data applied to different kinetic and isotherm models for analysis.

$$Q_t = (C_i - C_t) \times \left(\frac{V}{M}\right) \tag{4.2}$$

The percentage of Cr (VI) elimination (R%) was determined using Equation 4.3:

$$R\% = \left(\frac{C_i - C_t}{C_i}\right) \times 100\% \tag{4.3}$$

Here, V (l) stands for the solution's volume, M for the mass (g) of the added sorbent, C_i for the starting concentration, and C_t for the concentration at that moment. To reduce experimental uncertainties, each experiment was conducted three times under identical conditions, and the mean numbers were recorded.

4.3.7.1 Equilibrium experiment

Individual 50 mL plastic centrifuge tubes were filled with 20 milliliters of aqueous solutions of Cr (VI) varying in concentration from 0.1 to 1.0 mg/L. Using HCl or NaOH, the pH of each solution was brought to neutral. Each tube received 0.5 g of BC-SiO_2-DAPTMS adsorbents for equilibrium investigations. To separate the solid and liquid phases, the mixtures were shaken at 21 ℃ for 30 minutes at 70 rpm and then centrifuged for 5 minutes. For spectrophotometric analysis, 5 mL of each supernatant was placed into 15 mL plastic tubes. To comprehend the processes by which the adsorbents extract water-based metal ions, models of adsorption isotherms, such as the Freundlich and Langmuir, were used. Each isotherm in these models provides certain constants that characterize the adsorbent's surface characteristics and its affinity for metal ions, which were utilized to assess the interaction between the adsorbent and metal ions (Freundlich 1906; Langmuir 1916).

4.3.7.1.1 Langmuir Model

When a monolayer with a small number of uniformly dispersed sites forms on the surface of an adsorbent, the Langmuir model is applicable. The equation 4.4 represents it:

$$\frac{C_{eq}}{q_{eq}} = \frac{1}{Kq_{max}} + \frac{C_{eq}}{q_{max}} \tag{4.4}$$

In this case, q_{max} is the maximum adsorption capacity, C_{eq} represents the equilibrium concentration in the solution, K is the adsorption equilibrium constant, and q_{eq} refers to the amount of Cr (VI) adsorbed at equilibrium. Plotting C_{eq}/q_{eq} against C_{eq} yields a straight line, where the slope corresponds to $1/q_{max}$, and the intercept is equal to $1/Kq_{max}$.

4.3.7.1.2 Freundlich Model

Equation 4.5 of the Freundlich Model, which describes adsorption on a heterogeneous surface, accounting for binding sites that are non-identical and non-uniform.

$$lnq_{eq} = lnK_F + \frac{1}{n} lnC_{eq} \tag{4.5}$$

In this case, n denotes adsorption intensity, and K_F denotes adsorption capacity. Finding K_F and 1/n is aided by plotting lnq_{eq} against lnC_{eq}.

4.3.7.2 Kinetic experiment

To study the adsorption mechanism, kinetic tests were carried out under various sorption model settings. The adsorption behaviour of Cr (VI) onto BC-SiO_2-DAPTMS (4% and 10%) was carefully studied using the pseudo-first order (PFO) and pseudo-second order (PFO) models.

A pipette was employed to measure twenty milliliters of a 0.7 mg/L Cr (VI) aqueous solution into 50 mL polypropylene centrifuge tubes. Using HCl or NaOH, the pH of the mixture was brought to a neutral level. For equilibrium investigations, BC-SiO_2-DAPTMS (0.5 g) adsorbents were added to each tube. To separate the solid and liquid phases, the tubes were centrifuged after being shaken for five to sixty-five minutes at 70 rpm at room temperature (21 °C). For spectrophotometric analysis, 5 mL of each supernatant was then put into 15 mL plastic tubes.

The Cr (VI) adsorption mechanism onto BC-SiO_2-DAPTMS was thoroughly understood using PFO and PSO kinetic models to analyse the experimental data. Lagergren introduced a linear PFO kinetic model, which is explained below (Lagergren 1898). Equation 4.6 provides the model's integral form:

$$log(q_{eq} - q_t) = logq_{eq} - \frac{k_1}{2.303} t \tag{4.6}$$

The quantity of adsorbed Cr (VI) at equilibrium is denoted by q_{eq}, the amount adsorbed at time t (minutes) by q_t, and the pseudo-first-order adsorption rate constant is denoted by k_1. Adsorption kinetics can also be described using this model in a linear format.

The integrated linear form of equation 4.7's PSO reaction (Ho and McKay 1999) is as follows:

$$\frac{t}{q_t} = \frac{1}{k_2\, q_{eq}^2} + \frac{1}{q_{eq}} t \tag{4.7}$$

In this case, the pseudo-second order Cr (VI) adsorption rate constant is denoted by k_2. Graphing t/q_t against t reveals a linear connection. If the PSO kinetic equation is applicable, this linear connection enables the calculation of q_{eq} and k_2 from the plot's slope and intercept, respectively.

4.4 Results and Discussion

4.4.1 ATR-FTIR analysis

As seen by the FTIR spectra (Figure 4.2), the addition of the silane coupling agent containing amine groups (DAPTMS) to the BC-SiO_2 composite at different concentrations (4% and 10%) causes noticeable structural changes in the functional groups. These changes indicate new bonding interactions and structural modifications introduced with each concentration of DAPTMS, which directly impact the composite's adsorption efficiency and reactivity, especially in applications for heavy metal remediation. As shown in Figure 4.2. DAPTMS content increases to 4%, and the peaks associated with amine groups become more pronounced, indicating an enhanced amine presence. This increase in amine groups supports stronger electrostatic interactions with heavy metal ions, thereby improving adsorption efficiency. Additionally, the Si-O-Si bond formation and silane linkage are significantly intensified as the DAPTMS concentration rises, especially at 4% and 10%. This is evident from the characteristic Si-O-Si stretching around 1000-1100 cm^{-1} (Kim *et al.* 2018), which reflects a strengthened silane network where DAPTMS molecules link to both silica and cellulose, reinforcing the overall composite structure. At 10% DAPTMS, however, the

intensified Si-O-Si peak suggests a saturation point where silane linkage may be maximized, potentially introducing steric hindrance that could limit active site accessibility

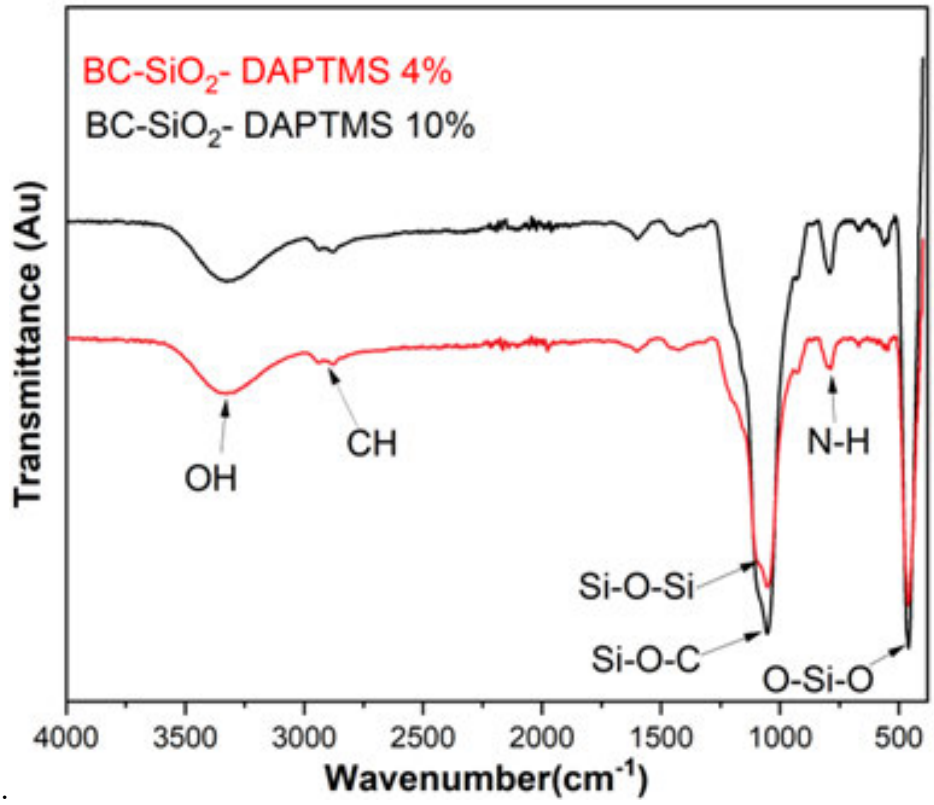

Figure 4.2 ATR-FTIR spectra of BC-SiO_2-DAPTMS (4 %) & BC-SiO_2-DAPTMS (10 %).

Further changes are observed in the O-H stretching region (3200-3500 cm^{-1}), where shifts and intensity reductions occur with increasing DAPTMS doses, particularly at 10%. This indicates reduced hydrogen bonding as amine and silane groups replace hydroxyl groups on the BC-SiO_2 surface. Such substitution, particularly at higher DAPTMS levels, may impact the composite's affinity for water and consequently alter its adsorption kinetics. The increase in amine functionality at higher DAPTMS levels enhances the composite's chemisorption capacity by introducing electron-donating groups that facilitate complexation with metal ions. NH_2 bending was identified as the cause of the peaks at 690 cm^{-1} and 720 cm^{-1} (Kim *et al.* 2018). The peak for BC-SiO_2-DAPTMS (10%) was more intense compared to that of the BC-SiO_2-DAPTMS (4%) composite. The 4% DAPTMS concentration appears especially effective, as it balances active site availability and material crystallinity for optimal adsorption. Conversely, at 10% DAPTMS, the FTIR spectra

suggest potential saturation, where excessive amine functionalization could lead to aggregation, possibly restricting the accessibility of binding sites for Cr (VI). In summary, FTIR analysis indicates that a DAPTMS concentration of around 4% achieves a balanced distribution of functional groups, enhancing BC-SiO_2's reactivity for Cr (VI) adsorption through increased amine group introduction and effective Si-O-Si network formation. Although higher doses increase functionality, they may also introduce steric effects that limit adsorption efficiency, underscoring the importance of dose optimization in designing composites for environmental applications.

4.4.2 XRD analysis

The BC-SiO_2-DAPTMS (4 and 10%) X-ray diffractograms, shown in Figure 4.3, display a similar pattern to that of BC-SiO_2–DAPTMS (2%) (Mazibuko *et al.* 2024). The XRD analysis revealed that the crystalline structure remained unchanged after DAPTMS functionalization. There are distinct peaks at $2\theta = 15^{o}$, 22^{o}, and 34^{o} in the XRD diffractograms of BC-SiO_2–DAPTMS (4 & 10%), which correspond to the crystallographic planes (101), (002), and (040) of the normal cellulose I structure (Mohd *et al.* 2016; Khanjanzadeh *et al.* 2018; Helmiyati and Suci 2019). The crystallinity index results in Table 4.1 indicate a notable increase in crystallinity with the addition of higher doses of DAPTMS to the BC-SiO_2 composite. Specifically, the crystallinity index for BC-SiO_2-DAPTMS at 4% is 93.79%, which rises to 97.77% with a 10% DAPTMS dose. This trend suggests that higher concentrations of DAPTMS promote a more ordered structure within the composite, enhancing its crystalline arrangement. The increased crystallinity at the 10% DAPTMS level is likely due to strengthened crosslinking and bonding interactions among silica, cellulose, and DAPTMS molecules, leading to improved structural integrity and resistance to thermal degradation.

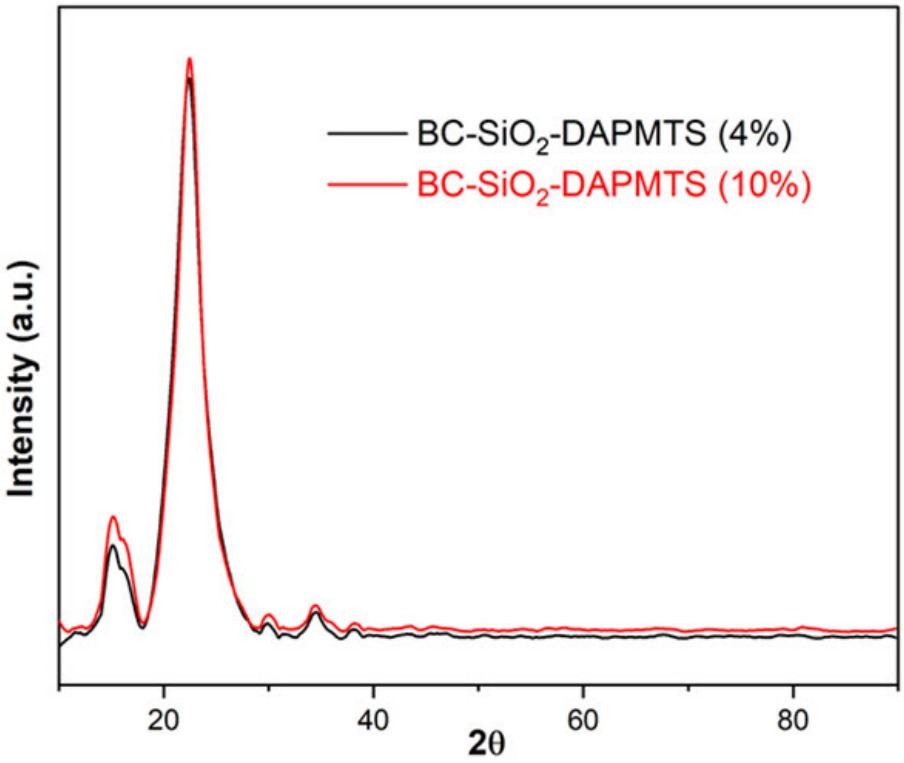

Figure 4.3 BC-SiO₂-DAPTMS (4 and 10%) X-ray diffractograms.

Table 4.1 BC-SiO₂-DAPTMS (4 and 10%) crystallinity indices.

Samples	Percentage Crystallinity (%)
BC-SiO₂-DAPTMS (4 %)	93.8
BC-SiO₂-DAPTMS (10 %)	97.8

However, while higher crystallinity enhances the composite's stability, it may also impact the accessibility of adsorption sites, potentially influencing the adsorption kinetics and efficiency, especially for heavy metal ions such as Cr (VI). The lower crystallinity observed in the 4% DAPTMS sample, in contrast, suggests a less rigid structure, which could improve the accessibility of active sites and facilitate ion diffusion, thereby supporting efficient adsorption rates. This variation underscores the importance of achieving a balance between crystallinity and functional flexibility to optimize the composite's performance as an adsorbent. While a high crystallinity level, as seen in the 10% DAPTMS sample, reinforces the composite's structural stability, it may

come at the cost of reduced site accessibility, which could compromise adsorption efficiency. Consequently, a 4% DAPTMS concentration might represent an optimal balance, offering sufficient crystallinity without limiting the accessibility of active sites. Overall, increasing the DAPTMS content enhances the crystallinity and structural stability of BC-SiO_2 composites but may restrict adsorption site accessibility. This finding highlights the need to carefully balance DAPTMS concentration to optimize both durability and adsorption efficacy for effective environmental remediation applications.

4.4.3 Thermogravimetric analysis

The TGA curves for BC-SiO_2-DAPTMS (4% and 10%) in Figure 4.4(a) show similar decomposition patterns to those observed for BC-SiO_2-DAPTMS (2%) in (Mazibuko *et al.* 2024), indicating the normal phases of heat breakdown of cellulose. Dehydration, depolymerization, and glycosyl unit breakup are the two primary degradation steps that the BC-SiO_2-DAPTMS (4 & 10%) samples go through. At higher temperatures, the cellulose chain breaks down, resulting in a considerable weight loss. Additionally, the DSC curves for BC-SiO_2-DAPTMS (4%) in Figure 4.4(b), compared to BC-SiO_2-DAPTMS (10%) in Figure 4.4(a), reveal similar thermal degradation peaks. As the DAPTMS dose rises, these curves show a clear second peak that is well separated, signifying enhanced thermal stability. Table 4.2's TGA of the BC-SiO_2-DAPTMS (4%) and BC-SiO_2-DAPTMS (10%) composites provides important information about their degradation behaviour and heat stability. At the first stage of deterioration, the BC-SiO_2-DAPTMS (4%) composite exhibits an initial mass loss of 8.88%. However, the second degradation stage has a slightly higher mass loss of 42.74%, due to the thermal breakdown of both cellulose and the higher concentration of DAPTMS. The ash content at 600℃ is 33.62%, indicating increased stability from the additional DAPTMS.

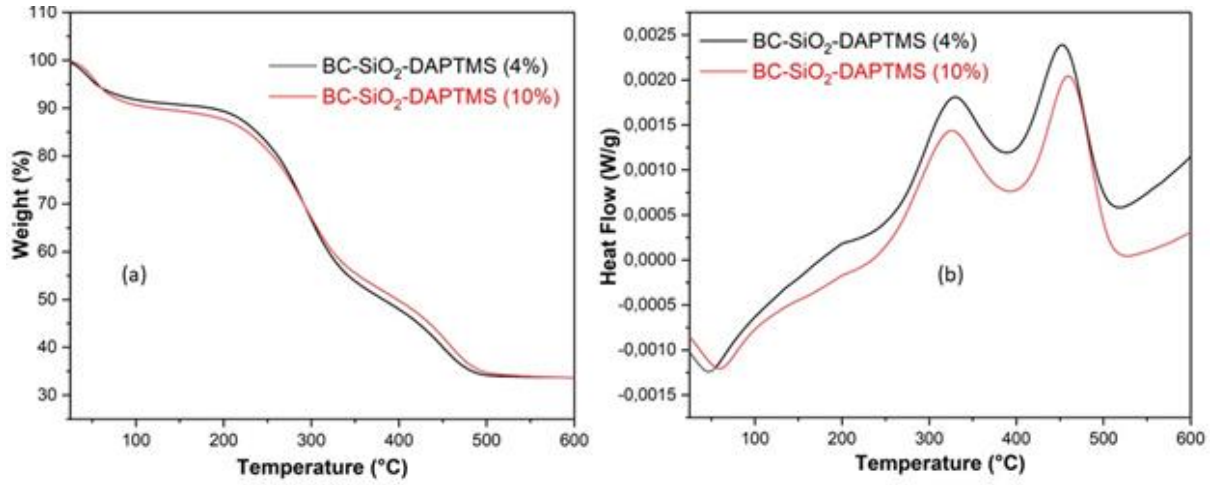

Figure 4.4 The TGA curves for BC-SiO_2-DAPTMS (4% and 10%) are displayed in (a); (b) compares the DSC thermograms of BC-SiO_2-DAPTMS (4 and 10%).

Because of its higher volatile content, the BC-SiO_2-DAPTMS (10%) composite has the largest initial mass loss (10.44%). A 39.61% mass loss in the second stage indicates cellulose breakdown, but more stability is provided by the increased DAPTMS concentration. The final mass loss is 16.16%, with an ash content of 33.64%, showing that increased DAPTMS concentration enhances the composite's stability. The ash content, which is the residue at 600°C, increases overall as the DAPTMS content increases, indicating a higher inorganic (silica) content and improved thermal stability. The level of functionalization increases with the increasing residue, indicating that the DAPTMS coating enhances both the structural integrity and thermal stability of the material, which are important for applications like heavy metal removal. Therefore, the composites changed with DAPTMS, especially those with higher DAPTMS concentrations, show improved stability, as they are better suited for demanding environmental applications like heavy metal remediation. Similar findings about the improvement of cellulose thermal stability after modification have been reported by several studies (Khanjanzadeh *et al.* 2018; Sabir *et al.* 2023).

Table 4.2 The weight loss throughout each degradation phase, as well as the residual ash content for BC-SiO_2-DAPTMS (4 and 10%).

Temperature °C		Weight %		Calculations (%)		
BC-SiO_2-DAPTMS (4%)						
Initial	**Final**	**Initial**	**Final**	**Mass loss (At each degradation point)**		**Ash content (Residue at 600 °C)**
25	150	99.6	90.72	8.88	1st stage	
150	400	90.72	47.98	42.74	2nd stage	33.62
400	600	47.98	33.62	14.36	3rd stage	
BC-SiO_2-DAPTMS (10%)						
Initial	**Final**	**Initial**	**Final**	**Mass loss (At each degradation point)**		**Ash content (Residue at 600 °C)**
25	150	99.85	89.41	10.44	1st stage	
150	400	89.41	49.8	39.61	2nd stage	33.64
400	600	49.8	33.64	16.16	3rd stage	

4.4.4 SEM analysis

The SEM analysis of BC-SiO_2-DAPTMS composites with 4% and 10% DAPTMS concentrations in Figure 4.5 reveals important insights into the surface morphology and dispersion of DAPTMS on the composite matrix. In Figure 4.5 (a-c), the BC-SiO_2-DAPTMS (4%) sample, SEM images display a relatively uniform surface with well-dispersed silica particles throughout the cellulose matrix. The 4% DAPTMS concentration appears to provide an optimal amount of amine silane coupling, resulting in effective bonding between silica and cellulose without excessive

agglomeration. This uniform dispersion likely enhances the composite's accessibility to adsorption sites, which is beneficial for applications in heavy metal remediation.

In contrast, in Figure 4.5 (d-f), the BC-SiO_2-DAPTMS (10%) sample shows a more uneven surface morphology, with visible clusters and agglomerations of silica and DAPTMS. This high concentration of DAPTMS may lead to excessive crosslinking and bonding, causing localized densification and aggregation of particles. These clusters reduce the available surface area and block some of the active sites, which could hinder the adsorption efficiency of the composite. Overall, the SEM analysis suggests that while the modification with DAPTMS enhances the interaction between silica and cellulose, an optimal concentration (such as 4%) is critical for maintaining uniform dispersion and maximizing surface accessibility. Higher concentrations (such as 10%) may negatively impact the composite structure by creating dense clusters, thus limiting its adsorption potential and practical effectiveness for environmental applications. Similar to Pinto et al., who developed novel SiO_2/cellulose nanocomposites through in-situ synthesis and polyelectrolyte gathering, SEM images revealed that smaller silica particles tend to agglomerate on the fiber surfaces, forming dense coatings (Pinto *et al.* 2008).

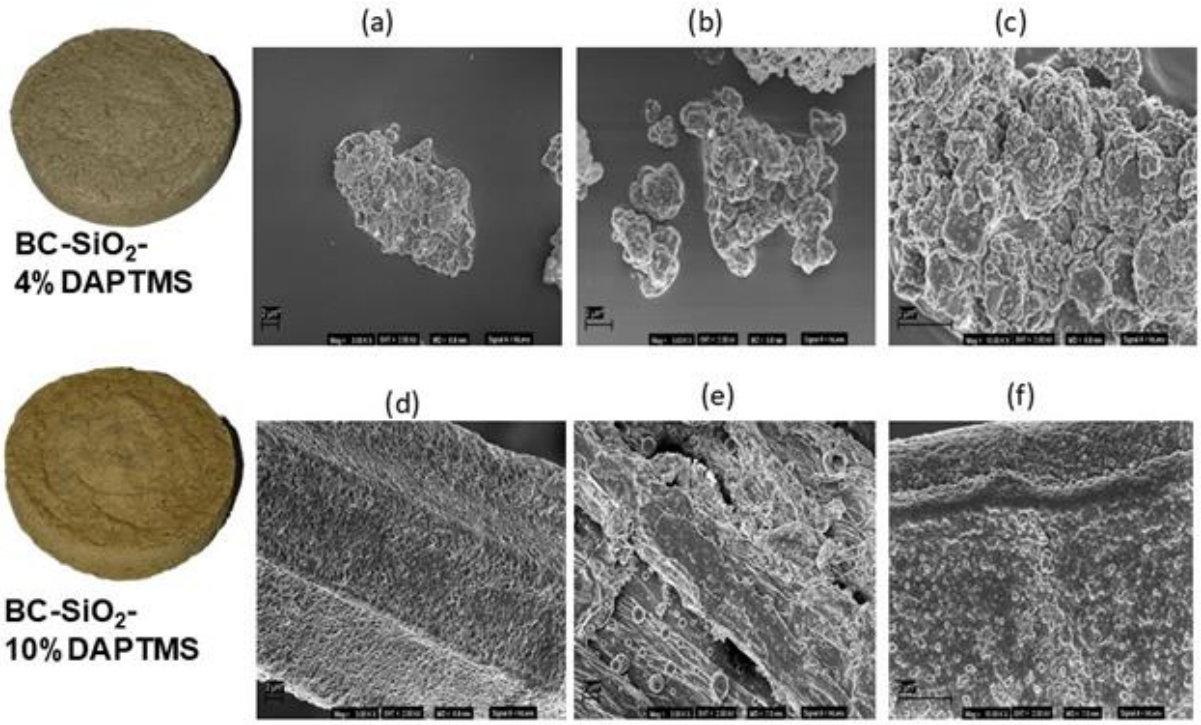

Figure 4.5 The SEM images demonstrate BC-SiO_2-DAPTMS composites with varying DAPTMS concentrations at various magnifications: images (a–c) show BC-SiO_2-DAPTMS (4%) at 3.00 KX, 5.00 KX, and 10.00 KX magnifications, while images (d–f) display BC-SiO_2-DAPTMS (10%) at the same magnification levels. This series provides a comparative view of the surface morphology for each concentration.

4.4.5 TEM analysis

The TEM analysis comparing BC-SiO_2-DAPTMS composites with 4% and 10% DAPTMS concentrations provides insights into how different doses of the amine silane coupling agent impact the structural integrity, particle dispersion, and bonding within the composite matrix. In Figure 4.6 (a-b), the BC-SiO_2-DAPTMS (4%) sample, TEM images show a well-dispersed distribution of silica particles across the cellulose matrix, suggesting effective integration facilitated by the amine groups in DAPTMS. The amine silane coupling agent promotes covalent bonding between cellulose and silica, which is evident in the smooth distribution and consistent particle size. This structure supports improved stability and tailored surface properties, allowing the composite to

maintain a high degree of accessible active sites. The uniform dispersion at 4% DAPTMS concentration enhances the overall integrity and functionality of the composite, making it particularly suited for applications like heavy metal adsorption. In contrast, in Figure 4.6 (c-d), the BC-SiO_2-DAPTMS (10%) sample exhibits areas of increased particle agglomeration and less uniform distribution. The higher concentration of DAPTMS likely results in excessive bonding interactions, leading to clustering within the composite matrix. This clustering can hinder the accessibility of active sites by reducing the overall surface area and creating a denser surface.

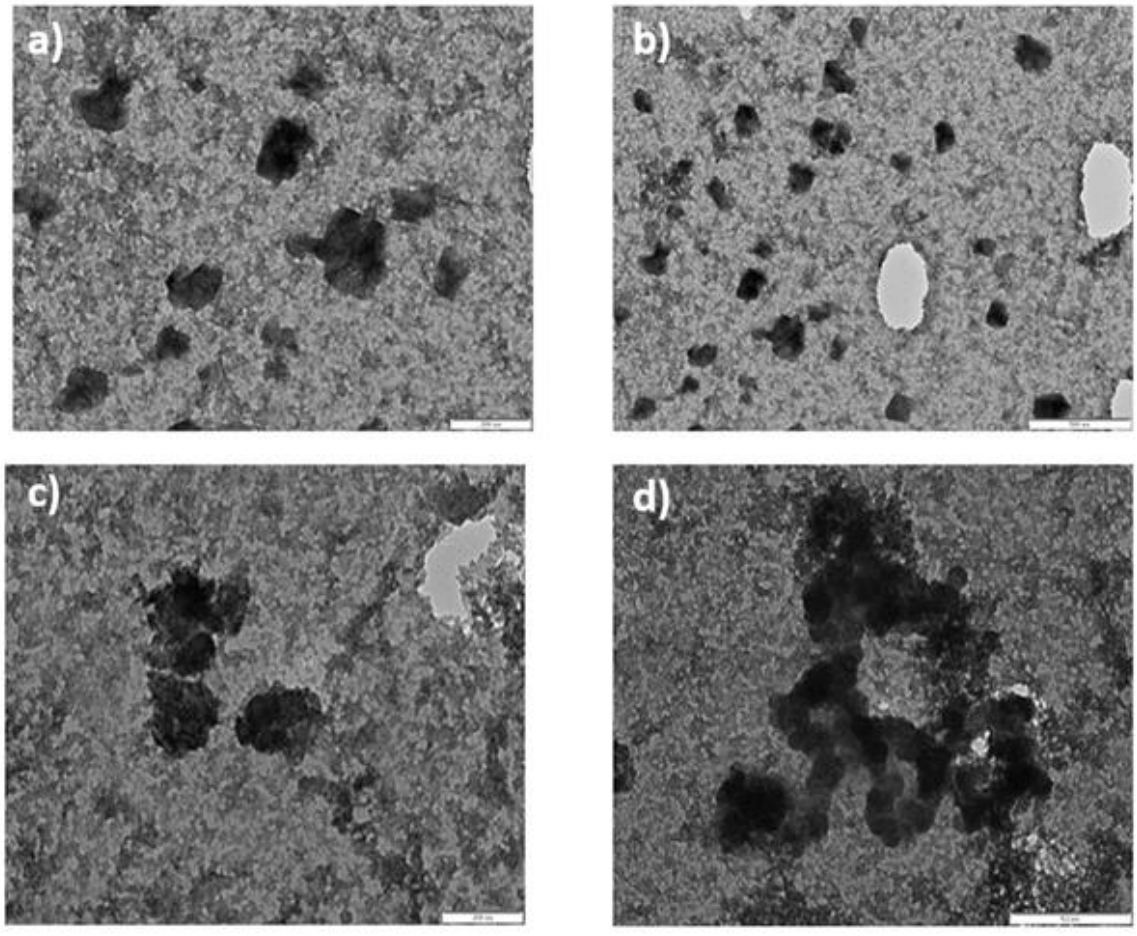

Figure 4.6 The BC-SiO_2-DAPTMS composites with varying DAPTMS concentrations at different magnifications are displayed in TEM images: BC-SiO_2-DAPTMS (4%) at (a) 200 nm and (b) 500 nm, and BC-SiO_2-DAPTMS (10%) at (c) 200 nm and (d) 500 nm.

4.4.6 Adsorption kinetics and isotherms

4.4.6.1 Initial concentration Effect

The plot in Figure 4.7(a) illustrates the removal efficiency of Cr (VI) at varied initial concentrations (Ci) ranging from 0.1 mg/L to 1 mg/L utilizing two composites: BC-SiO_2-DAPTMS (4% and 10%), each at a weight of 0.5g. At the lowest concentration (0.1 mg/L), BC-SiO_2-DAPTMS (4%) demonstrates the highest removal efficiency (88.76%), followed by BC-SiO_2-DAPTMS (10%) at 80.07%. As the concentration increases to 0.2 mg/L, the removal efficiency improves for all composites, with BC-SiO_2-DAPTMS (4%) reaching 92.79%, while BC-SiO_2-DAPTMS (10%) shows a removal of 84.13%. At higher concentrations (0.3 to 1 mg/L), BC-SiO_2-DAPTMS (4%) continues to show superior performance, achieving nearly complete removal, with efficiencies reaching 97.14% at 0.3 mg/L, and slightly decreasing at higher concentrations to 92.98% at 1 mg/L. BC-SiO_2-DAPTMS (10%) maintains a relatively consistent removal efficiency, starting at 95.53% at 0.3 mg/L and declining to 90.19% at 1 mg/L.

Overall, the plot in Figure 4.7(a) suggests that BC-SiO_2-DAPTMS (4%) is the most effective composite for Cr (VI) removal across a range of concentrations, with BC-SiO_2-DAPTMS (10%) following closely behind. The removal efficiency generally improves with concentration up to a certain point before stabilizing or slightly declining at higher concentrations, indicating the capacity limits of the adsorbents. This trend highlights the importance of composite formulation in determining the efficiency of Cr (VI) removal in different environmental conditions. A study by Wang et al. demonstrated that the fixed number of active adsorption sites in the adsorbent is the reason for the decline in the efficiency of Cr (VI) removal as the quantity of adsorbate rises. which remain constant despite the rising concentration of adsorbate ions. As a result, the available sites become saturated, leading to reduced adsorption efficiency (Wang, Li and Tao 2009; Mohd *et al.* 2016).

4.4.6.2 Weight dosage effect

The plot in Figure 4.7(b) shows the removal efficiency of a contaminant using two different composites, BC-SiO_2-DAPTMS (4%) and BC-SiO_2-DAPTMS (10%), at varying adsorbent weights ranging from 0.05g to 1.1g. As the adsorbent weight increases, the removal efficiency improves for all three composites, with BC-SiO_2-DAPTMS (10%) consistently demonstrating the highest efficiency. At the lowest adsorbent weight of 0.05g, BC-SiO_2-DAPTMS (4%) and BC-SiO_2-DAPTMS (10%) achieve 90.73 and 95.03%, respectively. This trend continues as the adsorbent weight increases, with BC-SiO_2-DAPTMS (10%) reaching nearly 95.46% removal efficiency at 1.1g. BC-SiO_2-DAPTMS (4%) follows closely, reaching 95.81% at the same weight. As the adsorbent weight increases from 0.5g to 1.1g, the differences between the composites become less pronounced, with all composites achieving removal efficiencies greater than 93%. This indicates that once the adsorbent weight reaches a certain level, further increases do not significantly enhance the removal efficiency. Kim et al.'s investigation showed that when the adsorbent dosage increased, Cr (VI) adsorption improved. The increased availability of sorption sites was credited with this improvement, which facilitated a higher percentage of Cr (VI) removal (Ofomaja 2008; Wang, Li and Tao 2009; Kim *et al.* 2018).

Overall, the data underscores that increasing the adsorbent weight improves contaminant removal, with BC-SiO_2-DAPTMS (10%) providing the highest efficiency across all weights. However, the removal efficiency stabilizes after reaching a certain weight, suggesting that optimal performance is achieved around 1g of adsorbent for the most effective contaminant removal.

4.4.6.3 Contact time effect

The Cr (VI) elimination efficiencies of two distinct composites, BC-SiO_2-DAPTMS (4 and 10%), are plotted for a period of 5 to 65 minutes in Figure 4.7(c). BC-SiO_2-DAPTMS (10%) consistently demonstrated the highest Cr (VI) removal performance, starting at 88.14% at 5 minutes and gradually increasing to 91.29% by the 65-minute mark. This suggests that the composite reaches a point of equilibrium after approximately 50 minutes, where further increases in removal

efficiency are minimal. On the other hand, BC-SiO_2-DAPTMS (4%) showed a similar trend but with a slightly lower removal efficiency. Beginning at 82.57% at 5 minutes, the removal efficiency increased more slowly, reaching 84.30% by 65 minutes. This composite's removal efficiency plateaued after around 55 minutes, with little change in the final readings. Although it demonstrated consistent improvement, it never reached the levels of the other two composites. Comparable studies have shown a consistent trend where adsorption capacities increase significantly with extended contact time. However, the adsorption percentage stabilizes and stays almost constant after equilibrium is reached (Das *et al.* 2000; Hokkanen *et al.* 2016; Tao *et al.* 2017).

Overall, while all three composites effectively removed Cr (VI), BC-SiO_2-DAPTMS (10%) exhibited the best performance, followed by BC-SiO_2-DAPTMS (4%), highlighting the positive correlation between DAPTMS concentration and the effectiveness of elimination of Cr (VI).

4.4.6.4 pH effect

The plot in Figure 4.7(d) illustrates the effectiveness of the elimination of Cr (VI) ions using two composites: BC-SiO_2-DAPTMS (4 and 10%), at various pH values (ranging from 1 to 10). As the pH increases, the removal efficiency generally decreases for all composites, with BC-SiO_2-DAPTMS (10%) consistently demonstrating the highest removal efficiency. At pH 1, the BC-SiO_2-DAPTMS (10%) composite achieves removal of 85.23%, while BC-SiO_2-DAPTMS (4%) in Figure 4.7(d) shows lower removal rates of 70.42%. As the pH rises to 2 and 3, the removal efficiencies for all composites improve, with BC-SiO_2-DAPTMS (10%) reaching 88.97% at pH 2 and 89.27% at pH 3. BC-SiO_2-DAPTMS (4%) and BC-SiO_2-DAPTMS (10%) also show a decrease in removal efficiency at higher pH. BC-SiO_2-DAPTMS (10%) remains the most effective, stabilizing at 85.84% at pH 10. This data indicates that acidic conditions (low pH) are more favourable for Cr (VI) removal (Benhamou *et al.* 2013), with BC-SiO_2-DAPTMS (10%) offering the best performance overall, suggesting that pH control is crucial for optimizing the effectiveness of these adsorbents in Cr (VI) remediation. According to a related work by Kim et al., acidic pH levels were optimal for Cr (VI) adsorption onto the adsorbents. The maximum adsorption capacity

was achieved at pH 3, indicating favourable sorption in strongly acidic environments (Kim *et al.* 2018).

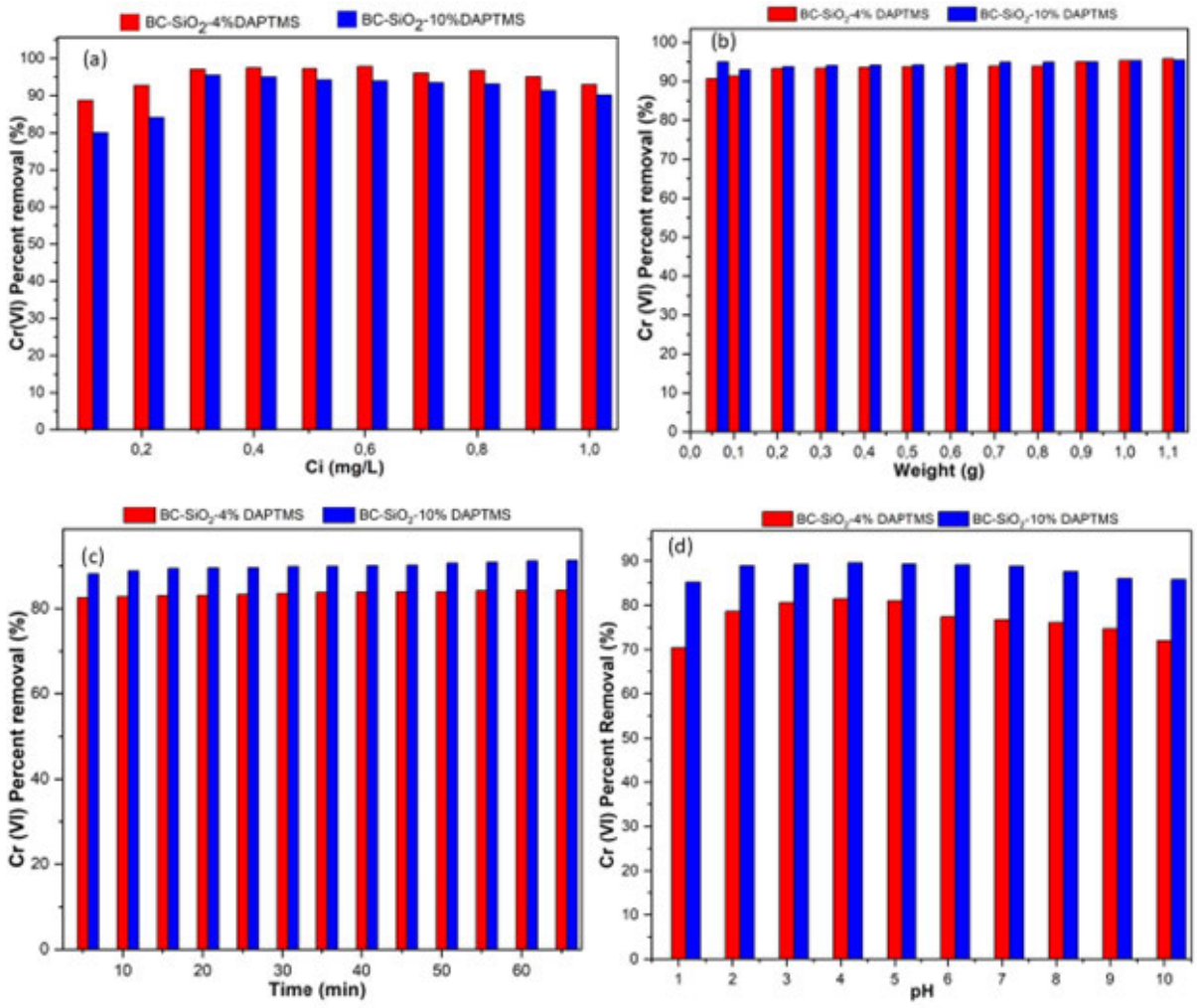

Figure 4.7 Effects of several operational parameters on the percentage of Cr (VI) elimination include (a) the initial concentration, (b) the adsorbent dose, (c) the contact time, and (d) pH.

4.4.6.5 The pH at Point of Zero Charge (pH_pzc)

For BC-SiO_2 composites functionalized with different amounts of DAPTMS (4 and 10%), the pH at Zero Charge Point (pH_pzc) increases noticeably as the DAPTMS content increases. This trend reflects the influence of amine groups from DAPTMS on the surface charge characteristics of the

composite, improving its effectiveness for adsorption. As shown in Figure 4.8, increasing the DAPTMS content to 4% raises the pH_pzc to around 10.05, allowing the composite to maintain a positively charged surface over a broader pH range and improving its effectiveness for adsorbing anionic species like Cr (VI) at near-neutral pH. At the highest DAPTMS concentration, BC-SiO_2-DAPTMS (10%) achieves a pH_pzc of around 11, enabling it to retain a positive charge even in mildly alkaline environments, thus making it particularly effective for anion adsorption in both acidic and near-neutral conditions.

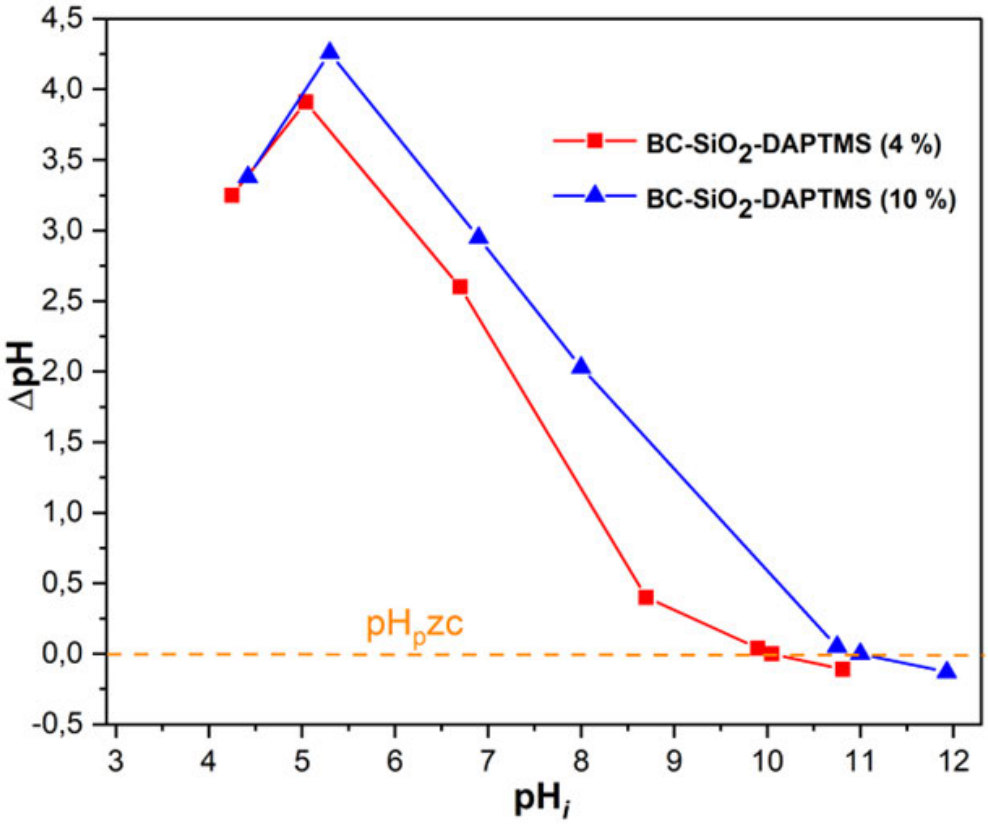

Figure 4.8 BC-SiO_2-DAPTMS, the pH at Zero Charge Point (pH_pzc) (4 (Red) and 10% (Blue).

This progressive increase in pH_pzc with higher DAPTMS concentration underscores the role of amine groups in shifting the surface charge of the composite, enhancing its versatility for anionic metal adsorption across a wider range of pH values. A study by Sun et al. similarly observed a shift in the Zero Charge Point from lower to higher values following amino functionalization. This shift

was ascribed to amino groups being protonated introduced during the grafting process, indicating that the amino-functionalized adsorbent acquired a positive charge (Sun *et al.* 2014).

4.4.6.5.1 Equilibrium Study

The adsorption isotherm study for Cr (VI) removal using BC-SiO_2-DAPTMS composites (4 and 10%) was assessed using both linear and non-linear fitting techniques for the Langmuir and Freundlich models (Table 4.3). The results revealed distinct adsorption behaviours for the two composites, highlighting the influence of DAPTMS concentration on adsorption performance. For the maximal adsorption capacity (q_{max}) and the Langmuir isotherm for the 4% composite was higher than the 10% composite under both linear and non-linear fitting methods, suggesting that the 4% composite has a slightly greater monolayer adsorption capacity. However, the Langmuir constant (K_L) was significantly higher for the 10% composite, indicating stronger adsorption affinity for Cr (VI). This shift toward positive K_L values suggests improved homogeneity in adsorption sites as the DAPTMS content rises. The correlation coefficients (R^2) propose that non-linear fitting provides the Langmuir model a better fit, particularly for the 4% composite (R^2 = 0.94034) compared to the 10% composite (R^2 = 0.95676) (Figure 9 (a and b). Similar results were observed by Qiu et al., who showed that the Cr (VI) adsorption was more accurately represented by the Langmuir isotherm model (Qiu *et al.* 2014).

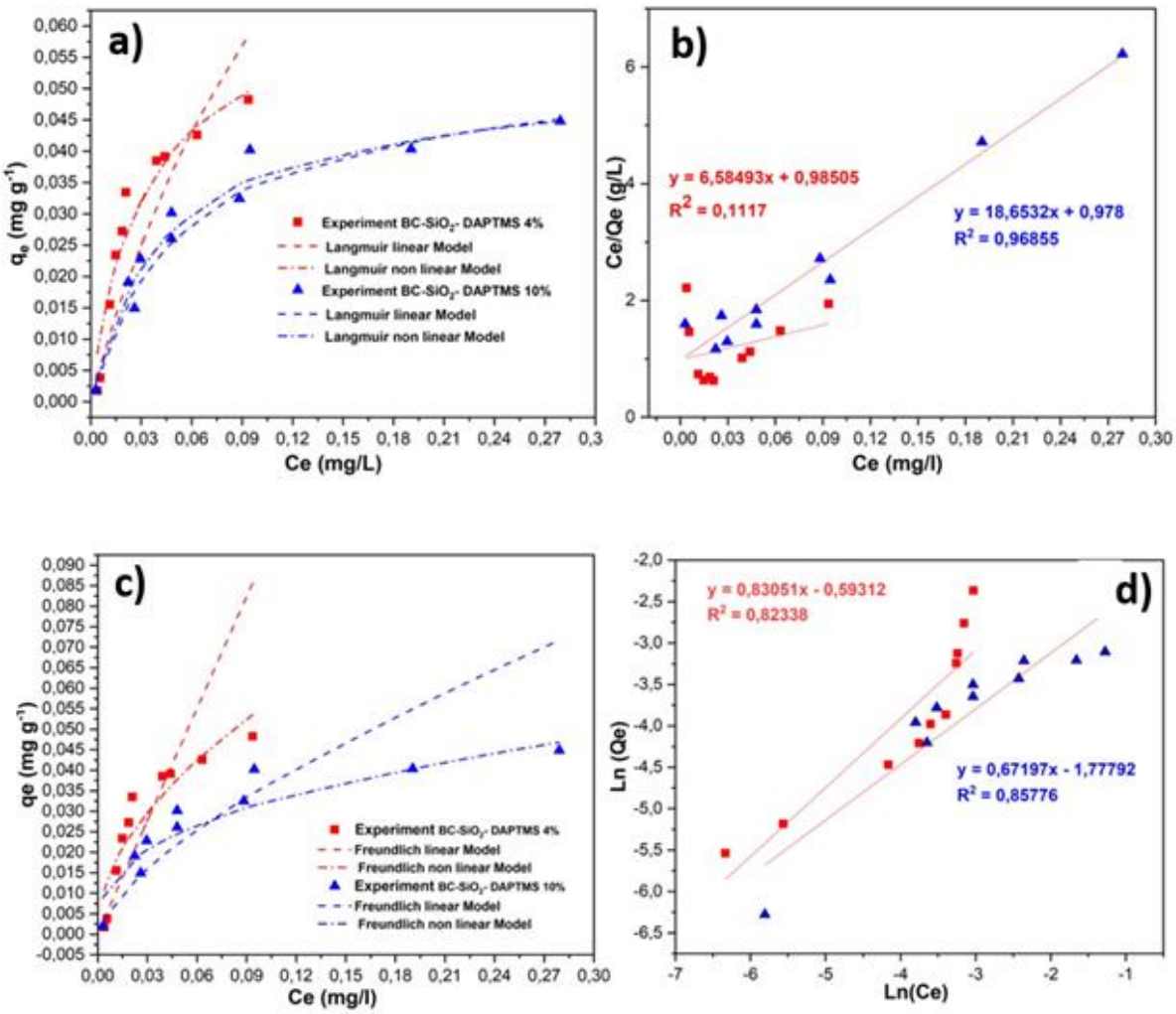

Figure 4.9 Cr (VI) ion solutions (0.1–1.0 ppm) were adsorbed onto BC-SiO2-DAPTMS (4 & 10%) at neutral pH (7) using the following adsorption isotherms: (a) Langmuir (linear & non-linear), (b) Langmuir (linear), (c) Freundlich (linear & non-linear), and (d) Freundlich (linear).

In the Freundlich model, the Freundlich isotherm demonstrated higher q_{max} values for the 4% composite across both fitting methods, aligning with its higher adsorption capacity. However, the Freundlich constant (K_F) was notably higher for the 10% composite, reflecting a greater intensity of adsorption. Non-linear fitting yielded superior R^2 values for the Freundlich model, especially for the 10% composite (R^2 = 0.98006), signifying that the adsorption process may involve heterogeneous surface interactions.

Overall, the findings indicate that while the 4% composite exhibits slightly higher adsorption capacities, the 10% composite demonstrates stronger adsorption affinities and better adherence to the Freundlich isotherm behaviour. This suggests that increasing the DAPTMS concentration enhances the adsorbent's surface interaction with Cr (VI), potentially because of more active sites available for adsorption (Figure 4.9 (a and b)). Comparable findings were reported by Chakraborty et al., who demonstrated that the Freundlich isotherm model successfully described the experimental results (Chakraborty *et al.* 2021).

Table 4.3 Characteristics of the adsorption isotherm for metal ion adsorption onto BC-SiO_2-DAPTMS (4 and 10%).

Adsorption isotherm	Parameter	Adsorbent BC-SiO_2-DAPTMS (4 %)		Adsorbent BC-SiO_2-DAPTMS (10 %)	
		Cr (VI)			
		Linear	Non-linear	Linear	Non-linear
Langmuir	q_{max} (mg/g)	0.15186	0.06498	0.05361	0.05161
	K_L	6.68484	34.17710	19.07271	23.60139
	R^2	0.11170	0.94034	0.96855	0.95676
Freundlich	q_{max} (mg/g)	0.89621	0.17842	0.16899	0.07469
	K_F	1.00866	1.96584	6.58493	2.73307
	R^2	0.82338	0.86610	0.85776	0.98006

4.4.6.5.2 Kinetic study

The PSO model outperformed the PFO model in the kinetic analysis of Cr (VI) adsorption onto BC-SiO_2-DAPTMS composites (4 and 10%). The plots in Figure 4.10 showed that while both models were assessed using the PSO model, both linear and non-linear fitting techniques,

especially under non-linear fitting, provide the best fit across all composites, as indicated by the high R^2 values close to 1. In Table 4.4, the BC-SiO_2-DAPTMS (4%) composite shows an increase in k_2 to 173.31 g/mg/min in the linear PSO fit, with an exceptionally high R^2 of 0.9999, while the PFO model produces a significantly lower R^2 of 0.9608 and a lower k_1 of 0.0364 g/mg/min. Non-linear fitting in the PSO model for this composite shows an even higher k_1 (1.13 g/mg/min) but with a lower q_{eq} of 0.0234 mg/g, which still does not match the consistency seen in the PSO model. For the BC-SiO_2-DAPTMS (10%) composite, the trend continues with the PSO model showing a superior fit. The linear PSO fit for this composite reveals a very high k_2 value of 255.11 g/mg/min and an R^2 value of 0.9999, indicating that the adsorption process follows a chemisorption mechanism with increased DAPTMS content. In non-linear fitting, k_2 slightly increases to 285.47 g/mg/min, while R^2 remains at 0.9996, confirming the robustness of the PSO model for this system. Interestingly, the non-linear PSO fit shows an exceptionally high k_1 of 2.50x106 g/mg/min, which appears to be an outlier and likely results from a computational or experimental anomaly, as it does not correspond to realistic adsorption dynamics.

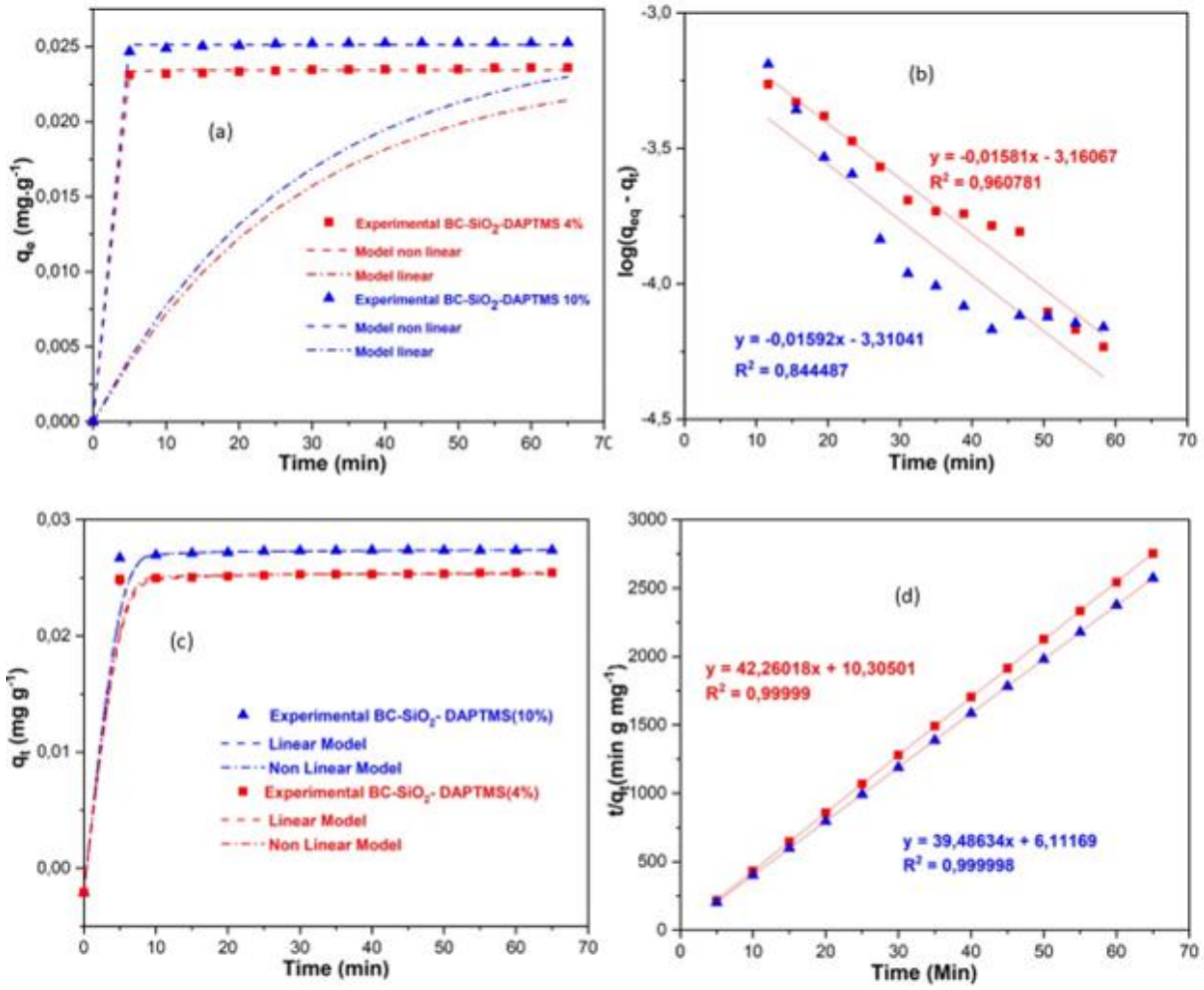

Figure 4.10 PFO and PSO adsorption plots for Cr (VI) ions (5 to 65 minutes) were analyzed using the BC-SiO_2-DAPTMS (4 and 10%) composite: (a) PFO linear and non-linear plots, (b) PFO linear plots, (c) PSO linear and non-linear plots, and (d) PSO linear plots, all at neutral pH (7).

Overall, the findings clearly show that, for all DAPTMS content levels, the PSO kinetic model best explains the Cr (VI) adsorption onto BC-SiO_2-DAPTMS composites. The pseudo-second order model's non-linear fitting approach regularly yields the highest R^2 values, demonstrating its dependability in describing the adsorption kinetics. As the DAPTMS content increases, k_2 values also increase, highlighting improved adsorption efficiency and suggesting that the adsorption process becomes more favourable at higher DAPTMS content due to a likely increase in available active sites for Cr (VI) ions. This improvement in fit, particularly under the PSO model, suggests

a chemisorption-dominated mechanism, as opposed to the physical adsorption typically indicated by the PSO model. Consistent with findings reported by Dong et al., the results indicated that the adsorption kinetics adhered to a PSO model (Dong *et al.* 2016; Su *et al.* 2022).

Table 4.4 Pseudo-first- and second order reaction rate parameters for linear and non-linear Cr (VI).

Parameters	Linear fitting						Non-linear fitting					
	Pseudo-first order kinetic model			Pseudo-second order kinetic model			Pseudo-first order kinetic model			Pseudo-second order kinetic model		
Composites	k_1 (g /mg min)	q_{eq} (mg/g)	R^2	k_2 (g /mg min)	q_{eq} (mg/g)	R^2	k_1 (g /mg min)	q_{eq} (mg/g)	R^2	k_2 (g /mg min)	q_{eq} (mg/g)	R^2
BC-SiO_2-DAPTMS (4%)	0.036	0.024	0.9608	173.306	0.024	0.999988	1.132	0.023	0.999507	363.211	0.024	0.998173
BC-SiO_2-DAPTMS (10%)	0.037	0.025	0.8445	255.113	0.025	0.999998	2.50×10^6	0.025	0.999346	285.472	0.025	0.999599

4.5 Conclusions

This study demonstrates that the success of modified bleached cellulose-SiO_2 composites in removing chromium (Cr (VI)) from wastewater is significantly influenced by the concentration of N-[3-(trimethoxysilyl)propyl]ethylenediamine (DAPTMS). Both the 4 and 10% DAPTMS-modified composites exhibited excellent adsorption capacities, with the 10% composite achieving higher removal efficiency due to the increased availability of functional amine groups. Structural characterization confirmed the successful functionalization of cellulose fibers with silica nanoparticles, which enhanced surface properties and provided additional active sites for Cr (VI) binding. BC-SiO_2-DAPTMS (4%) showed superior adsorption capacity, while BC-SiO_2-DAPTMS (10%) exhibited stronger affinities and higher overall efficiency, benefiting from increased active site availability. Optimal performance was achieved under acidic conditions, emphasizing the importance of pH control. Adsorption behaviour followed the Freundlich isotherm model, suggesting heterogeneous surface interactions, and the PSO kinetic model provided the best fit, indicating a chemisorption-dominated mechanism.

Lastly, the study underscores the significance of composite formulation and DAPTMS concentration in optimizing adsorbent performance. These findings offer valuable insights into improving BC-SiO_2-DAPTMS composites for Cr (VI) remediation, highlighting their potential application in environmental cleanup initiatives.

4.6 References

Agaba, A., Cheng, H., Zhao, J., Zhang, C., Tebyetekerwa, M., Rong, L., Sui, X. and Wang, B. 2018. Precipitated silica agglomerates reinforced with cellulose nanofibrils as adsorbents for heavy metals. RSC advances, 8 (58): 33129-33137.

Benhamou, A., Basly, J., Baudu, M., Derriche, Z. and Hamacha, R. 2013. Amino-functionalized MCM-41 and MCM-48 for the removal of chromate and arsenate. Journal of colloid and interface science, 404: 135-139.

Bois, L., Bonhommé, A., Ribes, A., Pais, B., Raffin, G. and Tessier, F. 2003. Functionalized silica for heavy metal ions adsorption. Colloids and Surfaces A: Physicochemical and Engineering Aspects, 221 (1-3): 221-230.

Chakraborty, R., Verma, R., Asthana, A., Vidya, S. S. and Singh, A. K. 2021. Adsorption of hazardous chromium (VI) ions from aqueous solutions using modified sawdust: kinetics, isotherm and thermodynamic modelling. International Journal of Environmental Analytical Chemistry, 101 (7): 911-928.

Das, D. D., Mahapatra, R., Pradhan, J., Das, S. N. and Thakur, R. S. 2000. Removal of Cr(VI) from Aqueous Solution Using Activated Cow Dung Carbon. J Colloid Interface Sci, 232 (2): 235-240.

Dong, Z., Zhao, J., Du, J., Li, C. and Zhao, L. 2016. Radiation synthesis of spherical cellulose-based adsorbent for efficient adsorption and detoxification of Cr (VI). Radiation Physics and Chemistry, 126: 68-74.

Freundlich, H. M. F. 1906. Over the adsorption in solution. J. Phys. chem, 57 (385471): 1100-1107.

Gao, J., Zhang, L., Liu, S. and Liu, X. 2022. Enhanced adsorption of copper ions from aqueous solution by two-step DTPA-modified magnetic cellulose hydrogel beads. International journal of biological macromolecules, 211: 689-699.

Helmiyati, H. and Suci, R. 2019. Nanocomposite of cellulose-ZnO/SiO2 as catalyst biodiesel methyl ester from virgin coconut oil. In: Proceedings of AIP Conference Proceedings. AIP Publishing LLC, 020063.

Ho, Y.-S. and McKay, G. 1999. Pseudo-second order model for sorption processes. Process biochemistry, 34 (5): 451-465.

Hokkanen, S., Bhatnagar, A., Repo, E., Lou, S. and Sillanpää, M. 2016. Calcium hydroxyapatite microfibrillated cellulose composite as a potential adsorbent for the removal of Cr (VI) from aqueous solution. Chemical Engineering Journal, 283: 445-452.

Jamroz, E., Kocot, K., Zawisza, B., Talik, E., Gagor, A. and Sitko, R. 2019. A green analytical method for ultratrace determination of hexavalent chromium ions based on micro-solid phase extraction using amino-silanized cellulose membranes. Microchemical Journal, 149: 104060.

Johari, K., Saman, N., Song, S. T., Chin, C. S., Kong, H. and Mat, H. 2016. Adsorption enhancement of elemental mercury by various surface modified coconut husk as eco-friendly low-cost adsorbents. International Biodeterioration & Biodegradation, 109: 45-52.

Khanjanzadeh, H., Behrooz, R., Bahramifar, N., Gindl-Altmutter, W., Bacher, M., Edler, M. and Griesser, T. 2018. Surface chemical functionalization of cellulose nanocrystals by 3-aminopropyltriethoxysilane. International journal of biological macromolecules, 106: 1288-1296.

Kim, J.-H., Kang, J.-K., Lee, S.-C. and Kim, S.-B. 2018. Synthesis of powdered and granular N-(3-trimethoxysilylpropyl) diethylenetriamine-grafted mesoporous silica SBA-15 for Cr (VI) removal from industrial wastewater. Journal of the Taiwan Institute of Chemical Engineers, 87: 140-149.

Lagergren, S. 1898. About the theory of so-called adsorption of soluble substances.

Langmuir, I. 1916. The constitution and fundamental properties of solids and liquids. Part I. Solids. Journal of the American chemical society, 38 (11): 2221-2295.

Lee, J., Kim, J.-H., Choi, K., Kim, H.-G., Park, J.-A., Cho, S.-H., Hong, S. W., Lee, J.-H., Lee, J. H. and Lee, S. 2018. Investigation of the mechanism of chromium removal in (3-aminopropyl) trimethoxysilane functionalized mesoporous silica. Scientific reports, 8 (1): 12078.

Malik, D., Jain, C. and Yadav, A. K. 2017. Removal of heavy metals from emerging cellulosic low-cost adsorbents: a review. Applied Water Science, 7: 2113-2136.

Mazibuko, M. T., Onwubu, S. C., Mdluli, P. S., Paul, V., Teboho, M. C. and Thabang, M. 2024. Amine-functionalized cellulose-silica composites for the remediation of hexavalent chromium (Cr IV) in contaminated water. Results in Chemistry, 11: 101796.

Mohd, N. H., Ismail, N. F. H., Zahari, J. I., Fathilah, W., Kargarzadeh, H., Ramli, S., Ahmad, I., Yarmo, M. A. and Othaman, R. 2016. Effect of aminosilane modification on nanocrystalline cellulose properties. Journal of Nanomaterials, 2016

Ofomaja, A. E. 2008. Sorptive removal of Methylene blue from aqueous solution using palm kernel fibre: Effect of fibre dose. Biochemical Engineering Journal, 40 (1): 8-18.

Okhrimenko, D. V., Budi, A., Ceccato, M., Cárdenas, M., Johansson, D. B., Lybye, D., Bechgaard, K., Andersson, M. P. and Stipp, S. L. 2017. Hydrolytic stability of 3-aminopropylsilane coupling agent on silica and silicate surfaces at elevated temperatures. ACS applied materials & interfaces, 9 (9): 8344-8353.

Pinto, R. J., Marques, P. A., Barros-Timmons, A. M., Trindade, T. and Neto, C. P. 2008. Novel SiO2/cellulose nanocomposites obtained by in situ synthesis and via polyelectrolytes assembly. Composites Science and Technology, 68 (3-4): 1088-1093.

Pohl, A. 2020. Removal of heavy metal ions from water and wastewaters by sulfur-containing precipitation agents. Water, Air, & Soil Pollution, 231 (10): 503.

Qiu, B., Gu, H., Yan, X., Guo, J., Wang, Y., Sun, D., Wang, Q., Khan, M., Zhang, X. and Weeks, B. L. 2014. Cellulose derived magnetic mesoporous carbon nanocomposites with enhanced hexavalent chromium removal. Journal of Materials Chemistry A, 2 (41): 17454-17462.

Sabir, M., Muhammad, N., Siddiqui, U., Khan, A. S., Syed, M. R., Rahim, A., Liaqat, S., Shah, A. T., Sharif, F. and Khan, M. A. 2023. Effect of nanocrystalline cellulose/silica-based fillers on mechanical properties of experimental dental adhesive. Polymer Bulletin, 80 (8): 9131-9148.

Salama, A., Abouzeid, R., Prelot, B., Diab, M., Assaf, M. and Hesemann, P. 2023. Preparation and adsorption performance of cellulose nanofibers/silica/calcium carbonate composites for water purification. Chemistry Africa, 6 (5): 2357-2367.

Selvaraj, S., Chauhan, A., Dutta, V., Verma, R., Rao, S. K., Radhakrishnan, A. and Ghotekar, S. 2024. A state-of-the-art review on plant-derived cellulose-based green hydrogels and their multifunctional role in advanced biomedical applications. International journal of biological macromolecules: 130991.

Sequeira, S., Evtuguin, D. V. and Portugal, I. 2009. Preparation and properties of cellulose/silica hybrid composites. Polymer Composites, 30 (9): 1275-1282.

Sharma, R. K. and Agrawal, M. 2005. Biological effects of heavy metals: an overview. Journal of environmental Biology, 26 (2): 301-313.

Sohaimy, M. I. H. A. and Isa, M. I. N. M. 2020. Natural inspired carboxymethyl cellulose (CMC) doped with ammonium carbonate (AC) as biopolymer electrolyte. Polymers, 12 (11): 2487.

Su, K., Zhao, D., Lu, A., Zhong, C., Shen, X.-C. and Ruan, C. 2022. One-pot green synthesis of poly (hexamethylenediamine-tannic acid)-bacterial cellulose composite for the reduction, immobilization, and recovery of Cr (VI). Journal of Environmental Chemical Engineering, 10 (1): 107026.

Sun, X., Yang, L., Li, Q., Zhao, J., Li, X., Wang, X. and Liu, H. 2014. Amino-functionalized magnetic cellulose nanocomposite as adsorbent for removal of Cr (VI): synthesis and adsorption studies. Chemical Engineering Journal, 241: 175-183.

Taha, A. A., Wu, Y.-n., Wang, H. and Li, F. 2012. Preparation and application of functionalized cellulose acetate/silica composite nanofibrous membrane via electrospinning for Cr (VI) ion removal from aqueous solution. Journal of Environmental Management, 112: 10-16.

Tao, J., Xiong, J., Jiao, C., Zhang, D., Lin, H. and Chen, Y. 2017. Cellulose/polymer/silica composite cotton fiber based on a hyperbranch-mesostructure system as versatile adsorbent for water treatment. Carbohydrate polymers, 166: 271-280.

Wang, J. and Chen, C. 2009. Biosorbents for heavy metals removal and their future. Biotechnology advances, 27 (2): 195-226.

Wang, L., Tang, C., Wang, X. and Zheng, W. 2019. Molecular dynamics simulation on the thermodynamic properties of insulating paper cellulose modified by silane coupling agent grafted nano-SiO2. AIP Advances, 9 (12)

Wang, X. S., Li, Z. Z. and Tao, S. R. 2009. Removal of chromium (VI) from aqueous solution using walnut hull. Journal of Environmental Management, 90 (2): 721-729.

Yoshitake, H., Yokoi, T. and Tatsumi, T. 2002. Adsorption of chromate and arsenate by amino-functionalized MCM-41 and SBA-1. Chemistry of materials, 14 (11): 4603-4610.

Chapter Five

Conclusion and Recommendations

5.1 Conclusion

The study successfully achieved its goal of preparing and characterizing amine-functionalized cellulose-silica composites for removing Cr (VI) ions from water solutions. The composites—BC, BC-SiO_2, and BC-SiO_2-DAPTMS—were synthesized and carefully characterized using ATR-FTIR, XRD, TGA, BET, SEM, and TEM techniques, showing important structural, thermal, and surface changes after functionalization. Adding different amounts of N-[3-(trimethoxysilyl)propyl]ethylenediamine (DAPTMS) to the cellulose-silica composites increased their ability to adsorb and stay stable by adding amine groups. These groups helped create electrostatic interactions and made the composites better at binding Cr (VI) ions.

Adsorption studies demonstrated that BC-SiO_2-DAPTMS composites, particularly those functionalized with 4% and 10% DAPTMS, exhibited superior performance in removing Cr (VI) under optimal acidic conditions. Kinetic analysis confirmed that the pseudo-second order model best described the adsorption process, indicating chemisorption as the dominant mechanism. Isotherm modelling highlighted the suitability of both the Freundlich and Langmuir models, suggesting a combination of monolayer and heterogeneous surface adsorption. These findings validate the potential of amine-functionalized cellulose-silica composites as efficient, sustainable, and scalable adsorbents for Cr (VI) remediation in wastewater treatment applications.

5.2 Revisiting the research objectives

1.5.1 Cellulose extraction from the banana stem:

1. To extract cellulose from agricultural residue by chemical processes.

The objective of extracting cellulose from Banana stem fibers through chemical processes was successfully achieved. Utilizing a series of alkali treatments with 2% NaOH and KOH, followed

by a 2% NaOCl bleaching step, effectively isolated the cellulose from the agricultural residue. The process, which involved drying, grinding, alkaline treatment, bleaching, and subsequent rinsing, yielded a purified form of bleached cellulose. The final product, obtained after neutralizing and drying, demonstrates the efficacy of this method for cellulose extraction from agricultural waste, specifically banana pseudostem, and offers a sustainable approach to utilizing agricultural residues for high-value cellulose materials.

2. To characterize the extracted cellulose using FTIR, TGA, TEM, SEM, and XRD to characterize the structure, morphology, thermal stability, and surface properties of the extracted cellulose.

The findings of this study show that extracted cellulose was successfully characterized using a suite of analytical techniques, providing detailed insights into its structure, morphology, thermal stability, and surface properties. FTIR confirmed the removal of non-cellulosic components, evidenced by the presence of characteristic cellulose peaks. TGA demonstrated enhanced thermal stability, indicating effective purification of cellulose. TEM and SEM revealed the cellulose's fibrous morphology and microstructural integrity, while XRD confirmed its crystalline nature. These analyses collectively validate the effectiveness of the extraction process and highlight the quality and characteristics of the extracted cellulose, underscoring its potential for various applications in material science and environmental remediation.

1.5.2 Synthesis of Amine-Functionalized Composites:

3. To prepare cellulose/silica composites functionalized with an amine-based coupling agent by in-situ sol-gel process. This method used an amine-based coupling agent and TEOS as the silica precursor.

The objective of synthesizing amine-functionalized cellulose-silica composites using an in-situ sol-gel process was successfully achieved. Through a modified approach, DAPTMS was effectively integrated as an amine-based silane coupling agent, alongside TEOS as the silica

precursor, to create the BC-SiO_2-DAPTMS composite. The process, involving a controlled addition sequence of cellulose, TEOS, water, ethanol, and NaOH catalyst, allowed for the formation of silica nanoparticles within the cellulose matrix. Subsequent introduction of DAPTMS at varying concentrations (2, 4, and 10%) successfully functionalized the composite with amine groups. This synthesis method resulted in a cellulose-silica matrix with targeted amine functionalities, establishing a versatile composite with potential applications in heavy metal adsorption and other environmental remediation processes.

4. To functionalize the synthesized composites with amine groups to enhance their Cr (VI) adsorption capacity. The functionalization process involves introducing varying amounts of the amine-based silane coupling agent to achieve different levels of amine functional groups on the cellulose-silica composite surface. This variation in amine-based silane coupling agent concentrations (2, 4, and 10%) is critical for investigating the impact of different functionalization levels on the adsorption capacity and effectiveness of the composite for Cr (VI)ion removal.

The functionalization of cellulose-silica composites with varying concentrations (2, 4, and 10%) of an amine-based silane coupling agent was accomplished, enhancing the composites' adsorption capacity for Cr (VI) ions. This strategic variation in functionalization levels enabled the study of how different densities of amine groups on the composite surface influence Cr (VI) adsorption efficiency. The results indicate that increased amine group concentrations on the composite surface significantly improve the composite's affinity and capacity for Cr (VI) ion removal, validating the functionalization approach as effective for enhancing adsorption performance. This functionalization method underscores the potential of tailored cellulose-silica composites in addressing heavy metal contamination and supports the development of advanced adsorbent materials for environmental remediation.

1.5.3 Characterization of Composites:

5. To characterize the amine silane-functionalized cellulose-silica composite using TGA, TEM, SEM, XRD, ATR-FTIR, and BET analysis to characterize the structure, morphology, thermal stability, and surface properties of the synthesized composites.

Comprehensive characterization of the amine silane-functionalized cellulose-silica composite was successfully performed using multiple analytical techniques, providing a detailed understanding of its structural, morphological, thermal, and surface properties. TGA revealed enhanced thermal stability of the composite, confirming successful functionalization. TEM and SEM provided insights into the composite's fibrous morphology and homogeneous silica dispersion. XRD confirmed the presence of crystalline silica structures, while ATR-FTIR validated the incorporation of amine groups on the composite surface. BET analysis highlighted the surface area and pore characteristics critical for effective adsorption. These characterization results affirm the synthesis process's effectiveness and the composite's potential application in Cr (VI) adsorption and other environmental remediation applications.

1.5.4 Adsorption Studies:

6. To determine the Cr (VI) ion concentration using UV/Visible Spectroscopy for trace levels adsorbed by amine silane-functionalized cellulose-silica composites.

The determination of Cr (VI) ion concentration at trace levels adsorbed by amine silane-functionalized cellulose-silica composites was effectively achieved using UV/Visible spectroscopy. This method enabled precise quantification of residual Cr (VI) ions in solution, providing insights into the adsorption efficiency of the functionalized composites. The UV/Vis analysis confirmed that varying levels of amine functionalization influenced the adsorption capacity, with higher amine concentrations resulting in greater Cr (VI) removal. These findings validate the use of UV/Visible Spectroscopy as a reliable technique for monitoring trace metal ion

adsorption and underscore the potential of the functionalized composites for effective Cr (VI) remediation in aqueous environments.

7. To conduct batch adsorption experiments to evaluate the adsorption capacity and kinetics of Cr (VI) removal by the functionalized composites.

Batch adsorption experiments were conducted to evaluate the adsorption capacity and kinetics of Cr (VI) removal by amine-functionalized cellulose-silica composites. The experiments revealed that the functionalized composites exhibit a high adsorption capacity for Cr (VI), with adsorption efficiency positively correlated with increased amine functionalization levels. Kinetic analysis showed that the adsorption process follows a pseudo-second order model, suggesting that chemisorption is the dominant mechanism. These results demonstrate the effectiveness of the amine-functionalized composites in Cr (VI) adsorption, offering insights into the optimal adsorption conditions and mechanisms, and supporting their potential use in water treatment applications.

8. To apply isotherm models (e.g., Langmuir and Freundlich) to understand the adsorption mechanism and calculate adsorption parameters.

The application of isotherm models, specifically Langmuir and Freundlich, provided valuable insights into the adsorption mechanism of Cr (VI) onto amine-functionalized cellulose-silica composites. Analysis using the Langmuir isotherm model indicated that adsorption occurs on a homogeneous surface with a finite number of active sites, yielding a maximum adsorption capacity. The Freundlich isotherm model suggested a multilayer adsorption process on a heterogeneous surface, further validating the composite's affinity for Cr (VI) ions. Calculated adsorption parameters from both models highlighted the strong interaction between Cr (VI) ions and the functionalized composite surface, supporting the composite's efficacy in Cr (VI) remediation. These findings enhance understanding of the adsorption behaviour and underscore the composite’s suitability for practical applications in water purification.

1.5.5 Optimization of Adsorption Conditions:

9. To investigate the effect of different parameters such as pH, contact time, initial Cr (VI) concentration, and adsorbent dosage on the adsorption performance.

The investigation into the effects of pH, contact time, initial Cr (VI) concentration, and adsorbent dosage on the adsorption performance of amine-functionalized cellulose-silica composites provided key insights for optimizing Cr (VI) removal. Optimal adsorption was observed in acidic pH conditions, which enhanced the electrostatic interaction between Cr (VI) ions and the amine groups on the composite surface. Increasing contact time and initial Cr (VI) concentration improved adsorption up to saturation, while adjusting adsorbent dosage revealed that higher dosages led to greater removal efficiency, up to an optimal level. These findings highlight the importance of carefully controlling these parameters to maximize the composites' effectiveness in Cr (VI) remediation, supporting their application in water treatment systems.

10. To optimize the adsorption conditions to achieve maximum Cr (VI) removal efficiency.

Optimizing the adsorption conditions was effective in achieving maximum Cr (VI) removal efficiency using amine-functionalized cellulose-silica composites. By fine-tuning parameters such as pH, contact time, initial Cr (VI) concentration, and adsorbent dosage, the study identified optimal conditions that significantly enhance adsorption performance. The results demonstrated that acidic pH, extended contact time, appropriate Cr (VI) concentration, and optimal adsorbent dosage collectively contribute to peak removal efficiency. This optimization underscores the composite's potential for highly efficient Cr (VI) remediation in practical applications, highlighting its suitability as an advanced adsorbent for water treatment.

5.3 Limitations

This study on amine-functionalized cellulose-silica composites for hexavalent chromium Cr (VI) remediation has certain limitations. Firstly, the experiments are conducted on a laboratory scale, which may not fully capture the complex conditions present in natural water bodies, such as varying pH, temperature fluctuations, and the presence of competing ions. Scaling up these findings for practical, field-based applications could introduce challenges not addressed in this study. Secondly, the study focuses solely on Cr (VI), limiting the generalizability of the results to other heavy metals, which may exhibit different adsorption behaviours. Additionally, while amine-functionalization enhances adsorption efficiency, the synthesis and functionalization processes can be resource-intensive, potentially affecting the composite's economic viability and environmental impact in large-scale applications. Future studies may need to explore cost-effective synthesis methods and long-term environmental implications to support broader applicability.

5.4 Recommendations

1. Further investigation on the pH effects: Conduct additional studies to explore a wider range of pH values and their impact on adsorption performance to identify optimal conditions for different water sources.
2. Long-term stability testing: Assess the long-term stability and reusability of the amine-functionalized cellulose-silica composites to evaluate their practical application in continuous water treatment processes.
3. Kinetic and thermodynamic studies: Expand on the kinetic and thermodynamic studies to fully understand the adsorption mechanisms and potential energy changes involved in Cr (VI) adsorption.
4. Field trials: Implement field trials to test the effectiveness of the composites in real-world contaminated water scenarios, validating laboratory results under practical conditions.
5. Explore alternative functionalization techniques: Investigate other functionalization techniques or different coupling agents that could further enhance the adsorption capacity of the composites.

6. Scale-up production: Explore the scalability of the synthesis process for industrial applications, ensuring cost-effectiveness and feasibility for large-scale production.
7. Evaluate other heavy metals: Test the adsorption capabilities of the functionalized composites for other heavy metals to assess their versatility and effectiveness in broader environmental remediation contexts.
8. Integration with other treatment methods: Consider integrating the composites with other water treatment methods, such as filtration or biological processes, to enhance the overall removal efficiency of contaminants.